This is to certify that the

thesis entitled

Fabrication of Continuous Carbon Fiber Reinforced Aluminum Matrix Composites Using An Acoustic Technique

presented by

Rao V Yallapragada

has been accepted towards fulfillment
of the requirements for

Master of Science degree in Materials Science

Thomas R. Bieler

Major professor

Date March 15, 1996

Fabrication of Continuous Carbon Fiber Reinforced Aluminum Matrix Composites Using An Acoustic Technique

By

Rao V Yallapragada

Thesis

Submitted to
Michigan State University
in partial fulfillment of the requirements
for the degree of

MASTER OF SCIENCE

Department of Materials Science and Mechanics
Michigan State University
East Lansing, MI 48824

1996

ABSTRACT

Fabrication of Continuous Carbon Fiber Reinforced Aluminum Matrix Composites Using An Acoustic Technique

By

Rao V Yallapragada

A novel method of producing continuous fiber reinforced metal matrix composites has been developed using a powder metallurgical route. Unidirectional carbon fiber reinforced aluminum composites are fabricated by coating 3000 filament fiber tows with aluminum (99.99% pure) powder by using acoustic energy to evenly distribute the powder around every fiber in the tow. The coated tow is cut into mats, stacked up and consolidated by vacuum hot pressing (570 ^{o}C, 30MPa, 45mins.). Two possibilities have been demonstrated: Fibers are precoated with a polymer (Nylon) which serves as a binder to hold the fine metal powder onto the fiber. However, the process can also can be carried out without a binder, which eliminates two steps in the process: adding the binder and the vacuum burnout of the polymer. This makes a continuous processing strategy possible.

Physical properties such as fiber volume fraction, density, and coefficient of thermal expansion have been measured. Fiber volume fractions from 25-50% are possible, with 100% densification. Mechanical properties such as flexural strength, modulus, and tensile strength have been measured and correlated with microstructures. Mechanical properties are 60-80% of the rule of mixture values. Microstructure analysis of the composite has been carried out, and correlated with property variations.

Composites fabricated with this technique have a homogeneous fiber distribution with less than 2% of fibers touching each other in a given cross section, and minimal interface

reaction products. Consolidation of the composite prepregs has been demonstrated using vacuum hot pressing, but other techniques such as hot isostatic pressing (HIP) is also possible. This technique can be extended to other systems of fibers and metals, intermetallics, and ceramics. Compared to other techniques for making continuous fiber metal matrix composites such as metal infiltration, plasma spraying, chemical vapor deposition (CVD), physical vapor deposition (PVD), and fiber/foil lay-up processes, the proposed technique has the potential to provide improved properties, as well as cost effective scale-up potential for mass production. All of these desirable qualities together are not possible with techniques currently described in the literature.

The low coefficient of linear thermal expansion and high thermal conductivity make this material suitable for thermal management applications in aerospace and electronic packaging industries where the heat generated by the components has to be dissipated, and in applications where high dimensional stability is required.

To my parents

ACKNOWLEDGEMENTS

My sincere appreciation goes to Dr. Thomas Bieler for his guidance, support and encouragement through the entire research period. It had been a pleasure to work with him and I have learned a lot from him during my stay at Michigan State University.

I am especially grateful to Satyanarayana Kudapa for helping me prepare the manuscript and I also like to thank Mr. Wu for his help in doing some of the experimental work.

I thank my parents, sisters and brothers for their support and encouragement throughout my career.

Finally, I wish to thank Pia Trochez for her love, support and encouragement in enabling me to complete this work.

TABLE OF CONTENTS

LIST OF TABLES

LIST OF FIGURES

CHAPTER 1

Introduction

1.1 Definition of Metal Matrix Composites

Metal matrix composites, in general, have two components: one is the matrix material (an alloy is an usual matrix material), and reinforcement is the second component. The difference between metal matrix composites and other two or more phase alloys comes from the differences in processing of the composite. The matrix and the reinforcement are mixed together in the production of the composite. This distinguishes a composite from a two or more phase alloy, where the second phase forms as a particulate, eutectic or eutectoid reaction, etc. This implies that a composite begins as two separate components, i.e., the matrix and the reinforcement [1].

1.2 Types of Metal Matrix Composites

The classification of metal matrix composites depends on the type of the reinforcement. Metal matrix composites can be reinforced by strong second phases of three-dimensional shapes (particulate), two dimensional shapes (laminar) or one dimensional shapes (fibrous). Each of these categories has its own characteristics and advantages. Depending on the mechanical properties and differences in fabrication techniques of each category, they fall

into considerably different areas of applications [2].

The metal matrix composites offer a series of advantages that are important for the utilization of structural materials. They are high strength, high modulus, high toughness, impact properties, low sensitivity to changes in temperature or thermal shock, high surface durability and low sensitivity to surface flaws, high electrical and thermal conductivity, excellent reproducibility of properties and excellent technological back ground with respect to a) design, b) manufacture, c) shaping and forming, d) joining, e) finishing, and f) service durability information or the combination of the above properties [2].

The chemical compatibility and mechanical (stress) compatibility are a serious problem in metal-matrix composites since the temperature of fabrication is higher and the elastic-modulus coefficients of the matrix are much higher. The problem of chemical compatibility has been solved either by using low temperature fabrication techniques or by choosing thermodynamically stable components. The thermal-mechanical compatibility problem has been solved either by using a ductile matrix that can take up all the differential strain necessary in thermal cycling or by selecting a matrix and a reinforcement with matching thermal expansion coefficients [2].

The high strength of engineering alloys as matrix materials can replace structural ceramics or organic materials in composite materials. The strength of the matrix plays a significant role with respect to composite properties at some angle away from the reinforcement direction. The matrix controls the properties such as transverse strength, torsional strength, and interlaminar shear strength. This is true in creep and fatigue loading as well as under static loading conditions. The matrix also controls the strength of the joints or bonding to the composite. The higher strength metal also conserves the amount of high-cost reinforcement necessary for a given structure [2].

The high moduli of metal alloys compared to those of organic materials have a significant role in high-modulus composites. Figure 1.1 compares several fiber reinforced composite materials based on specific modulus. This Figure indicates that fiber reinforced

metal matrix composites have a higher shear specific modulus. The stiffness ratios are very important in dynamic structures such as turbine-engine blades and large airfoils [2].

In general, the reinforcement in composite materials is a linear elastic solid and does not possess good impact properties. Therefore, the high toughness and impact properties of metal alloys are very important. During plastic deformation under impact conditions, the ductile matrices such as aluminum, titanium, or nickel-chromium alloys absorb energy. This is an important design parameter in dynamic structure applications. Additionally, the ductile matrix enhances the fracture toughness by allowing the blunting of cracks and stress concentration by deforming plastically [2].

For composite structures, the insensitivity of metal properties to changes in temperature is beneficial as matrix materials. The inferior thermal shock resistance of ceramic materials when compared to metals restrict their use to limited applications only. In the case of organic-resin matrices, the properties change drastically with change in temperature, especially when approaching the glass transition temperature of the polymer. At elevated temperatures, the resins tend to soften and their resistance to oxidation and corrosion decreases significantly. Similarly, the engineering aluminum, titanium, and nickel-based alloys are much less sensitive to changes in temperature or thermal cycling [2].

Surface flaws do not show significant impact on structural engineering alloys. These alloys have significantly durable surfaces. The high thermal and electrical conductivity of metal-matrix alloys permit the diffusion and elimination of electrical concentrations from point sources. One of the most significant advantages of metal matrices is their excellent reproducibility of wrought metal properties. Especially in the case of dynamic structures, no other engineering material can be as precisely controlled to mechanical and physical specifications as these metal alloys [2].

The development of an excellent technological background enhanced the usage of metal matrix alloys in high modulus composites. Some of the present uses of these materials are in design of engineering structures, in the manufacture of complex hardware, including

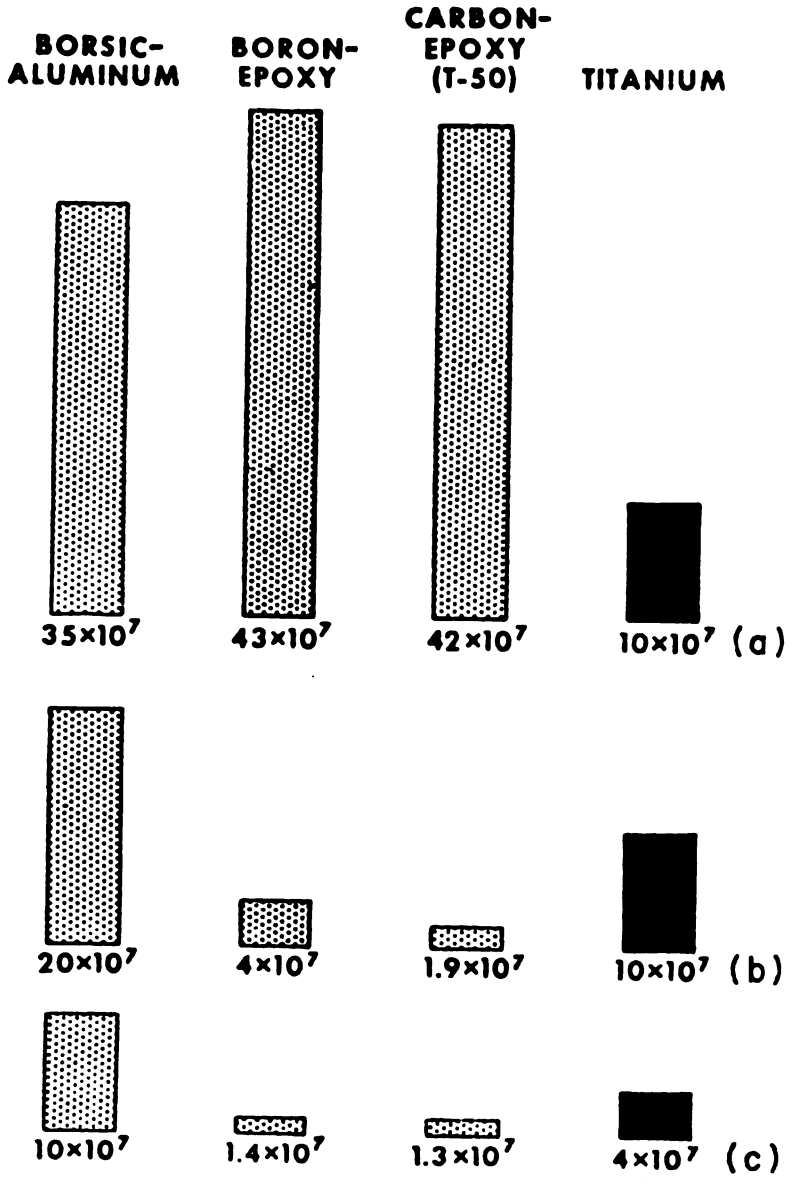

Figure 1.1: Comparison of unidirectionally reinforced composite materials used in aerospace based on their specific modulus. a) Longitudinal modulus, b) Transverse modulus, and c) Shear modulus [2].

shaping, forming, and joining operations, and in the development of finishing coatings, together with comprehensive information on service durability. In this thesis, the focus will be on continuous fiber reinforced metal matrix composites with special emphasis on continuous carbon fiber reinforced aluminum matrix composites [2].

CHAPTER 2

Continuous Fiber Reinforced Metal Matrix Composites

2.1 Introduction

Fiber reinforced composite materials are suitable materials for applications in aerospace and engineering structures because of their attractive mechanical properties ranging from cryogenic to high temperatures and enhanced resistance to specific environments. These materials have been under development for more than 20 years but the development was initially focussed on continuous fiber metal matrix composites. Aerospace applications were the first targets for these materials [1].

Unlike most metals and alloys, fiber reinforced metal matrix composites are anisotropic and the degree of anisotropy depends on the degree of fiber orientation [1]. In general, metal matrix composites consist of a ductile matrix containing strong brittle fibers. The role of the fibers is to carry the load and the matrix acts as medium to transfer the load to the fibers. The efficiency of load transfer depends on the bond strength at the interface. In particular, strongly bonded interfaces are required with ductile reinforcements for the brittle matrix composites having high toughness, and weakly bonded interfaces for brittle (fibers) reinforcements. Ductile phases can contribute to toughening by bridging contri-

butions from the deforming particles. Debonding along the fiber/matrix interface at the crack front, which is governed by the inherent bond strength of the interface is required for toughening by brittle fibers and whiskers. The debonding at the interface allows the fibers to remain intact in the immediate crack wake and subsequent fiber pull-out contributes to the toughening [3].

If the efficiency of the interface is high, the mechanical properties of the composite depend more on the properties of the fibers than the properties of the matrix. This means that the matrix can be selected based on oxidation and corrosion resistance or other required properties [1].

2.1.1 Existing Fabrication Methods of CFRMMCs

The production of CFRMMCs involves two stages. The first stage is production of precursors which is synonymous to the production of prepregs in the fiber reinforced plastics technology. In the second stage, the precursors are cut into desired lengths, stacked, and consolidated by diffusion bonding to produce structural components [4].

2.1.2 Fabrication of Composite Precursors

New fabrication techniques to make CFRMMCs were developed in 1970s and 1980s. Improved processes to produce near net shape composites in a cost effective manner will be the key to the success of any processing technique. The CFRMMCs or MMCs fabrication methods can be classified into 3 different categories [5]:

1. Liquid state fabrication.

2. Solid state fabrication.

3. In situ fabrication.

2.1.3 Liquid State Fabrication

All the methods in this category involve liquid metal infiltration of fibers or fiber preforms. The infiltration can be carried out under atmospheric or inert gas pressure or under vacuum. In this type of processing, the long (continuous) fibers have to be properly aligned and distributed before infiltrated by the metal. The primary requirement for this process to succeed depends on the wettability of molten metal on fiber surface. The molten metal penetrates around the fiber bundles by capillary action, vacuum infiltration, or pressure infiltration. Squeeze casting is a specialized version of liquid metal infiltration [5].

Squeeze Casting

In this technique high pressures are applied to the liquid metal during solidification and is shown in Figure 2.1. The first step in this process is the introduction of porous fiber preform into the die. Then the molten metal is poured into a preheated die mounted on a hydraulic press. Molten metal is made to penetrate the fiber preform by applying the pressure. The matrix solidifies under pressure and piston is ejected after solidification. The fiber volume fraction and orientation have significant role in controlling the resistance against wear and seizure or galling [5].

Metal-Melt (Liquid Infiltration) Process

In this technique, a fiber bundle is pulled through a molten metal bath to produce the precursor with large enough fiber volume fraction. Figure 2.2 shows the fibers pulling through the molten metal bath. This process was successfully used to produce boron-aluminum cables with pure aluminum as matrix material, silicon carbide filaments in an aluminum alloy matrix (6061 alloy), maraging steel-aluminum tapes, and carbon/aluminum composites. The most effective use of liquid infiltration to produce composite cables was in the case of carbon fibers. Fabrication of this composite included two stages. In the first stage the fiber

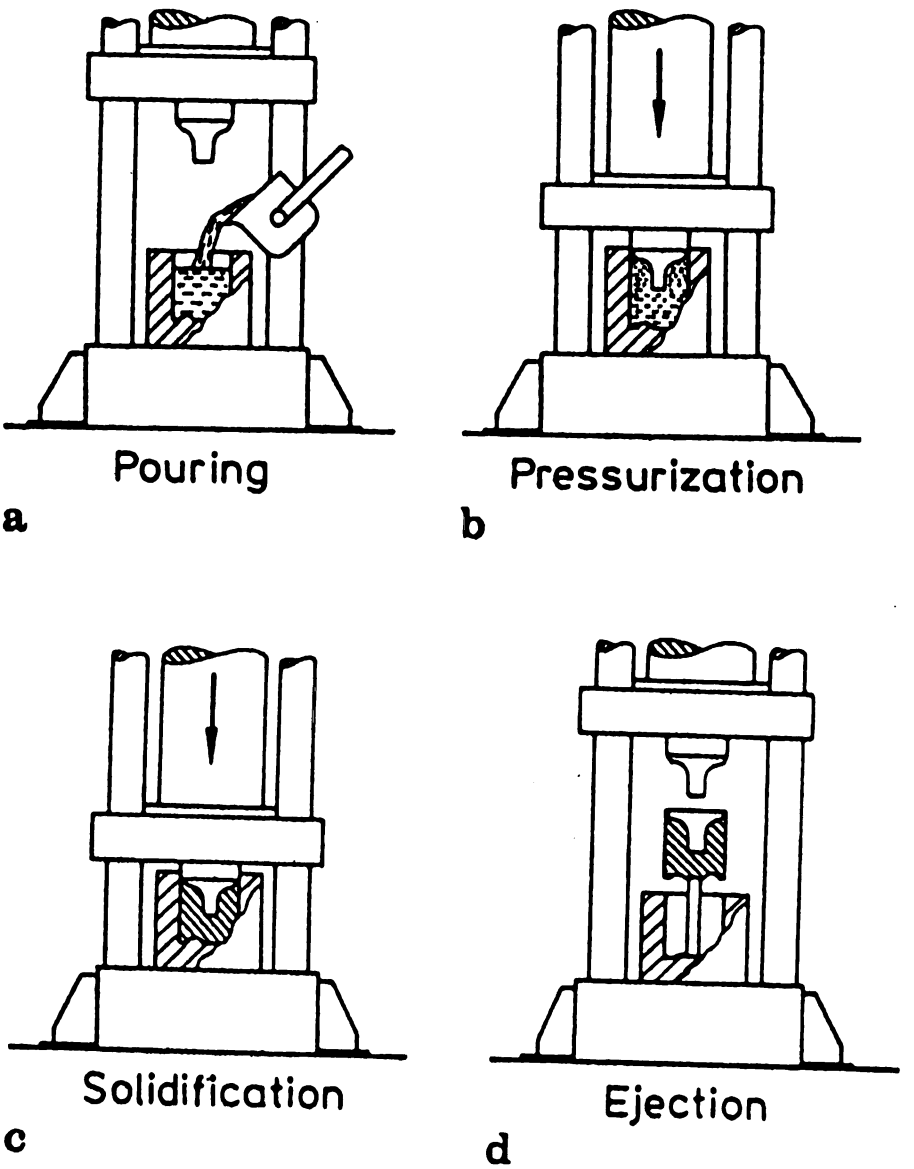

Figure 2.1: Squeeze Casting [5].

surface was coated by a mixture of titanium and boron to promote wettability of aluminum on carbon surface. Then the fiber bundle was pulled through the molten aluminum alloy bath. The strength of the cable with v_f of 0.35 - 0.4 was found to be 1.0 to 1.3 GPa.

Divecha back in 1974, suggested an interesting method of prebonding the fibers and a matrix, which could be used to make precursors as well as structural elements. In this technique, a thin cable of matrix material was wound onto a fiber and such wound fibers were stacked and an ideal fiber distribution was expected to be obtained.

The disadvantages with this liquid infiltration technique are poor wetting of fiber by molten metal, excessive reaction between fibers and metal due to high processing temperatures, and nonuniform fiber distribution.

2.1.4 Solid State Fabrication

In this process, alternate layers of properly placed fibers and metal foils are stacked to obtain the desired volume fraction and orientation. A resin based sacrificial binder might be used to keep the fibers in place depending on the fibers in use. The preformed materials are consolidated by diffusion bonding. The application of heat and pressure in vacuum causes the metal to flow around the fibers and make a bond with the next layer, enclosing and gripping the fibers in between [5]. Figure 2.3 gives the flow chart for composite fabrication by diffusion bonding. Starting materials are pure metals or metal alloys in the form of thin foils as matrix materials with filaments/fibers bundles, and whiskers as reinforcements. The fibers in the form of mats and woven cloth are more complicated to use in diffusion bonding than in liquid infiltration methods. The surface of the components must be clean to improve the interdiffusion which in turn enhances the bond strength between the fiber and matrix. Therefore, surface treatment of fibers in alkaline or acid solutions is often required. The surface treatment of aluminum foils with carbon tetrachloride to remove the surface oxide Al_2O_3 is an example [6].

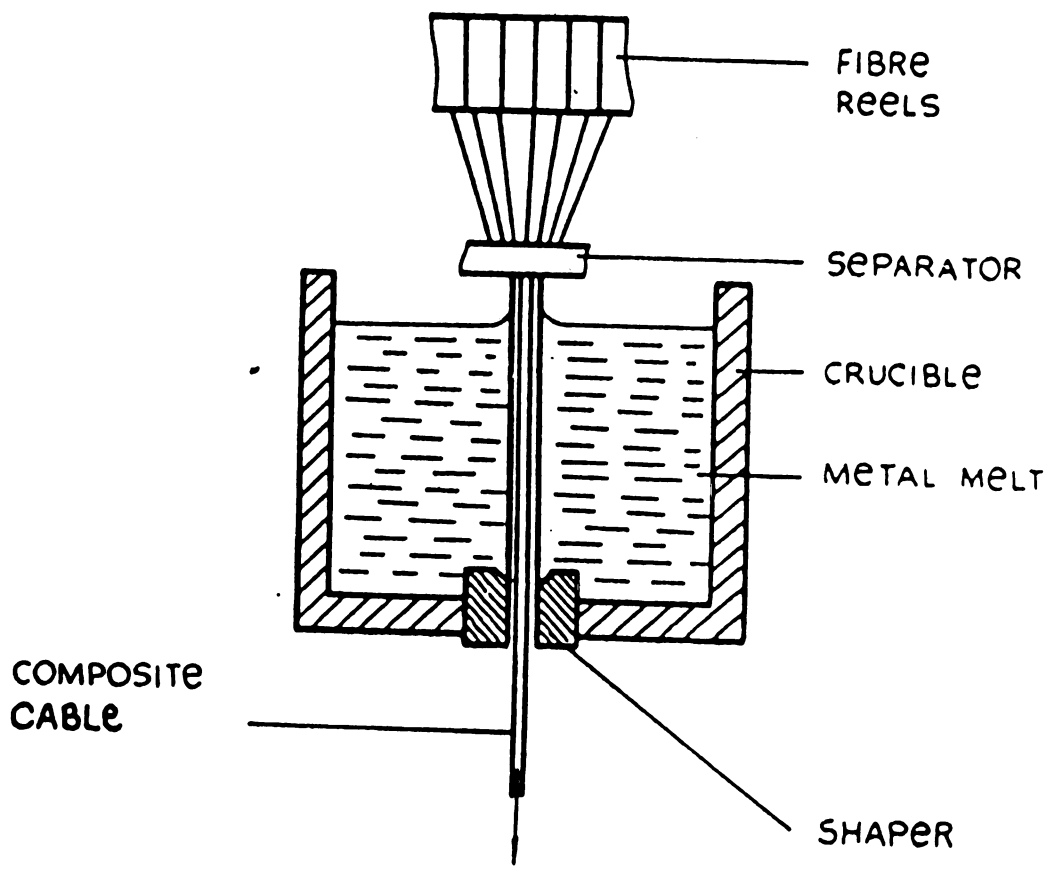

Figure 2.2: Fiber bundle pulled through a molten metal bath to produce composite cables [4].

The arrangement of reinforcements and fibers varies from one system of fibers to another. The monofilaments or fiber bundles are wound onto a drum made of good thermal conducting metal for C, SiC/W, SiC and Al_2O_3. Then the preforms are made by coating the metal on the fiber surface by plasma spraying, physical vapor deposition, and chemical vapor deposition (described later in this section). The low cost plasma spraying is most often used to produce sheets with good adhesion between fiber and matrix [6].

The preformed sheets are cut and stacked in predetermined orientations to achieve the required fiber volume fraction and thickness. The important step in diffusion bonding is the application of temperature and pressure, which gives good bonding between fiber and matrix, enhances the composite density by eliminating voids, and improves the strength of the composite by plastically deforming the matrix. The efficiency of consolidation depends on consolidation pressure, temperature, time of consolidation, and atmosphere [6]. This technique has limited usage because of the limited number of foils available, fiber volume fractions are often small, and fiber diameters are too large [7].

Plasma Spraying

The process starts with winding the fibers onto a cylindrical mandrel with a fixed pitch. Then the fibers are coated by spraying molten metal drops onto mandrel surface using a plasma jet. The composite layer with a weak matrix is cut to get a precursor sheet or tape. This has to be densified and sintered to produce a particular structural component. The instant freezing of the liquid droplets gives a fine microstructure of the matrix around the fibers, and thus reduces the fiber surface area that could have been wetted in the case of moderate cooling rates [8]. This instant freezing causes porosity and lower the mechanical properties. In addition, melting and subsequent rapid cooling of a matrix alloy during plasma spraying can also change the structure of the matrix and deteriorates the properties of the composite. Another disadvantage is the change in composition of the matrix due to oxidation if the process is carried out in air or in an impure inert gas atmosphere.

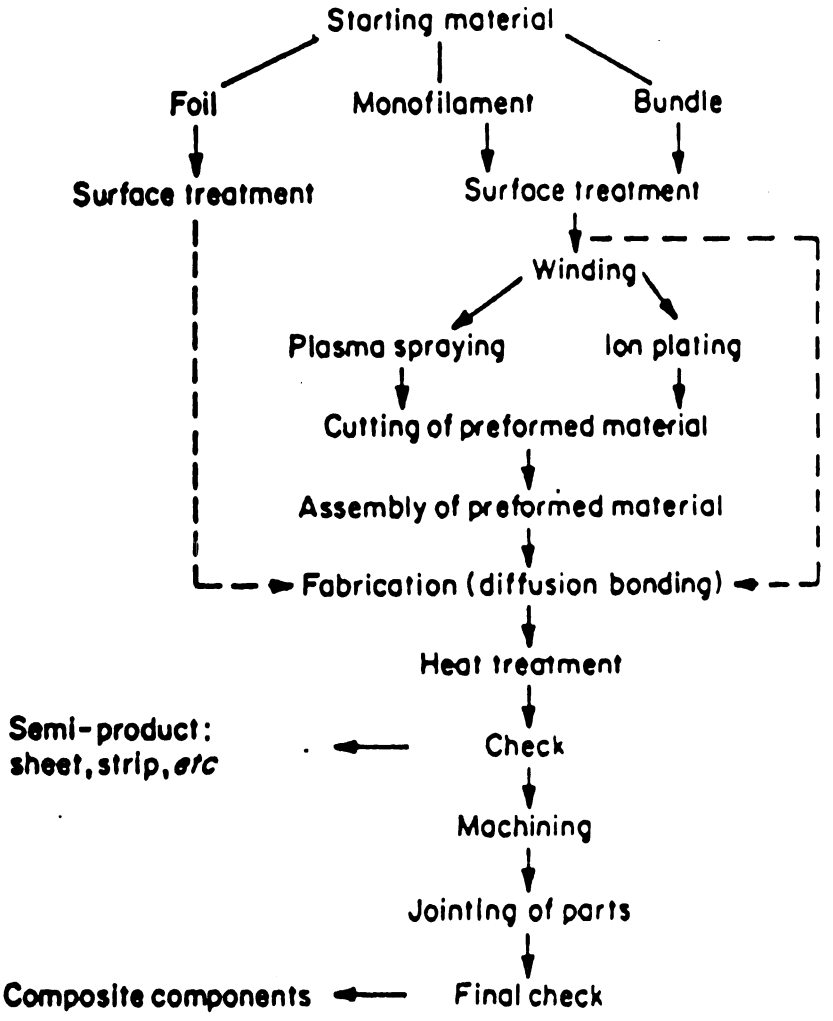

Figure 2.3: Flow chart for composite fabrication by diffusion bonding [6].

Microcracks will also form during rapid solidification due to thermal stresses [9].

Chemical Vapor Deposition (CVD)

In CVD process, the chemical components are vaporized and decompose or react with another vaporized chemical and get deposited on the fiber surface. The undesired chemical components escape as gases. This process is frequently used to coat the fibers with wetting agents to improve the wettability or diffusion barrier coatings to prevent the fiber matrix interactions. This technique has been used to coat carbon fibers with Al/Al alloys to make the composites [10, 11, 12, 13]. Some of the elements/compounds deposited on carbon fibers include TiB, Cu, Ni, TiC, TiN, and SiC by using CVD process. The important parameters in the CVD process are the chemicals and the temperature of the reaction chamber. The disadvantage of this process are that the process is slow and expensive.

Physical Vapor Deposition (PVD)

This process is similar to CVD but the basic difference is that the matrix material is deposited on the fibers without the help of any chemical components (wetting agents). Evaporation, ion plating, and sputtering are the three basic PVD processes in use to produce metal matrix composites. Carbon fiber reinforced aluminum composites were fabricated using PVD technique [14, 15]. This process is very attractive because of the versatility in composition and microstructure of the coating. Pure metals or metal alloys can be deposited on the fibers and no effluents are used or created using this process. The disadvantage is that the process is slow and expensive.

2.1.5 In-Situ Fabrication

Many researchers have fabricated metal matrix composites during working of mixtures of individual constituent phases (Courtney *et al.* [16, 17]). This kind of approach usually

works for cast or directionally solidified ingots where controlled unidirectional solidification gives a two phase microstructure with one phase existing in a lamellar or fibrous form. It has also been utilized to mix blends of elemental metallic powders to fabricate metal matrix composites. In this technique, elongated reinforcements are created by deformation. Extrusion, rolling or drawing are some of the deforming processes that can be used to deform the constituents into fibrous or lamellar morphology. The reinforcing phase must be ductile to achieve this. Ni-W (W as reinforcement), Cu-Cr (Cr as reinforcement), and Fe-Cu (Fe as reinforcement) systems are some of the examples of in-situ composites [18].

This technique can not be applied to all metallic systems because of the restrictions on the quantity of second phases in the blend and the differences in the flow stress of the constituents. One more disadvantage is that the reinforcing phase (minor constituent) will not elongate into fibers or platelets if the reinforcing phase has much higher flow stress. An example is the Cu-11.3 wt% Mo system where the Mo particles retain their shape even at a true strain of 7. Despite these limitations, large positive deviations in tensile strength compared to rule-of-mixture values are observed for fibrous composites. An example is the Cu-16% volume fraction Fe system as shown in Figure 2.4 [18].

For certain metallic systems this technique offers significant advantages [18]:

- Metallic constituents are inexpensive when compared with nonmetallic reinforcements
- Traditional metal working operations can be performed
- Mismatch in thermal expansion coefficients of the reinforcement and matrix are minimized when compared with nonmetallic reinforcement and matrix
- Higher strengths will be obtained than the predicted rule-of-mixture values (eg. Cu-16% volume fraction Fe)

The disadvantages are:

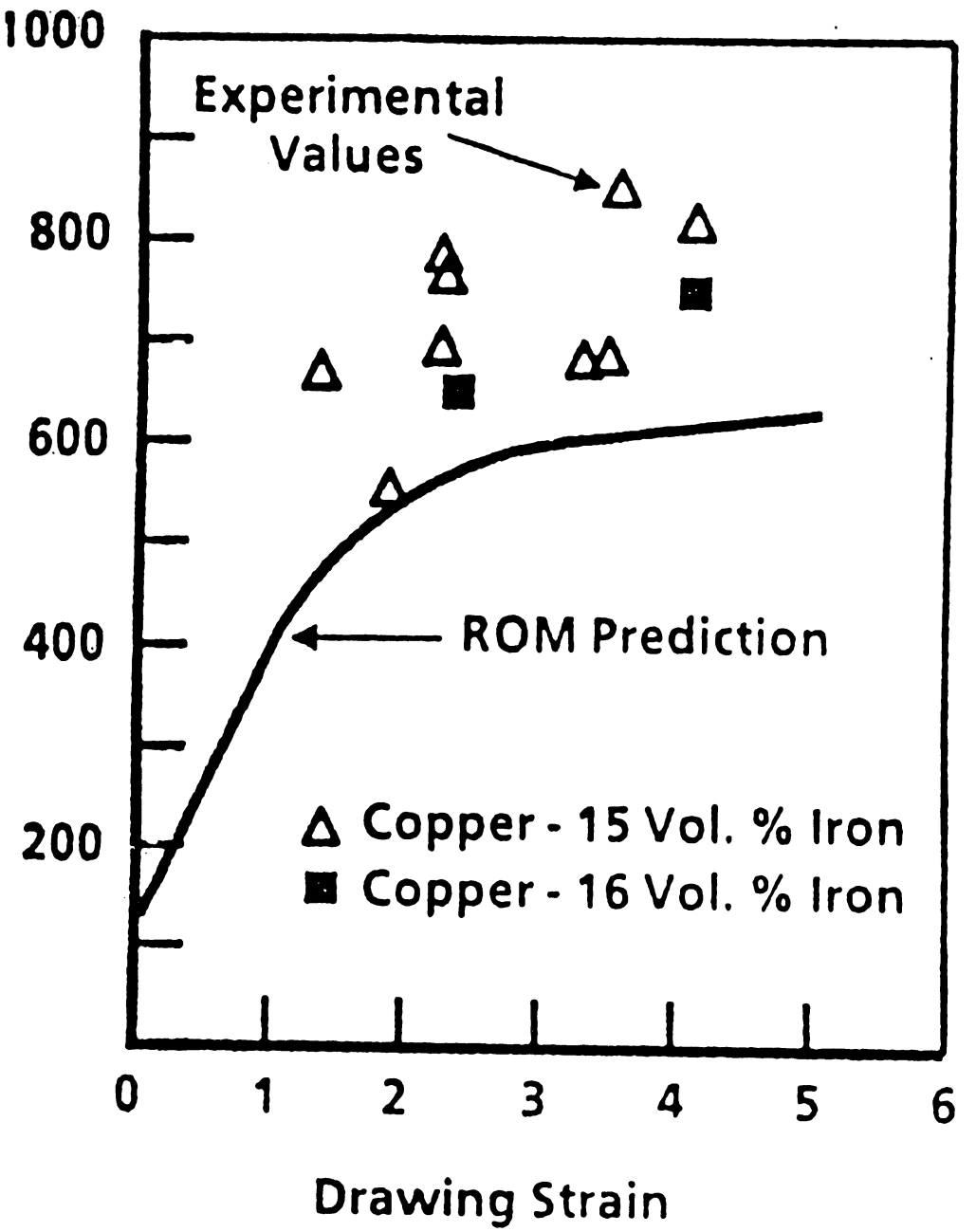

Figure 2.4: Observed and predicted tensile strengths for Iron-Cu in-situ composites [18].

- Restrictions on the product shapes if very high true strains (≈ 7) are needed
- Very high strains limit the thermal resistance of the composite to recovery and re-crystallization
- There are limited number of material systems that respond to high strains
- The reinforcement limits the increase in elastic modulus of the composite [18]

2.2 P/M Route of Making CFRMMCs

2.2.1 Introduction

As described earlier, the reinforcement for metal matrix composites are filaments, whiskers, and particulates. Continuous fiber composites give best mechanical properties only along the fiber direction. However, if biaxial or triaxial stress states are encountered, whiskers or particulate reinforced composites will exhibit much more isotropic properties. The bi-axial stress state problems can be addressed by cross-ply lay-ups of continuous fiber piles and three dimensional weaving, a technology not yet been implemented for metal matrix composites would address the problems of triaxial property uniformity [18].

2.2.2 Strengthening Considerations

The control of mechanical properties depends on the concept of combining metals (matrix) with reinforcement. Under ideal conditions the composite exhibits mechanical and physical properties defined by the rule-of-mixtures [18]:

$$P_c = P_m V_m + P_r V_r$$

where:

P_c = the property of the composite

P_m = the property of the matrix

P_r = the property of reinforcement

V_m = volume fraction of the matrix

V_r = volume fraction of the reinforcement

The Figure 2.5 shows the mechanical properties attainable in aluminum metal matrix composites as a function of length of reinforcement, elastic modulus, and volume loading [18].

The improvement in strength, elastic modulus, fracture toughness, and density in the case of continuous fiber reinforced aluminum metal matrix composites is based on the assumption that the rule-of-mixtures is followed by the composite. In fact, this holds good in the case of continuous fibers as reinforcement, and if there is no interface reactions to degrade the strength of the fiber and bonding between matrix and fiber. An agreement between the strength predicted by the rule-of-mixtures and measured values was achieved in the case of stainless steel fiber reinforced aluminum composite (Figure 2.6) [18].

From the above discussion one can conclude that the continuous filaments would be the best choice as reinforcements. However, the use of continuous fibers/filaments in metal matrix composites imposes certain restrictions. The preparation and lay-up of continuous fiber/filament in the matrix are complex and this makes the processing very expensive. The filaments reinforcement is currently restricted to simple geometries such as planar or axisymmetric shapes. Therefore, alternative reinforcements are being studied to reduce the processing cost of metal matrix composites while retaining the attractive properties. Use of less expensive discontinuous reinforcements, powder metallurgy, and casting techniques are some of the approaches to bring down the processing cost. However, lower the cost

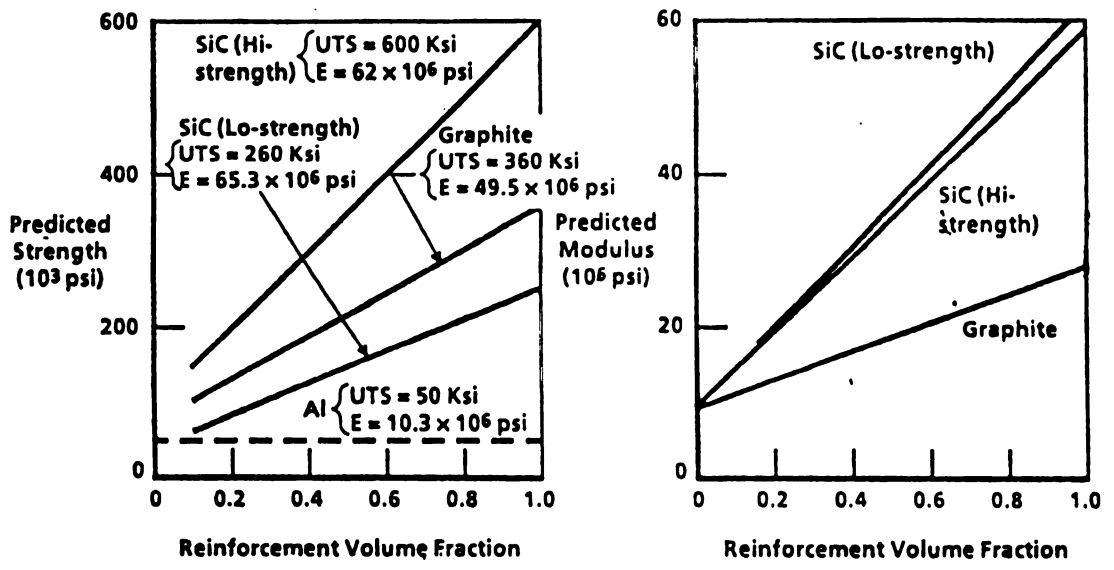

Figure 2.5: Predicted values of UTS and Elastic Modulus for continuous fiber reinforced aluminum matrix composites [18].

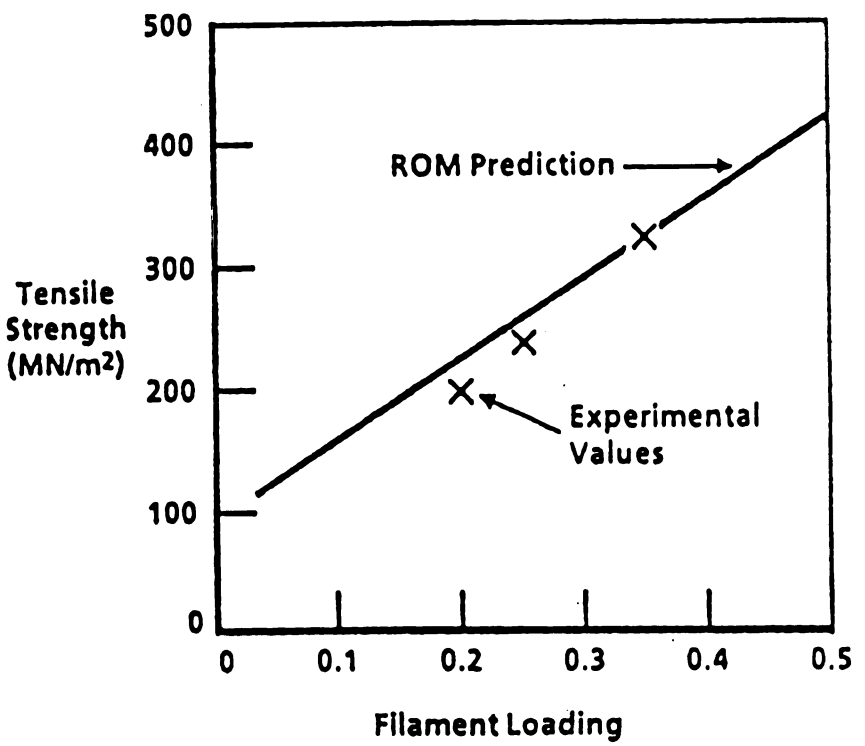

Figure 2.6: Comparison between measured and predicted values of UTS for continuous stainless steel fiber reinforced aluminum composite [18].

gives lower levels of property enhancements. The inferior properties compared to continuous fiber reinforcements is the result of decrease in stress transfer from the matrix to the reinforcement. The efficiency of stress transfer depends on the length (l) of the reinforcement and its critical length (l_c) by the relationship:

$$S_c = S_f[V_f^*(l - l_c/2^*1) + E_m/E_f^*(1 - V_f)]$$

where:

S_c = composite strength

S_f = strength of the reinforcement

V_f = reinforcement volume fraction

l_c = minimum reinforcement length for full load transfer from the matrix to the reinforcement

$$(l_c = d * S_f/S_m)$$

where

d = fiber diameter

and

S_m = matrix strength

l = actual length of reinforcement

E_m = elastic modulus of the matrix

E_f = elastic modulus of the reinforcement

Figure 2.7 shows that relatively modest increases in strength are obtained for fiber lengths near the critical fiber length. The efficiency of load transfer from the matrix to the reinforcement increases with increase in l/l_c. At l/l_c=16, the discontinuously reinforced composite

will exhibit approximately 96% of the increase in strength exhibited by a continuously reinforced composite [18].

In spite of these theoretical advantages, there are certain practical problems with maintaining the integrity of high-aspect-ratio discontinuous fibers during fabrication and working. Thus, the focus is now on particulates as reinforcements. But the low aspect ratio ($\approx$ 1) of particulates offers lower properties as compared to high aspect ratio fibers [18].

2.2.3 Advantages of P/M Process

The advanges of producing metal matrix composites using powder metallurgy techniques over liquid processing or diffusion bonding are:

1. Lower processing temperatures can be used and this minimizes the interaction between the matrix and the reinforcement and this in turn improves the mechanical properties of the composite.

2. In particular cases powder metallurgy techniques allows the preparation of composites that can not be prepared by liquid processing [18].

The production of particulate or whisker reinforced composites is easier using powder metallurgy blending techniques rather than casting techniques. Continuous fiber reinforcement is more expensive than the particulate reinforcement of similar composition. Several companies are currently working on the development of powder metallurgy particulates or whisker reinforced metal matrix composites. DWA, the advanced material division of ARCO Chemical Company, formerly Silag, and Novamet are currently working in this area. An unique feature is associated with each of their processing techniques. DWA and Silag use their proprietary blending processes to combine their composite components. The basic difference is that Silag uses SiC whiskers manufactured from rice hulls rather than particulates. Novamet also uses particulate, but blends the reinforcement and matrix by mechanical alloying techniques [18].

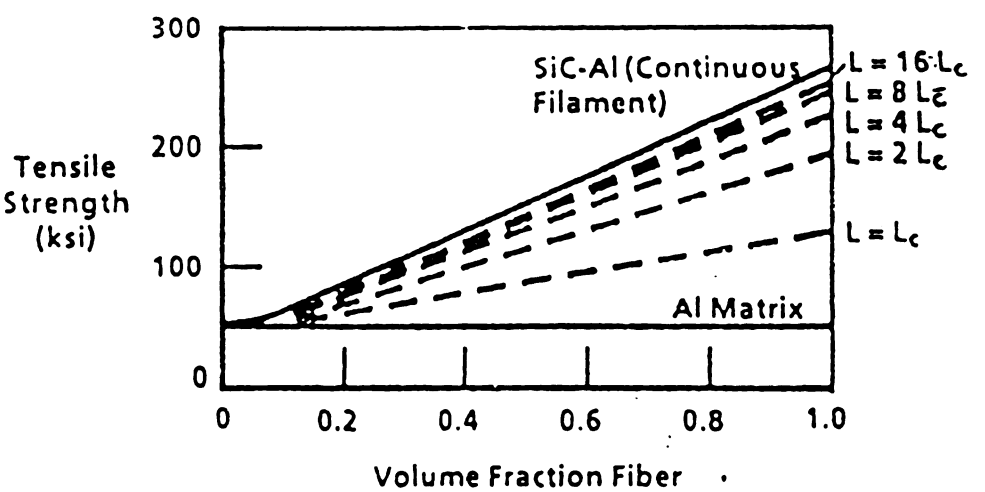

Figure 2.7: Composite strength as affected by whisker length and volume loading [18].

Despite their differences in processing methods or reinforcements, these products show some similarities. These products are being used in military or aerospace industries, and are quite expensive when compared with noncomposite products ($50 - $100/pound vs. $5 - $10/pound as billet). Additionally, the relation between volume fraction of the reinforcement and corresponding mechanical properties is similar in all the three processes. Figure 2.8 shows that the measured values of elastic modulus are close to the predicted values for continuous fiber/filament reinforcement. The Figure also shows that the measured tensile strength values are below the predicted values by the continuous fiber/filament reinforcement model, although they are superior to the predicted values by discontinuous models, at least at the lower volume loadings. The shortfall in strength is a result of poor bonding between the reinforcement and the matrix. This problem has been addressed in the continuous filaments by using particular filaments that are specially tailored to improve the interfacial bond strength [18].

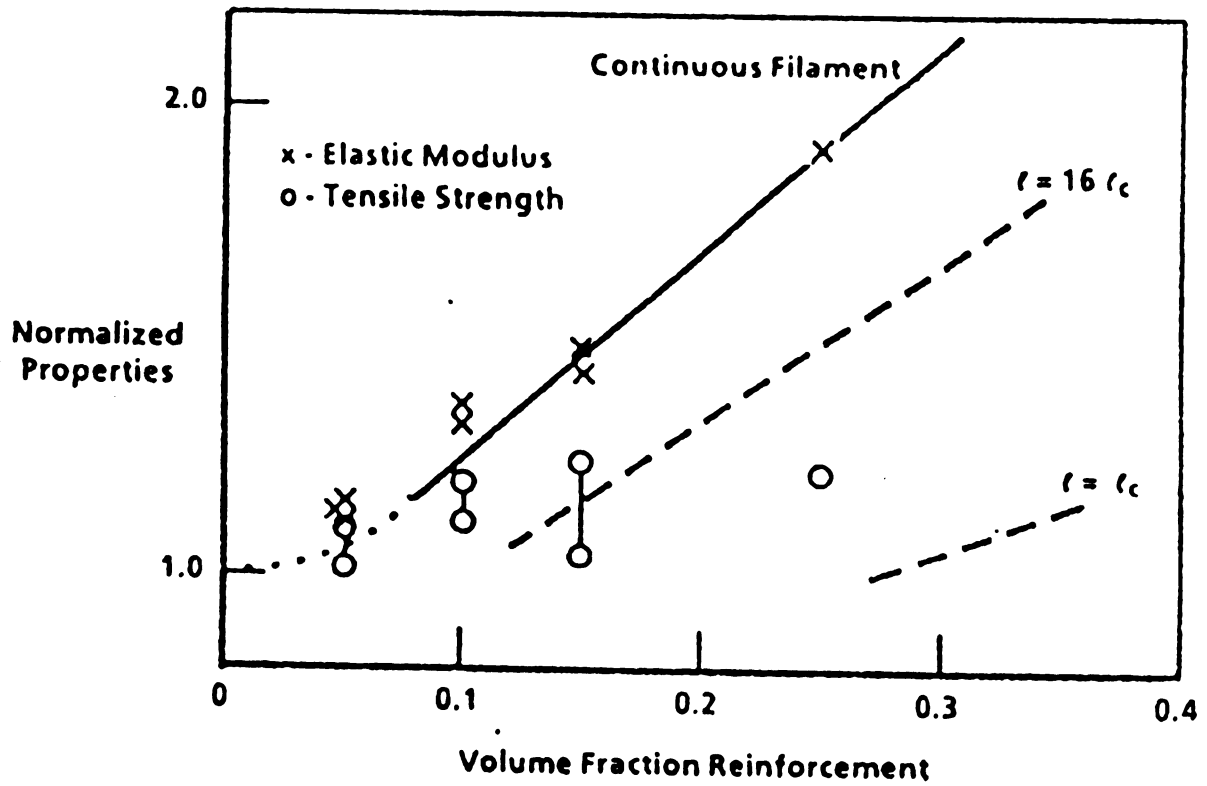

Figure 2.8: Comparison of normalized values of elastic modulus and ultimate tensile strength vs. volume fraction reinforcement. Predicted values of continuous and discontinuous reinforcement are also shown [18].

CHAPTER 3

Carbon-Aluminum Composites

The high strength and stiffness, low density, and potential for large-scale production make carbon/graphite fibers attractive as reinforcements in metal matrix composites. However, the lack of compatibility between carbon fibers and metals during fabrication restricts the development of these composites. Aluminum, magnesium, nickel, and cobalt are fairly compatible with carbon fibers. Titanium can also be a matrix material but it can not be considered unless protective coatings are applied to prevent the formation of carbide. However, carbon-aluminum composites attracted much attention in space applications industry because of their light weight, high stiffness, and very low thermal expansion coefficient. These properties and the cost of production make this material competitive for many applications in aircraft, missiles, electrical machinery, rocket propulsion systems, launch vehicle structures, and spacecraft [4]. An interesting example is the large antenna boom cum waveguide designed for NASA space telescope. Depending on the orientation in space, some of the components of the boom will be exposed to direct sunlight and a temperature difference of hundreds of degrees exists. Therefore carbon fiber reinforced aluminum will be the best choice with $\alpha \approx 0$ without any weight penalty. Pure aluminum can not be used because its high thermal expansion coefficient (24×10^{-6}/K) makes it distorted. The carbon-aluminum's very low coefficient of expansion is due to almost zero longitudinal expansion coefficient of carbon fibers [5].

Aircraft applications of carbon fiber reinforced aluminum composites are in skins, struts, spars, wing boxes, and helicopter blades. The high temperature resistance of these composites up to 500 ^{0}C makes these composites suitable for reentry shieldings for missiles and compressor blades for gas turbine engines. Carbon fiber aluminum composites find applications in launch-vehicle structures require light weight for stiffening of large diameter cylindrical sections, interstages, adapters, and tank and equipment support structures. Spacecraft applications are in shells and trusses in the primary structures, and booms, solar-cell panels, equipment mounts, and antennas in auxiliary structures. If the cost of production comes down, aluminum-carbon composites can find applications in non-aerospace industries like rapid-transit and deep submergence vehicles and rotating parts in electrical generators [4].

3.1 Fabrication of Carbon-Aluminum Composites

Different pathways have been developed to manufacture carbon fiber reinforced aluminum metal matrix composites. These include liquid metal processing, diffusion bonding, spray forming, etc., or a combination of these methods [19]. These techniques are described below.

They were first produced in 1961 by Kopenall and Parikh [20] with aluminum-4% Cu as matrix and graphite fibers as reinforcement. Chopped graphite fibers were mixed with the alloy powder in a ball mill, and hot extruded at a temperature ranging from 690 ^{0} to 1100 ^{0}F. The composite had 20-40 w/o of graphite and the maximum strength obtained was 242 MN/m^{2} (35, 000 psi). Sara *et al.* [21] used liquid infiltration techniques to force molten aluminum into graphite fiber bundles. This technique is shown in Figure 3.1. The mold was preheated to 750 ^{0}C and aluminum was forced at pressures of 2.48 (360 psi) and 7.46 MN/m^{2} (1080 psi) in two different experiments. Sara *et al.* [21] concluded from the experiments that pressure alone was not sufficient to infiltrate aluminum, and the improvement

in wetting of fibers by aluminum was necessary [21].

Sara [21] also worked on coating the fibers to minimize the interaction between aluminum and carbon, promote wettability, and infiltration of aluminum into fiber bundles. Carbon/graphite fibers were coated with TiC, Ta, Ni, and Ag. Satisfactory coatings were obtained for TiC and Ta, but in the case of fibers coated by TiC, the tensile tests indicated that fibers were degraded by the coating process. Al_4C_3 was observed in the interface region of fibers and the matrix. In the case of Ta, no reaction products were observed and the fibers were readily wetted by aluminum. The nickel coating readily reacted with aluminum and formed significant quantities of Al_3Ni and thus nickel is unsuitable as a coating. Dewetting was noticed in case of Ag due to the presence of solution of Ag in aluminum during infiltration [21].

Electroplating aluminum from a non-aqueous electrolyte was investigated by Buschow and Esola in 1969 [22]. They codeposited graphite fibers and aluminum simultaneously to produce the composites with short fibers having l/d ratio up to 100:1 and in small volume never exceeding 0.11. Schmidt and Hellman in 1969 electroplated aluminum on substrates by using aluminum hydride as a source material in contact with a decomposition catalyst. Several hundred feet of graphite yarn was coated this way, and the thickness of aluminum coating was found to be 0.3μm but the bond between fiber and aluminum was poor and the coating could be removed easily [22].

LaIacona in 1971 [23], coated Thornel-50 fibers with electroless nickel, spread on A1100 aluminum foil, held together by spraying an acrylic solution and hot pressed at 1000 ^{0}F. The fiber volume fraction was 8 v/o. This process could not be commercialized because high fiber volume fractions were not possible [23].

Howlett *et al.* in 1971 [24] tried to produce graphite-aluminum composites by coating and hot pressing, electroforming, hot extrusion of blends of powder and fibers, and liquid infiltration. Coplating of aluminum and chopped fibers from an ethereal plating solution in an inert atmosphere was futile. Flocking of the fiber which in turn shorted out the electrodes

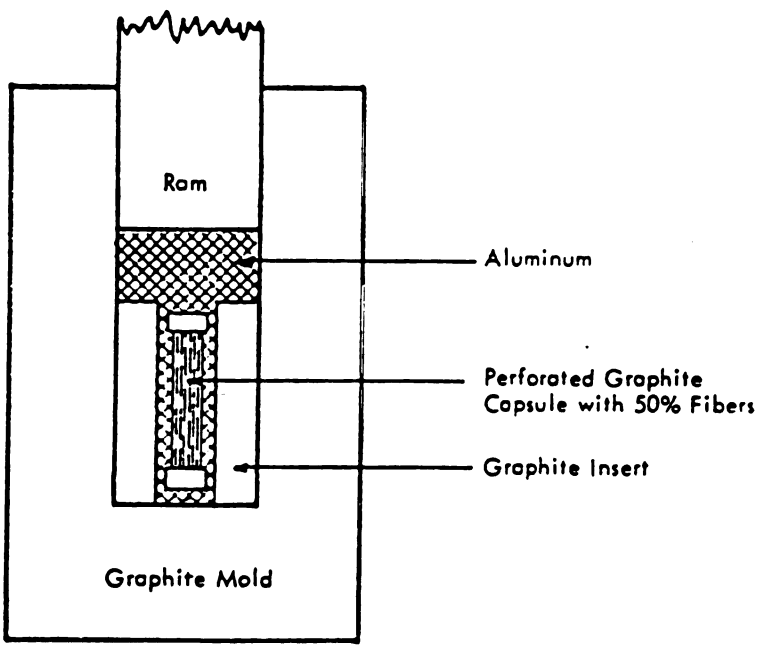

Figure 3.1: Pressure infiltration technique to make carbon-aluminum composite [21].

was the main problem. No solution was found to the experimental difficulties [24].

Howlett *et al.* [24] also coated graphite fibers with aluminum by vacuum deposition. techniques and consolidated. The fiber distribution was good but the strength of the composite was very low. Peeling of the matrix from the fiber and shadowing were other problems with this technique. The method was discontinued because of the difficulty in penetration [24].

Several techniques were attempted by Howlett *et al.* [24] to hot-work the blends of aluminum powders and chopped graphite fibers. The blends were wet mixed using an organic binder in an extremely volatile carrier liquid to yield mixtures containing 12-25 v/o fibers. The mixture was placed in an aluminum container and extruded at 400-600 ^{0}C after binder was evaporated. In order to avoid fiber damage, high extrusion temperatures, low extrusion ratios, and low fiber fractions were maintained. The strength of the composite having 11 v/o fiber was 25,000 psi [24].

DeLamotte and coworkers [25] in 1972 continuously cast aluminum-carbon fiber composites. The technique is shown in Figure 3.2. Nickel coated 1μm carbon fiber tow was passed through the crucible containing aluminum melt and then drawn through the die located at the bottom of the crucible to produce a continuous wire. The liquid metal wets the fibers and solidifies in the die, producing continuous wire [25].

Davis and Bradstreet [26] in 1970, consolidated aluminum-electroplated thornel fibers by diffusion bonding. The coated fibers were placed between layers of aluminum foils and hot pressed. The composite was fully dense with no porosity, but the fiber content was only 9v/o. Higher fiber contents (25 v/o) were obtained by consolidating coated fibers alone without the use of any metal foils. Some uncoated fibers and fibers with unusually thick plating were observed in the microstructure analysis. Metallographs also revealed fairly uniform fiber distribution with little fiber-to-fiber contact. Tensile strengths of 40-50 ksi were obtained and fiber pull out during testing indicated unsatisfactory bond between fiber and the matrix [26].

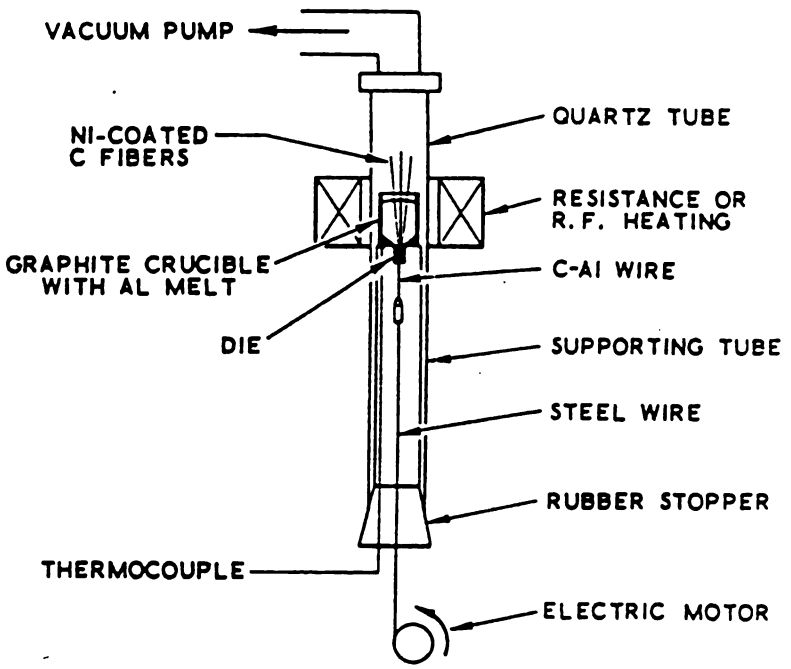

Figure 3.2: Wire drawing apparatus for producing continuously cast aluminum-carbon composite [25].

Baker *et al.* [27] electroplated carbon fibers with aluminum by winding the fibers on a stainless steel drum. Prespreading of the fibers was done for good penetration of metal into fiber tows. Plating was carried out using diethyl ether based organic bath and the processing was done in a dry inert atmosphere to eliminate water to avoid the danger of explosions. After coating, the sheets were removed from the mandrel and consolidated by diffusion bonding or liquid phase bonding. The composites had fiber contents of 30-40 v/o with tensile strengths ranging from 400-500 MN/m^2 which were considerably lower than the predicted rule-of-mixture values [27].

Blankenburgs (1969) [28], manufactured carbon-aluminum composites using powder metallurgy route. The composite was made by blowing aluminum powder (oxide content $\approx$ 1%, particle size 5-8μm) onto RAE type carbon fiber (UTS=240 ksi, E=48$\times$ 10^6 psi, density=1.8 gr/cm^3), followed by consolidation. The coated fibers were chopped off and extruded at 600 ^{0}C [28].

Ramakrishnan *et al.* [19, 29] in 1990, utilized continuous slurry technique (P/M route) to fabricate continuous carbon fiber reinforced aluminum matrix composites. Torakya T 300, 3000-50B carbon fibers and a slurry having a composition of 0.2 wt% of aqueous solution of sodium alginate with 20 vol% of aluminum powder were used for making the preforms. The sizing on the carbon fibers was removed by using acetone before they were made to pass through the slurry continuously. The dried (vacuum at 50 ^{0}C) preform was cut into pieces, stacked, and vacuum hot pressed (30 MPa, 600 ^{0}C, 900 seconds) to make the composite. These researchers found that the tensile strength increases with increase in fiber volume fraction. They also found that the composite is capable of retaining most of its room temperature tensile strength at elevated temperature and pressures (73 MPa at 400 ^{0}C). Soni *et al.* [29] studied the room temperature and elevated temperature tensile strength of carbon fiber reinforced aluminum matrix composites made using slurry technique [29]. The results are reported in the next chapter. X-ray photo-emission spectra of the above fractured composite indicated the formation of Al_4C_3 at the interface [19, 29].

CHAPTER 4

Mechanical Property Measurements of Carbon-Aluminum Composites

4.1 Introduction

Mechanical properties of continuous fiber reinforced metal matrix composites primarily depend on their interfacial bonding. In particular, it is now universally accepted that brittle matrix composites having high toughness require strongly bonded interfaces for ductile reinforcements and weakly bonded interfaces for brittle (fiber) reinforcements. Ductile phases can be effectively toughened by bridging contributions from the deforming particles. On the other hand, debonding is required along the fiber/matrix interface at the crack-front for toughening by brittle fibers and whiskers, which is governed by the inherent bond strength of the interface. This debonding at the interface thus permits the fibers to remain intact in the immediate crack wake, and subsequent pull out of fibers contribute to the toughening [3].

Most of the tensile test data in the literature is based on rule of mixtures (ROM) and the strengths achieved were reported in terms of percentage of rule of mixtures (%ROM). Islam *et al.* [30] summarized the consolidation parameters and the mechanical properties of carbon-aluminum composites. Maximum tensile strength of 1014 MPa was obtained in

HM 3000/201 composite (fiber coated with TiB_2) hot pressed at 568 ^{0}C, 24 MPa for 25 mins. This value corresponds to 98% of rule of mixture values. Ohsaki *et al.* [14] reported the properties of carbon fiber reinforced aluminum composites made by ion-plating process followed by vacuum hot pressing. The tensile strength obtained was 40 kg/mm^2. Patankar *et al.* [31] obtained a tensile strength of 240 MPa for the carbon fiber reinforced Al-12% Si alloy composite fabricated by infiltrating the fibers pretreated with K_2ZrF_6 followed by hot pressing. Asanuma *et al.* [32] utilized plasma spraying technique followed by roll diffusion bonding to produce carbon-aluminum composites.

The control of interfacial reactions during fabrication and service is an important parameter to achieve optimum mechanical properties. The wettability of aluminum against carbon improves [33] above 1000 ^{0}C, however, in carbon fiber reinforced aluminum matrix composites, the interfacial reaction takes place at above 500 ^{0}C [28, 34] or even below it. Aluminum carbide crystals form at the surface of the fiber, not as a continuous layer, but as platelets perpendicular to the fiber axis. In contact with molten aluminum, Pitch-based and PAN-based carbon fibers act differently. Initially, the tensile strength of both types of fibers decreases rapidly and decreases gradually with time afterwards. In case of Pitch-based carbon fibers, the rate of degradation is less than that of PAN-based fibers. The number of Al_4C_3 crystals on Pitch-based fibers is less than that on the PAN-based carbon fibers. Several other investigators analyzed the degradation effect of carbon fibers by molten aluminum on the tensile strength of the composite. Upp *et al.* [35] found that the degradation was minimum with short exposure times at temperatures up to 560 ^{0}C. Blankenburgs [28] and Khan [36] reported the degradation at 500 ^{0}C, and Harrigan [37] reported the degradation at a temperatures of 485 ^{0}C. The large mismatch between the thermal expansion coefficients of carbon and aluminum is also believed to reduce the strength of the composite due to the generation of high local strains resulting in debonding at the interface [29].

4.1.1 Tensile Testing

Except Ramakrishnan [19], Baker [38], and Blankenburgs [28], all other investigators concentrated on carbon fiber reinforced aluminum matrix composites manufactured at higher temperatures through liquid metal infiltration technique. Ramakrishnan [19] and Soni *et al.* [29] concentrated on the composite manufactured by P/M route at lower temperatures. They used PAN-based carbon fiber reinforced aluminum matrix composite having 16% fiber volume fraction to study the room temperature and elevated temperature tensile strength. The composite was fabricated by making preforms with a slurry technique followed by vacuum hot pressing under optimum conditions (600 ^{0}C, 90 MPa, 15 min) [19]. The specimens were heated up to a temperature ranging from 100 ^{0}C to 600 ^{0}C for 24 hours. Then the tensile strength was evaluated at room temperature. The elevated temperature tensile strength of the composite was evaluated at temperatures ranging from 100 ^{0}C to 400 ^{0}C.

Soni *et al.* [29] found that the room temperature tensile strength of the composite could be enhanced from 88.47 MPa to 177.57 MPa. Ramakrishnan *et al.* [19] also found out from fractography that there is adequate bonding between the matrix and fiber and ESCA studies indicated the formation of Al_4C_3 at the interface.

Soni *et al.* [29] performed the tensile testing at room temperature on a number of specimens exposed to different temperatures ranging from 100 to 600 ^{0}C. These test data shows that the tensile strength almost remains constant till 400 ^{0}C and decreases later on (Figure 4.1). Fractography of the composites heated up to 500 ^{0}C and 600 ^{0}C shows the increase in growth of Al_4C_3 with increase in exposure temperature above 400 ^{0}C. Soni *et al.* [29] believe that above 400 ^{0}C, the increase in growth may be due to increase in diffusion of aluminum in carbon than carbon in aluminum and below 400 ^{0}C, the Al_2O_3 layer present may prevent the diffusion and thus the growth of Al_4C_3 is less. They also believe that the formation of more brittle Al_4C_3 reduces the tensile strength of the composite above 400

^{0}C by reducing the effective diameter of the fiber. Additionally, the non-uniform growth of Al_4C_3 into the fiber surface generates notches and reduces the strength of the fiber due to stress concentration.

The tensile test results of above mentioned researchers showed that the elevated temperature tensile strength decreased with increasing temperature. The strength is 73 MPa at 400 ^{0}C which is comparable to matrix tensile strength at room temperature (Figure 4.2). No growth of carbide layer had been found at the interface for the samples tested at 200 ^{0}C and 400 ^{0}C. However, as the load was applied for a short duration, the possibility of growth of carbide layer due to strain induced diffusion was neglected. Soni *et al.* [29] believe that the softening of the matrix at higher temperatures, large mismatch in coefficient of linear thermal expansions of fiber and matrix which results in debonding at the interface, and more fiber pull out are the reasons for the decrease in tensile strength. Soni *et al.* [29] also believe that the sharp decrease in strength even at low temperatures is due to the oxidation of fibers. The fibers get oxidized since the cracks develop in the carbide layer expose the fiber to atmospheric oxygen.

Baker and Bonfield [38] studied the fracture of aluminum coated carbon fibers. For the experiments, the above researchers used three types of carbon fibers-Courtaulds HM-S, HM-U and HT-S (HM-high modulus, HT-high tensile strength, S-a proprietary surface treatment, U-no surface treatment). These fibers were coated with aluminum (99.999% pure) by vapor deposition in a vacuum of less than 10^{-5} Torr. Some fibers were tensile tested at room temperature and the rest were annealed at different temperatures for different times and tensile tested at room temperature. The tensile tested specimens were examined under electron microscope and x-ray diffraction studies were carried out before and after removing the aluminum coating on the fiber.

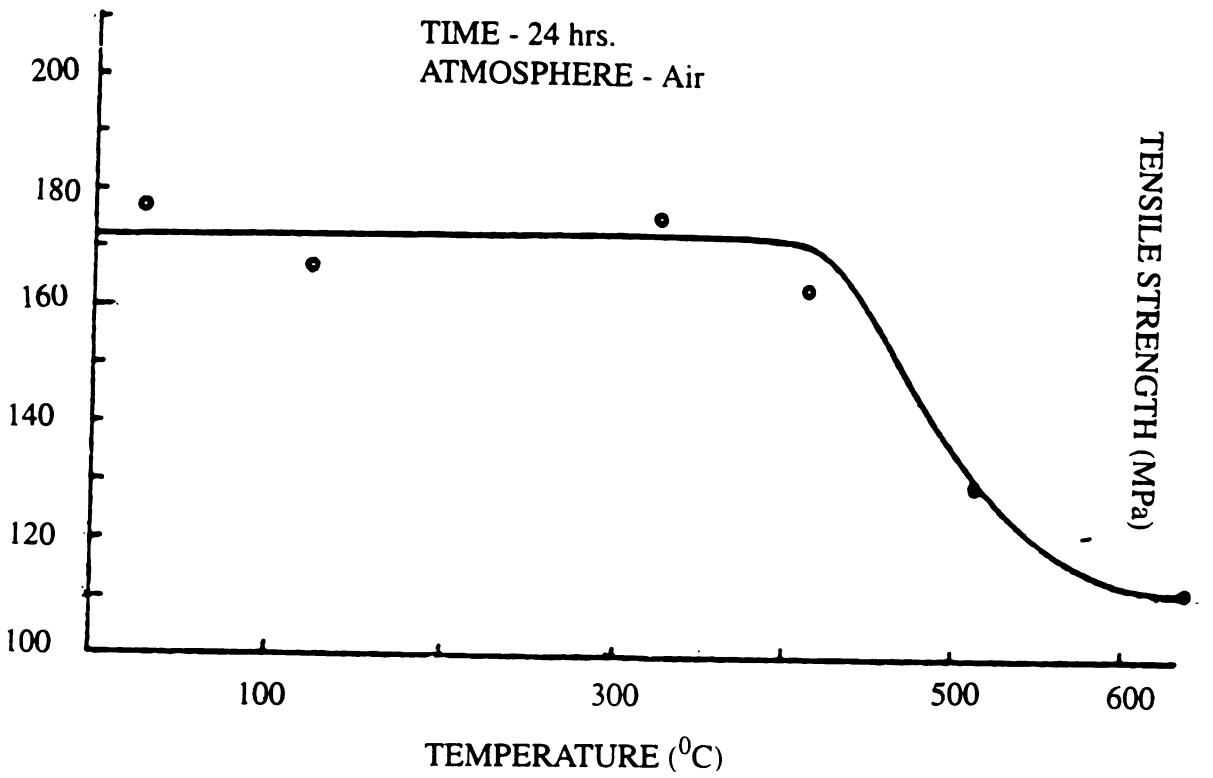

Figure 4.1: Variation of room temperature tensile strength of the composite with exposure temperature [29].

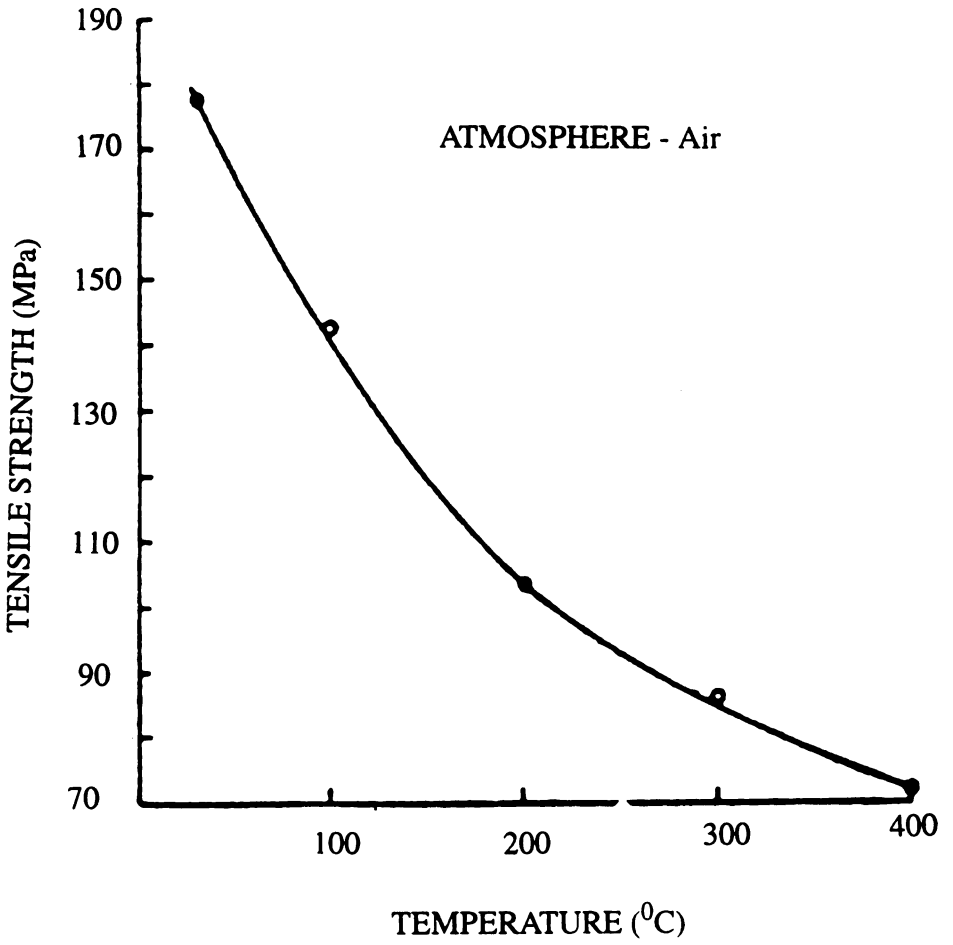

Figure 4.2: Variation of elevated temperature tensile strength of the composite with temperature [29].

Effect of Annealing Temperature on Aluminum Coated Carbon Fibers

Baker *et al.* [38] observed from the tensile test data that the aluminum coating did not significantly affect the room temperature tensile strength (UTS) and Young's modulus (E) of the coated fiber when compared with that of bare fiber. Additionally, the above researchers did not observe any change in the values of 'E' and 'UTS' of uncoated carbon fibers annealed at 650 ^{0}C for 100 hrs. and 850 ^{0}C for 100 hrs. For HT-S fibers coated with 180nm of aluminum, the room temperature UTS reduced after annealed at temperatures > 475 ^{0}C. Baker and Bonfield also noticed that the degradation in UTS increased with an increase in annealing temperature up to 650 ^{0}C and a minimum UTS value of approximately 30% of the original strength value was produced. Similar behavior was observed for HM-S and HM-U fibers with a reduction in UTS after annealing at > 550 ^{0}C and a minimum UTS value at 45% of the original strength (Figure 4.3). In contrast, Baker *et al.* [38] did not notice significant change in the Young's moduli of the three types of fibers.

Effect of Aluminum Coating Thickness on UTS & E of the Composite

Baker and Bonfield [38] also studied the effect of aluminum coating thickness on the room temperature UTS of three types of fibers (HM-S, HM-U and HT-S) annealed at 600 ^{0}C for 100 hrs. The studies showed that UTS decreased with an increase in the original aluminum thickness from 46 to 540nm (Figure 4.4).

Structural Observations

Baker *et al.* [38] found that x-ray techniques were not sufficiently sensitive to identify aluminum or aluminum carbide lines for the fibers with coating thickness < 90nm, but for these specimens as well as for all other coating thicknesses, the electron diffraction patterns indicated the formation of Al_4C_3 (Figure 4.5) after suitable anneals.

Baker *et al.* [38] concluded from the structural observations that the degradation in UTS

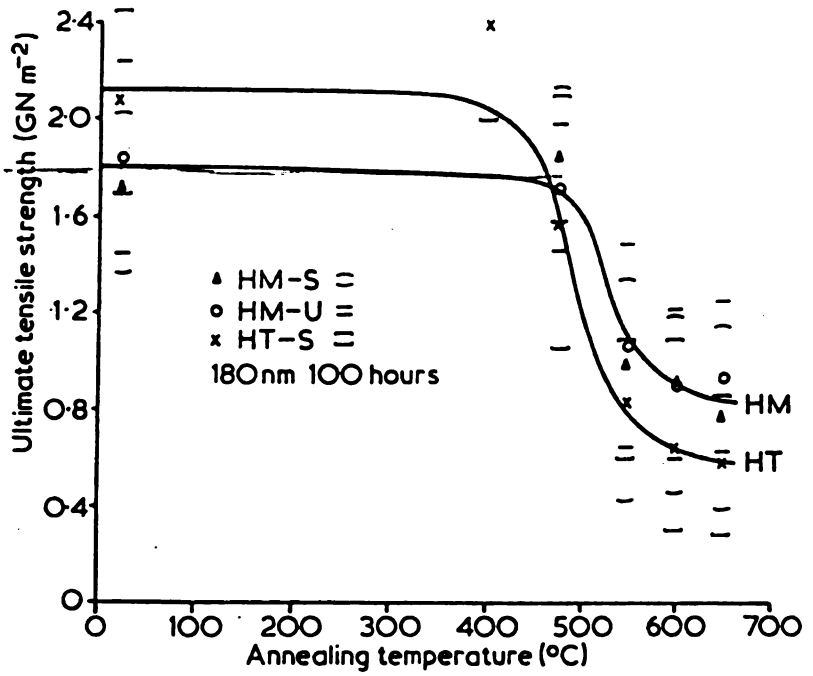

Figure 4.3: Effect of annealing temperature on the room temperature UTS of aluminum coated (180nm) carbon fiber composite [38].

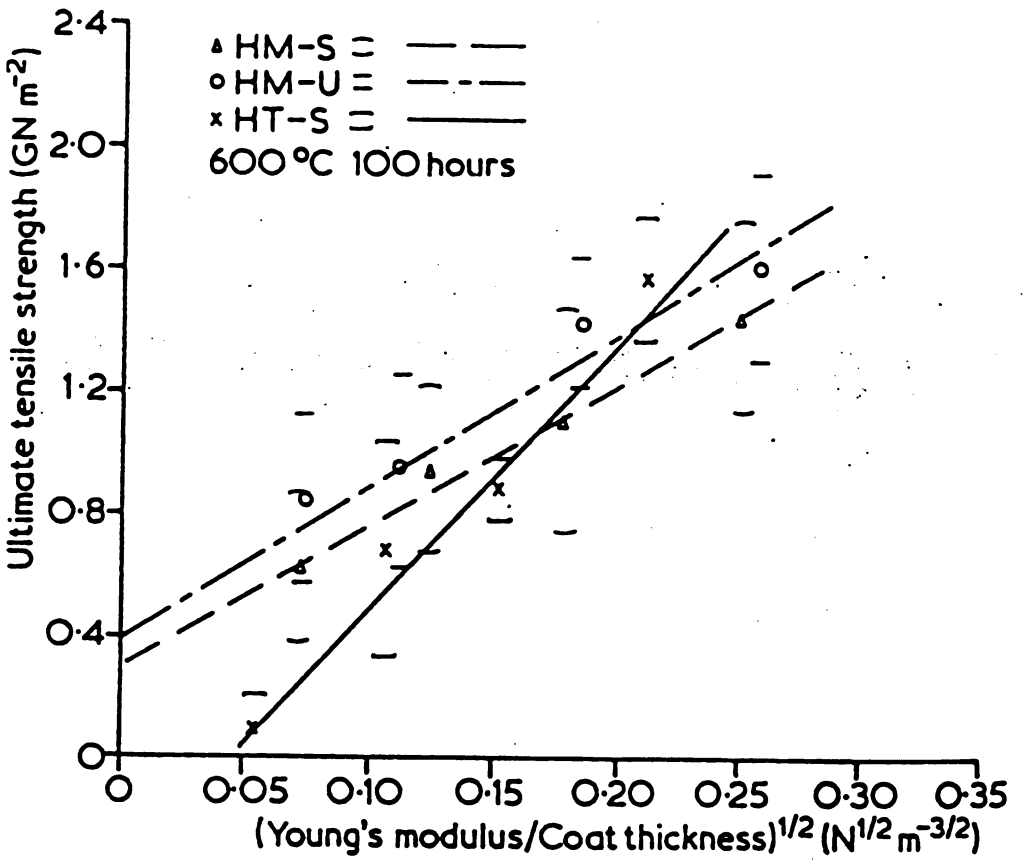

Figure 4.4: Effect of aluminum coating thickness on the room temperature UTS of carbon fiber composite, after annealing at 600 ^{0}C for 100 hrs [38].

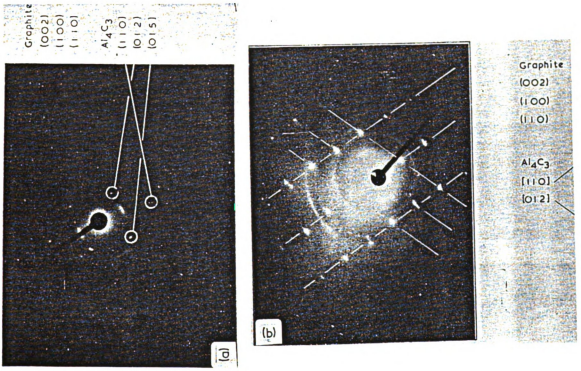

(a) (b)

Figure 4.5: Electron diffraction patterns of a) HM-S fiber coated with 46nm of Al, annealed at 600 ^{0}C for 24 hrs, b) HM-U fiber, coated with 180nm of Al, annealed at 650 ^{0}C for 24hrs with carbon diffraction rings and Al_4C_3 diffraction spots [38].

of the carbon fibers was associated with the presence of Al_4C_3 in the surface coating due to annealing. They also suggested that fracture propagated from the cracks in the reacted surface coatings. With a complete aluminum carbide coating, the maximum possible crack length normal to the fiber axis is equal to the thickness of the aluminum carbide, which in turn is related to the thickness of the original aluminum coating. Baker and Bonfield claim that this model is consistent with the observation that the UTS, after annealing for a given time and temperature, decreases as the aluminum coating thickness increases.

CHAPTER 5

Physical Properties of Graphite Reinforced Aluminum Composites

5.1 Thermal Behavior

The thermal behavior of metal matrix composites has not been extensively studied when compared with mechanical behavior since the mechanical properties of the composite have to be shown to be significantly better than that of the matrix material. Then the thermal behavior will be studied extensively. Metal matrix composites have a wide range of applications in high temperature environments and thus the mechanical behavior of MMCs in high temperatures has been studied extensively. The distribution of temperature has to be determined in order to study the mechanical behavior. The temperature is obtained by solving the heat conduction equation in a composite where the specific heat and thermal conductivity must be known. Then the stresses due to temperature are solved by using the thermoelasticity equations for which the coefficient of thermal expansion 'α' has to be found. Thus, the analysis of mechanical behavior of metal matrix composites requires the analysis of thermal behavior as a prerequisite step [1].

5.1.1 Coefficient of Thermal Expansion (CTE)

The behavior of thermal expansion of MMCs has been the most extensively studied characteristic of all thermal behavior characteristics, since it has a significant effect on the mechanical behavior of the composites in high temperature applications such as engine components and space structures. In these applications, the dimensional stability and changes in mechanical properties of the composite over a long period of time are the most important design considerations. The CTE of the composite plays an important role in the dimensional stability and the mismatch in CTEs between the matrix and fibers has dominant effect on mechanical properties [1].

Greenfield [39] measured the properties of the aluminum matrix composite with chopped carbon fibers as reinforcements. Aluminum was chosen for its low density. The purpose of his experiments was to determine the thermal expansion and conductivity of the composites. Therefore, the presence of impurities was minimized and no additives were used to help improve the mixing process or enhance the quality of the interface.

Aluminum powders with average diameter approximately same as the graphite filaments were chosen to attain homogeneous mixtures. The mixture of short fibers and aluminum powder was prepared by tumbling in a rotating cylindrical container and then vacuum hot pressed into one or two inch diameter cylindrical billets. Different hot pressing conditions were utilized and the resulting specimens were evaluated.

Greenfield's studies showed that the CTE was non-linear between 20 ^{0}C and 300 ^{0}C and lower CTEs resulted for aluminum-graphite composites compacted at higher pressures and temperatures (Figure 5.1). The measured values of CTE are listed in Table 5.1. During hot pressing, the alignment of the fibers becomes transverse to the direction of compression. From the graph it is clear that for fiber volume fractions above 0.3, the ratio of CTE_c[1]/CTE_m[2] increases to a value of 1.2. This ratio decreases for the directions per-

[1] coefficient of thermal expansion of the composite.
[2] coefficient of thermal expansion of the matrix.

Table 5.1: CTE (μm/mK) for C/Al composite [39])

Metal	20 - 100 ^{0}C	20 - 200 ^{0}C	20 - 300 ^{0}C
Al	21.4	24.2	28.8

pendicular to compression axis. The properties are radially symmetric since the billet is symmetric.

Hale [40] presented a general review on coefficient of thermal expansion in composites. According to his review there will be significant differences in the properties because of the difference in properties of the fibers and matrix such as elastic behavior, degree of anisotropy, aspect ratio, and volume fraction of the fiber. Takao and Taya [41], and Withers [42] utilized Eshelby's equivalent inclusion technique [43] to determine the elastic and thermo-elastic behaviors of short fiber composites. These models predict that there will be a decrease in thermal expansion along the direction of fiber alignment and an increase in transverse direction because of small to negative thermal expansion of graphite. Recent work by Withers *et al.* [42] has provided analytical techniques to predict the properties of non-aligned fiber distributions, if the fiber distribution is known. Figure 5.2 is a result of this analysis when all graphite fibers are aligned in an aluminum matrix and when all fibers oriented randomly in a plane with an aspect ratio of 20. In an analysis of experimental measurements, Greenfield [39] has taken values for elastic constants and CTE for graphite from Takao and Taya's [41] experiments for an indication of expected trends, although the physical constants of the fiber employed in this experiment are somewhat different. Greenfield [39] utilized the relationships derived from those obtained by Whithers and showed that the aligned fibers have a greater effect on the thermal expansion than planar arrays. However, a planar array has significant influence on the anisotropic thermal expansion properties. The experimental data shows that the redistribution of fibers resulting from hot pressing results in lower values of CTE than predicted for planar distribution of fibers. However,

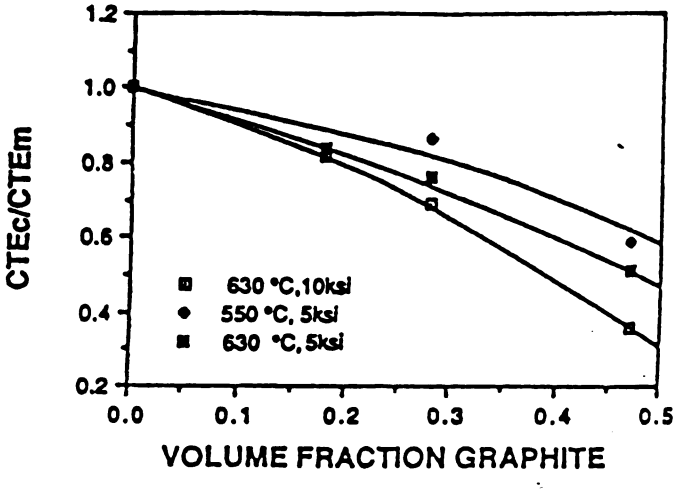

Figure 5.1: Effect of hot pressing pressure and temperature on coefficient of thermal expansion of the composite [39].

CTE values for the graphite fibers derived from mesophase Pitch were more negative in the longitudinal direction than the values used in the analysis by Greenfield [39], and more extreme properties are expected to result from an analysis for oriented fiber distributions with a high-modulus Pitch-based graphite.

5.2 Corrosion Behavior of Aluminum-Graphite Composite

Two types of corrosion at room temperature can take place in continuous fiber reinforced composites-galvanic corrosion that takes place between the fibers and the matrix and pitting corrosion with in the matrix itself. These two corrosion reactions occur when a metal matrix composite has been exposed to aqueous solutions such as salt water. Galvanic corrosion commonly occurs in metal matrix composites because of the mismatch in electrochemical potentials between the fibers and matrix, which provides a local cell if exposed to an aqueous solution [1]. Trzaskoma, Aylor *et al.* [44], and Paciej *et al.* [45] studied the galvanic corrosion in a number of metal matrix composite systems. Corrosion behavior in graphite fiber -aluminum composites was reported by Aylor and Kain [44]. The composite was exposed to different sea water conditions. Aylor *et al.* found that graphite fiber-aluminum composites are less resistant to corrosion. Initially pitting on the surface is the dominant mode and later corrosion penetrate the matrix and fibers through the aluminum foil. These results were corroborated by the studies carried out by Aylor *et al.* [44], and Vassilaros *et al.* Galvanic corrosion will be active as soon as the pitting corrosion breaks the surface of aluminum foil, leading to the depletion of aluminum (Figure 5.3) [1].

Kendall [46] reported the corrosion behavior in graphite-aluminum composites exposed to distilled water and 3.5% NaCl solution at different temperatures for 1000 hrs. NaCl increases the rate of corrosion (Table 5.2). The rate of corrosion in the composite was

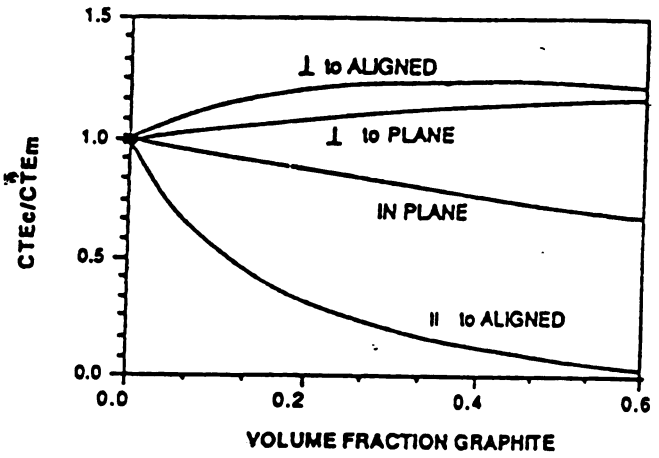

Figure 5.2: Predicted relation between thermal expansion and CTE_c/CTE_m using Withers' method [39].

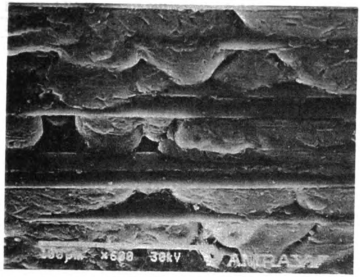

Figure 5.3: Corrosion behavior in graphite-aluminum composite exposed to sea water splash/spray test for 30 days [44].

compared with that of 356 aluminum which is used as a standard and is the matrix material in the composite. Kendall [46] found that the composite corrodes one to four times than 356 aluminum depending on the exposure conditions. Kendall [46] believes that the increase in the rate of corrosion in graphite-aluminum composite is due to the galvanic coupling effect between the graphite fibers and aluminum matrix [46].

Table 5.2: Corrosion behavior in graphite-aluminum composite exposed to distilled water and NaCl [46].

-	356 Aluminum		356 aluminum-25 v/o Thornel-50	
Environment	(23 ^{0}C)	(50 ^{0}C)	(23 ^{0}C)	(50 ^{0}C)
Distilled Water	Nil	Nil	1.2	1.2
3.5% NaCl solution	1.1	4.9	4.7	9.8

CHAPTER 6

Interfaces in Carbon Fiber Reinforced Aluminum Matrix Composites

The mechanical and physical properties such as high specific modulus, specific strength, thermal and electrical conductivity, and the dimensional stability make graphite fiber reinforced aluminum matrix composites attractive for use in advanced engineering applications. Graphite fiber reinforced aluminum matrix composites fabricated by the liquid infiltration do not generally exhibit ROM tensile strengths. There are a number of problems that must be solved before these materials can be commercially produced. These include limiting the interfacial reactions between fiber and matrix, control of fiber/matrix bond strength, understanding the wettability between the fiber surface and the molten alloy, and controlling the distribution of fibers in the composite.

Yoon *et al.* [47], Li *et al.* [48], and Zhang *et al.* [49] studied the interface reactions of different types of carbon fibers, and the effect of the reactions on the fiber strength and mechanical properties of C/Al composites. Yoon *et al.* [47] concentrated on the interface reactions of different types of carbon fibers, the effect of reactions on fiber strength, and impacts of certain inter-metallic compounds on the mechanical properties of C/Al composites fabricated by diffusion bonding. PAN-based and Pitch-based fibers were heat treated to evaluate the effect of interfacial reactions on the strength and reactivity of the fiber. In fact,

the heat treatments were carried out under various conditions on a set of a mono-filament evaporated composite that was produced by coating an aluminum layer of $1.2\mu m$ thick on the surface of carbon fibers using ion-plating method. The heat treated specimens were treated with 5N NaOH solution to dissolve aluminum and then the specimen surface was observed under SEM. Tensile testing was also carried out to study the deterioration of fiber strength due to interfacial reactions. In addition to the above tests, the heat treated specimens were pulverized and immersed in alcohol and fragments of specimens were poured on the carbon reinforced micromesh strainer to identify the interface reaction products using a TEM.

Preforms (sheets) of PAN-based carbon fiber reinforced aluminum were made by plasma spraying, followed by hot pressing within the solid phase temperature range of aluminum in vacuum (5×10^{-4} Torr). Tensile testing was carried out on the specimens with 20% fiber volume fraction, consolidation pressure of 78.5 MPa applied for 15 min. at temperatures of 500 ^{0}C, 550 ^{0}C, 600 ^{0}C, and 640 ^{0}C respectively and then studied the interface between carbon fibers and reaction products, as well as the bonding at the interface between reaction products and aluminum matrix using a TEM. Each specimen was heat treated for 10 hrs at 640 ^{0}C and thinned by mechanical polishing and ion polishing to 100-200 $\mathring{A}$.

The strength of the fibers decreased with increasing treatment temperature (Figure 6.1). For PAN-based fibers, a large decrease in fiber strength above 550 ^{0}C indicates the greater effect of treatment temperature rather than the treatment time on fiber strength (Figure 6.1). In case of Pitch-based fiber, the decrease in strength was observed at or above 600 ^{0}C (Figure 6.1). Degradation of the fiber strength was greater for PAN-based fibers than that of Pitch-based fibers. The SEM observations indicated that one of two different specimens of each type of carbon fiber (PAN & Pitch) heat treated for 4 hrs. at 640 ^{0}C, and each specimen whether heat treated or not, was dissolved (Al coating) in the NaOH solution. The researchers also noticed that there was no strength decrease during the coating process for the fibers that were not heat treated.

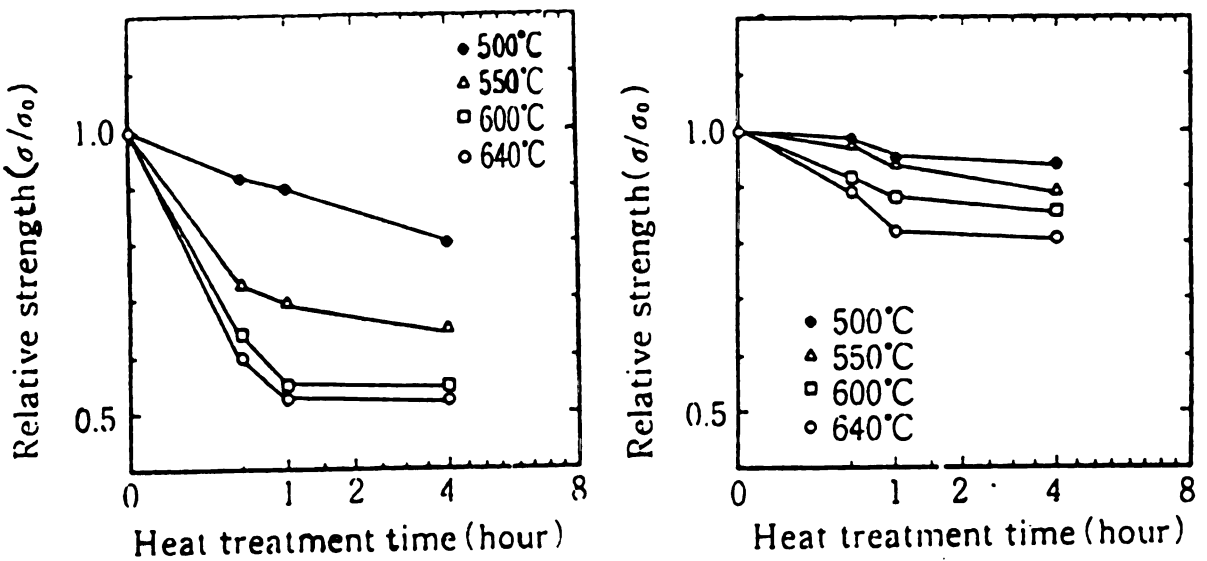

Figure 6.1: Effect of heat treatment time on the relative strength of a) PAN-based fibers, b) Pitch-based fibers [47].

Coarseness and irregularities were observed on the surfaces of PAN-based carbon fibers heat treated for 4 hrs. at 640 ^{0}C and voids were noticed on the surface of Pitch-based carbon fibers. The notches on the surface of PAN-based carbon fibers were created by strong chemical reaction, or the voids on the surface of the Pitch-based carbon fibers, made the Yoon *et al.* [47] to conclude that the fiber strength decreased as a result of stress concentration due to locally reduced diameters on the fiber.

The electron diffraction patterns of Al and Al_4C_3 with (110), (012) planes were identified in the interface of aluminum coated Pitch-based fibers annealed for 4 hrs. at 640 ^{0}C. In the case of PAN-based carbon fibers, diffraction patterns of Al_4C_3 were observed only at or above 550 ^{0}C and such patterns were observed at or above 600 ^{0}C for Pitch-based carbon fibers. This fact proves that the interfacial reactivity is higher in the PAN-based than in the Pitch-based fibers. This difference in the reactivities might be due to the orientation of the plane molecules composing these carbon fibers and their heterogeneous surface structures [47]. Hagiwara *et al.* reported that the graphite structure containing the basal plane represented by the relatively inactive (001) plane and the prism plane represented by the active (100) and (110) planes, tend to allow the surface oxide to be formed. The specific surface energies on the basal plane and that on the prism plane are 0.14 Jm^{-2} and 4.8 Jm^{-2} respectively so that the interfacial reactivity of any kind of carbon fibers must be variable with the area ratio of basal plane and prism plane on the fiber surface [47].

Figure 6.2 shows the effect of consolidation temperature on the tensile strength of C/Al composite. The fractographs after tensile tests of the composites hot pressed at 500 ^{0}C showed the fiber pull-outs and poor penetration of aluminum into the fibers. In contrast, at 640 ^{0}C, aluminum fully penetrated into the fibers, and the diffusion within the embedded aluminum was apparent. The researchers (Yoon *et al.* [47]) concluded from the above observations that the interfacial bonding was insufficient and the stress was not fully transmitted through the interface. They also concluded that better interfacial bonding could be achieved at a higher consolidation temperatures, but a decrease in the composite strength

due to more interfacial reaction should be taken into account.

The bright-field image and diffraction pattern of the composite consolidated at 640 ^{0}C showed that Al_4C_3 was formed at the interface between carbon and aluminum. Khan [36] mentioned that Al_4C_3 forms at the interface as a result of the diffusion of carbon atoms into aluminum since the former is smaller than the latter considering the atomic sizes. The lattice images of the interface of C/Al composite illustrates that the random lattice structure of carbon is bonded non-directionally to Al_4C_3 (003), whereas the bond between interface of Al_4C_3 and Al has the same directional orientation as Al_4C_3 (003) and Al (111). From the bond energies point of view, the latter interface should be more stable than the former.

Microstructure of the Interface and Inter-Fiber Regions in P-55 Reinforced Al Alloys

The interface in continuously reinforced composites plays a major role by transferring the load from fiber to fiber through the matrix. It also toughens the matrix by deflecting cracks at the fiber-metal matrix through an interface fuse mechanism [50, 36]. In composites, interfaces are required for full transmission of traction to assure that reinforcing phases such as fibers are fully load bearing to enhance the stiffness of the composite and to promote redundant deformations in a ductile matrix that in turn increases the overall deformation resistance in it. Stress concentrations develop across the interface due to the difference in the deformation resistance between the fibers and matrix. These stress concentrations initiate cavitaion and incipient fracture phenomenon that becomes unstable and results in the premature termination of service by overall fracture. When such fracture is inevitable, it is desirable that as much dissipative work be associated with it as possible to result in tough and energy absorbing structures. In design, whether the toughness associates with the propagation of a single crack, and carries the conventional implications of fracture toughness, or is more diffuse and widespread over the entire structure is important. The instability in all of these terminal phenomena can be delayed by the systematic decoupling of the reinforcing elements that on the verge of critically stressed. To the extent that this

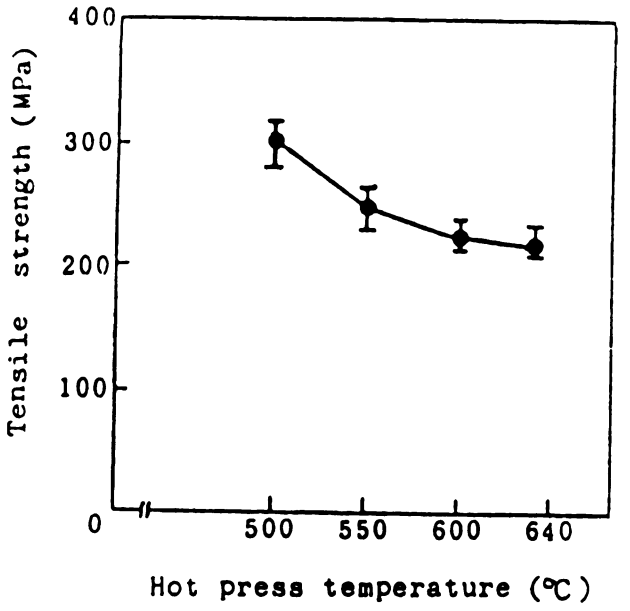

Figure 6.2: Effect of consolidation temperature on tensile strength of carbon fiber/Aluminum composite [47].

can be successfully accomplished, subcritical damage can be spread over large volume elements, to result in a quasi-plastic response of the entire composite on the large scale. The control of terminal properties of interfaces and have them act as mechanical fuses at appropriate predetermined levels of critical tractions can result in desired systematic decoupling of the reinforcing fibers or other heterogeneties.This is in principle possible but requires a high degree of understanding of both the micromechanics of interfaces and the factors that affect their cohesive strength and fracture toughness [50, 36].

In metal matrix composites, the chemical reactions between the fibers and the metal matrix forming reaction products can initiate cracks in the fibers due to the positive material misfit along the fiber-matrix interface. To protect the fiber damage, suitable non-reactive coatings are applied. These coatings can provide the opportunity for tailoring the strength and toughness of the interfaces with fiber to achieve the mechanical fuse action described above to isolate damage. The damage may have originated among the neighboring fibers and is transmitted across the matrix to the fiber, or it may have been generated by the reaction products forming on the outer interface between the matrix and the protective coating [50, 36].

Li *et al.* [48] studied the microstructure of the interface and inter-fiber regions in P-55 (carbon) reinforced aluminum alloys fabricated by pressure infiltration. AMOCO's P-55 fiber (tensile strength: 184 GPa, tensile modulus: 399.5 GPa) in the sized condition was used with A1100, A357 (0.45-0.6% Mg, 6.5-7.5% Si (nominal)), Ti doped Al, and Al-4.5% Cu as matrix materials. The fiber preform was manufactured by filament winding and cryopacking technique. The composite was cast by pressure infiltration of molten metal into pre-evacuated preforms and the volume fraction of the fiber was maintained at 0.55. All the important processing parameters, e.g. melt temperature, fiber (preform) temperature, infiltration pressure differential, and cooling rate were optimized and independently varied and controlled. The interfaces were slightly inclined from orthogonality because of the variability in fiber alignment during preform fabrication and infiltration processing.

Microstructure of Interface in P-55 Graphite Fiber Reinforced A1100 Castings

TEM results of Li *et al.* [48] indicated that the size and quantity of Al_4C_3 varies with cooling rate (Figure 6.3). Faster the cooling rate (23 k/min.), fewer the Al_4C_3 interfacial reaction products. Large amounts of Al_4C_3 was observed for the specimen with a cooling rate of 6.5 k/min. It was found that the specimen with more rapid cooling rate had better tensile strength.

Lower tensile strengths were noticed by Zhang *et al.* [48] for the specimen with more excessive carbide formation than specimens processed with a shorter solidification time. The results also indicate that a small amount of Al_4C_3 does not lower the mechanical properties. According to Cornie *et al.* [51], Ochiai [52], and Shorshorov [53], a critical amount of Al_4C_3 formation is needed in order to lower the tensile strength of fiber.

In the case of more rapidly cooled specimen (23 k/min.), Al_4C_3 needles grow discontinuously on the surface of the graphite fiber leaving the remaining graphite/aluminum interface free of reaction products. It has been found from the microstructures that Al_4C_3 does not form epitaxially along the graphite (001) planes. No preferred orientation of carbide reaction was observed with respect to graphite fibers. The measured lattice fringe spacing (8.3 Å) confirmed the formation of Al_4C_3 that corresponds to (003) plane spacing of Al_4C_3. Selected area diffraction patterns show the hexagonal [030] and [200] directions respectively (Figure 6.4). The lattice fringes with 3.35 Åspacing corresponds to the basal (002) planes of graphite.

Microstructure of Interface in P-55 Graphite Fiber Reinforced Al-0.34% Ti Castings

Being a peritectic system, Al-Ti requires higher infiltrating metal temperatures than unalloyed Al or eutectic systems. Therefore, the melt temperature and solidification have a significant influence on the interfacial reactions [48]. The studies made by Zhang *et al.* [49] revealed that the fibers extracted from castings infiltrated with a T_m of 708 ^{0}C were

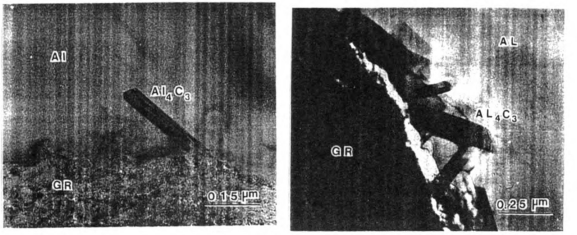

(a) (b)

Figure 6.3: a) Microstructure of interface in P-55 reinforced A1100 cooled at 23 C/min. [48], b) Microstructure of interface in P-55 reinforced A1100 cooled at 6.5 C/min. [48].

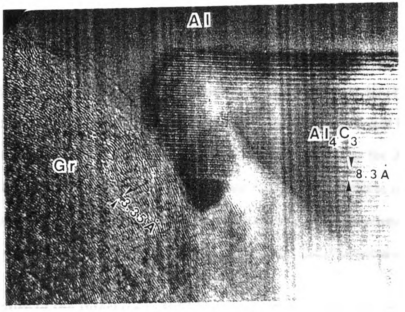

Figure 6.4: HRTEM micrograph showing the growth of Al_4C_3 from the fiber surface into A1100 matrix. a) [030] direction; b) [200] direction [48].

not degraded. The tensile and flexural strength were also optimized at this infiltration temperature. Reduction in composite strength and leached fiber strength were observed for the castings infiltrated at 748 ^{0}C. For the specimens cast at 708 ^{0}C, the grain size is about 10 times smaller than that of the unalloyed aluminum matrix cast under similar conditions (Figure 6.5). Increase in T_m to 708 ^{0}C, resulted in larger grain size ($\approx 1\mu$m). The studies made by Li *et al.* [48] also revealed that the amount of carbide formation increased with increase in metal infiltration temperature from 708 ^{0}C to 748 ^{0}C. Larger amounts of Al_4C_3 was observed in P55/A1100 castings than the Ti doped composite manufactured under similar conditions/processing parameters.

Li *et al.* [48] occasionally observed the intermetallic compound Al_3Ti in the inter-fiber regions. The frequency of appearance of Al_3Ti increased with increasing T_m. The electron diffraction pattern of Al_3Ti shows the orientation relationship: (211) Al/ (100) Al_3Ti, which matches the data in the literature [27]. Because of many orientation and favorable surface energy relationships, Al_3Ti acts as an effective nucleation catalyst for Al [27, 28]. The above data and observations show that Ti doping has beneficial effects on the composite. The formation of Al_3Ti refines the grain size of the matrix and small amounts of Ti reduces the activity of carbon in solution in Al that in turn reduces the formation of Al_4C_3.

Microstructure of the Interface in P-55 Graphite Fiber Reinforced A357 Castings

Li *et al.* [48] and Zhang *et al.* [49] observed regions free of Si precipitates in the TEM studies (Figure 6.6). They also observed needle shaped precipitates of Mg_2Si, a Si bridge (Figure 6.7) between two graphite fibers with stacking faults, and a few Al_4C_3 reaction products (Figure 6.8). Si addition to the matrix reduces the activity of C in Al and thus minimizes the formation of Al_4C_3. Si also reduces the melting point of Al alloys and thus allows the use of lower preform temperature and lower T_m. From the mechanical property measurements, Zhang *et al.* [49] noticed fiber degradation and poor composite properties. The above mentioned researchers related these effects to the location of Si and the bridging

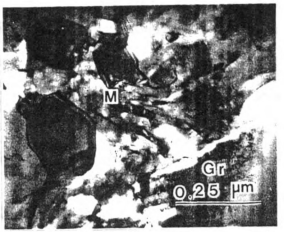

Figure 6.5: Microstructure of Al-0.34% Ti, reinforced with P-55 fiber at a T_m (molten metal temperature) of 708 ^{0}C [48].

between fibers (Figure 6.7). Zhang *et al.* [49]and He *et al.* [54] postulate that the Si bridges are responsible for the embrittlement and fiber degradation.

Microstructure of Interface in P-55 Graphite Reinforced Al-4.5% Cu Castings

Microstructure analysis by Li *et al.* [48] revealed that this composite and Al-Cu alloys had similar structures in the interfacial regions. Overaged penny shaped platelets of Al_2Cu, and large amounts of Al_2Cu phases precipitated during solidification were found in the microstructure.

Zhang *et al.* [49] studied the effect of processing parameters on mechanical properties of pressure infiltrated composite castings. This research group correlated the interface of specific processing/microstructure relationships on the flexural and tensile strength of cast composites. For continuous fiber reinforced composites, flexural strength measurements help evaluate the composites since they also probe interfacial shear properties.

The mechanical testing by Zhang *et al.* [49] on P-55/Al-0.34% Ti composite, showed that flexural and tensile strengths decreased with increasing infiltration temperature T_m. Flexural strength was maximum at 708 ^0C and this was not observed in the tensile test data (Figure 6.10). The fracture surface of this composite clearly shows the fiber pull-out and hence displays the effects of mechanical fuse mechanism [50]. The fractography of the composite infiltrated at 748 ^0C indicates a brittle failure (Figure 6.9). The above results show the fiber degradation and high interface bond strength resulting in poor axial properties.

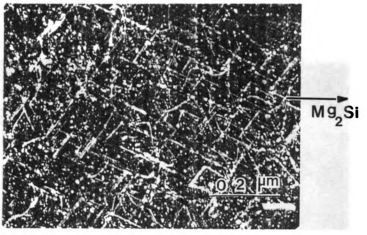

Figure 6.6: Microstructure of P-55/A357 showing precipitates of Mg_2Si from solid solution [48].

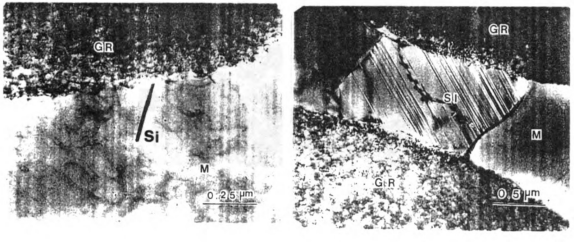

(a) (b)

Figure 6.7: Large Si second phase as bridge between fibers in the inter-fiber region of P-55/A357 casting fabricated at a) 665 ^{0}C, b) 525 ^{0}C [48].

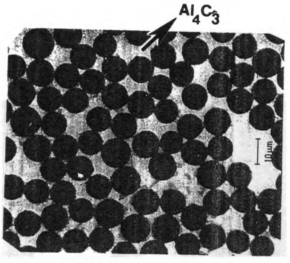

Figure 6.8: Micrograph showing the rare occurrence of Al_4C_3 in the interface region of P-55/A357 casting [48].

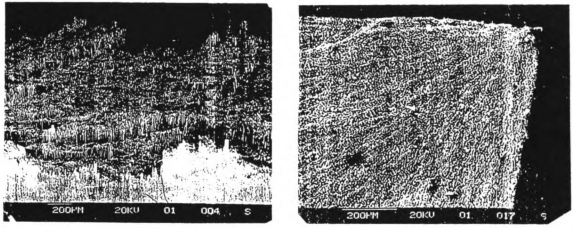

(a) (b)

Figure 6.9: Fractographs showing the fiber pull out and brittle failure in P-55/Al-0.34Ti composites infiltrated at a) 708 ^{0}C, b) 748 ^{0}C [49].

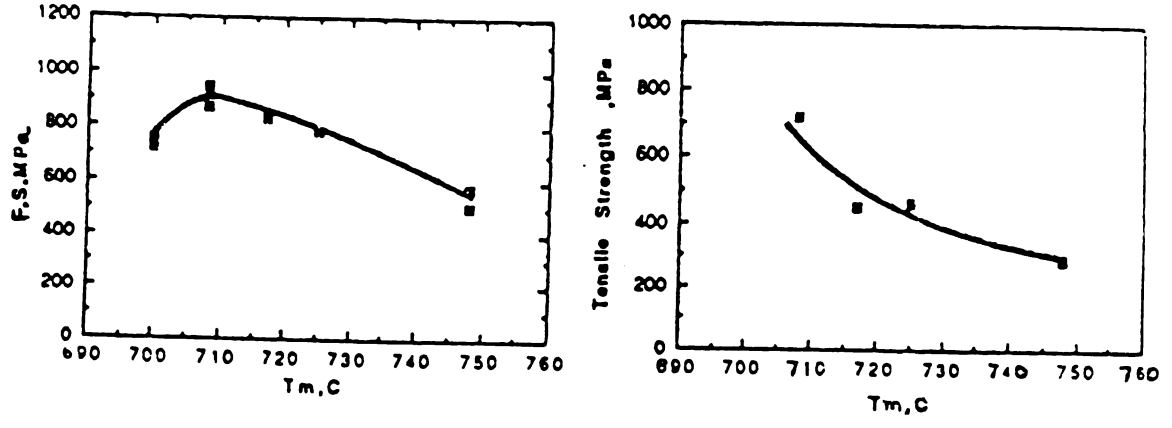

(a) (b)

Figure 6.10: a) Flexural strength vs. molten metal temperature (T_m) of P-55/Al-0.34Ti castings, b) Tensile strength vs. molten metal temperature (T_m) of P-55/Al-0.34Ti castings [49].

CHAPTER 7

New Fabrication Method

Fabricating continuous fiber reinforced metal matrix materials has always been a problem for material producers. The liquid infiltration technique would have been the first choice if the fiber was wetted by the matrix material because of its simplicity and continuity. Suitable fiber coatings or alloy additions can be applied to improve the wettability but the interfacial reaction is hard to control due to over-exposure to molten metal and high processing temperatures. Uneven fiber distribution is another problem in liquid infiltration technique. Other processing techniques such as electroplating, spraying, chemical vapor deposition (CVD), and physical vapor deposition (PVD) can be used to get high quality composites, but they are slow and expensive. A new processing technique based on P/M route to make CFRMMCs will be described in this chapter.

7.1 Original Process

The new fabrication technique is the modification of a continuous fiber reinforced polymer matrix composites process developed by the composite materials and structures center at Michigan State University [55].

In the original process, carbon fiber tows are made to pass through a series of chambers to produce a prepreg tape of a polymer matrix composite (Figure 7.1 and Figure 7.2).

A motor drives the fiber tows to pass above a speaker and the sound waves coming off from the speaker spread the fibers apart as the fibers pass through a series of stainless steel rollers. (Figure 7.3, Figure 7.4, and Figure 7.5). The spreaded fibers then enter an optional pretreatment chamber to modify the fiber surface or to apply a thin coating of binder material to improve adhesion between matrix and fibers. Then the fibers are made to pass through an impregnation chamber (aerosolizer), where small polyamide particles (10μm diameter) are suspended in air with the help of a rubber membrane placed on top of a speaker. The powder particles get attached to the fiber surface due to the electrostatic forces generated from the static charges held by the fine particles. Then the coated fibers are made to pass through an oven for 15 seconds and get heated to 165 ^{0}C-170 ^{0}C for sintering to occur to form globules of polymer. The fibers are then wound on to a take up drum. The prepreg tape is then cut into pieces of desired length, stacked-up, and vacuum hot pressed.

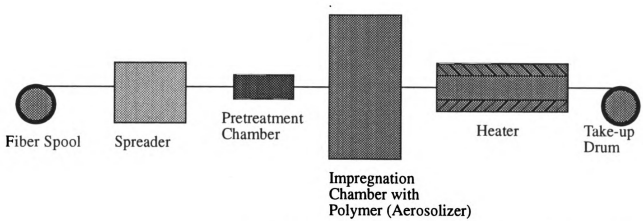

Figure 7.1: Experimental set up to coat fibers with polymer [55].

7.1.1 Modification of Original Process - Production of Precursors Using a Binder

The original process can be modified by adding a new chamber to coat the fibers with metal powders to produce CFRMMCs (Figure 7.6). In the modified process, the polymer prepregs are cut into 5cm pieces and suspended inside the new chamber (aerosolizer in Fig 7.7) where they will be coated with fine metal powder (matrix material). The sticky polymer (nylon) acts as a binder between the fibers and the matrix. The precursors are then stacked up and consolidated by vacuum hot pressing. This has not been done continuously but continuous processing is possible (Figure 7.6). Each element in the experimental set-up has been tested. Inorder to evaluate each element safely, the coating of the metal powder on the fiber surface was done in an argon atmosphere.

Production of Precursors Without a Binder

CFRMMCs can also be made by not using any polymer binder. This is possible since the metal powders form oxide coatings that can hold a static charge strong-enough to attract the metal powder particles to the fiber and hold them long enough to be consolidated.

Bare carbon tows are suspended in the aerosolizing chamber and evenly coated with aluminum powder particles. Subsequently, sections of bare fiber tows coated in this way are laid up in a stack and consolidated in the conventional way by hot pressing with minimum handling. Some layers that had lesser amounts of powder had additional powder sprinkled on top of the layer.

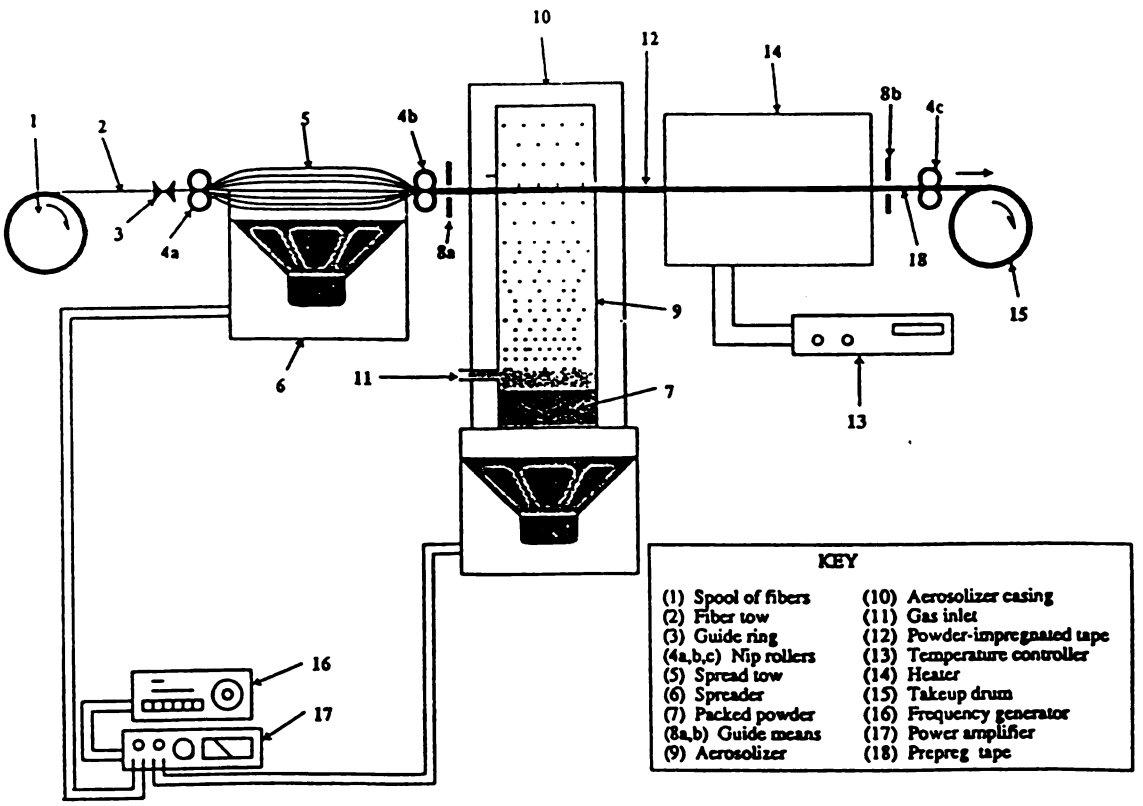

Figure 7.2: Schematic of powder prepregging process [55].

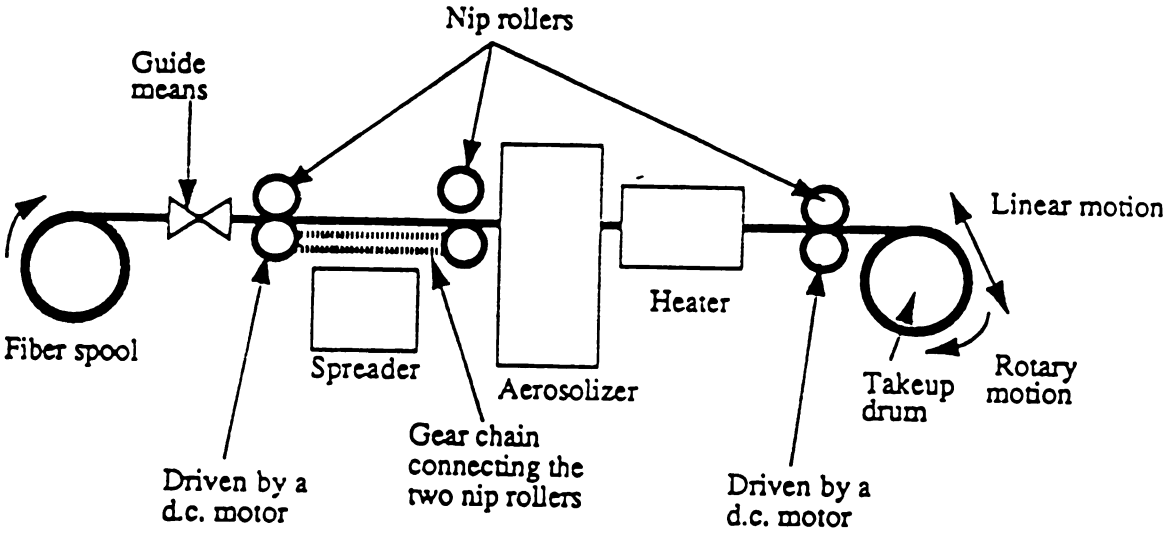

Figure 7.3: Fiber motion in powder prepregging process [55].

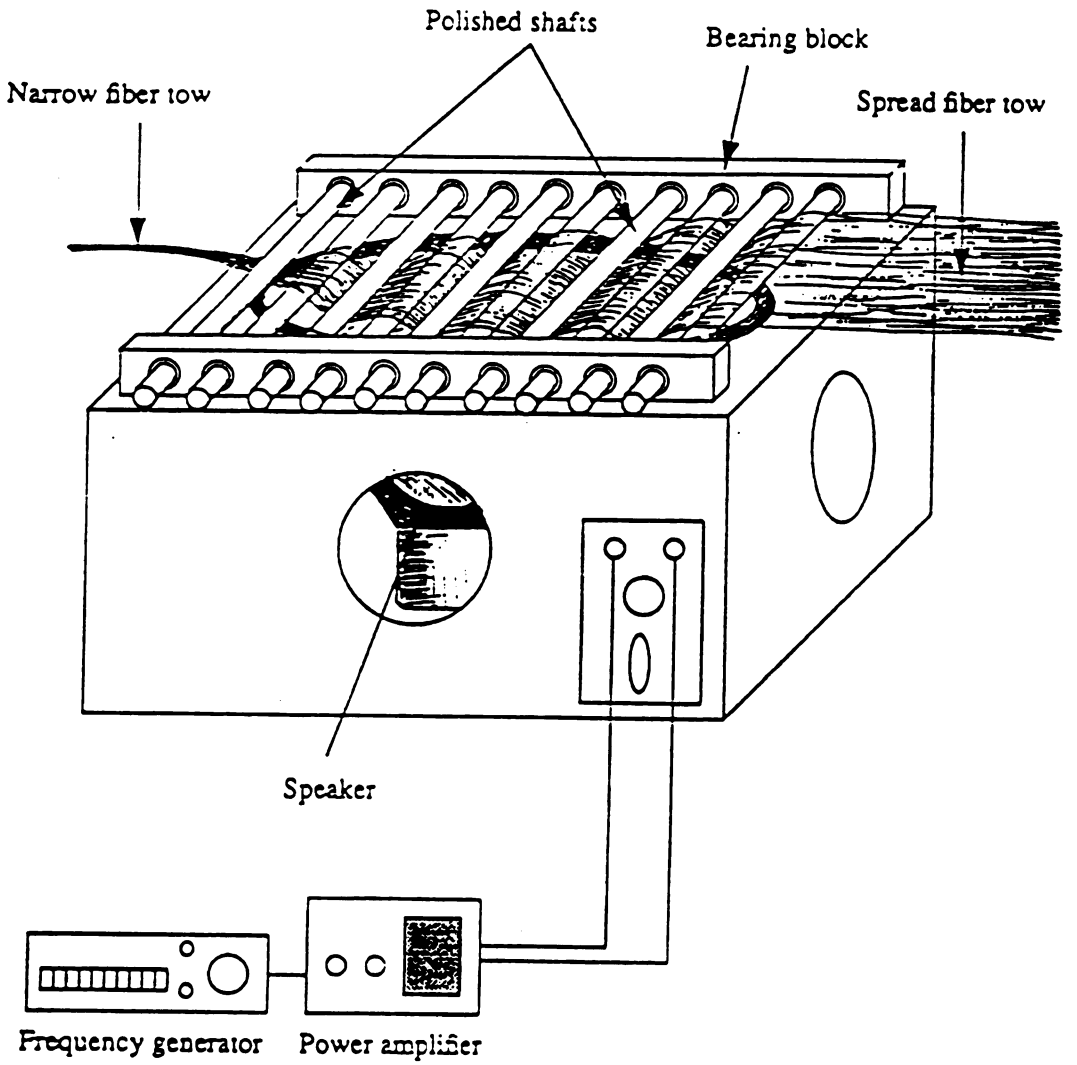

Figure 7.4: Spreader to spread the carbon fibers before coated with polymer [55].

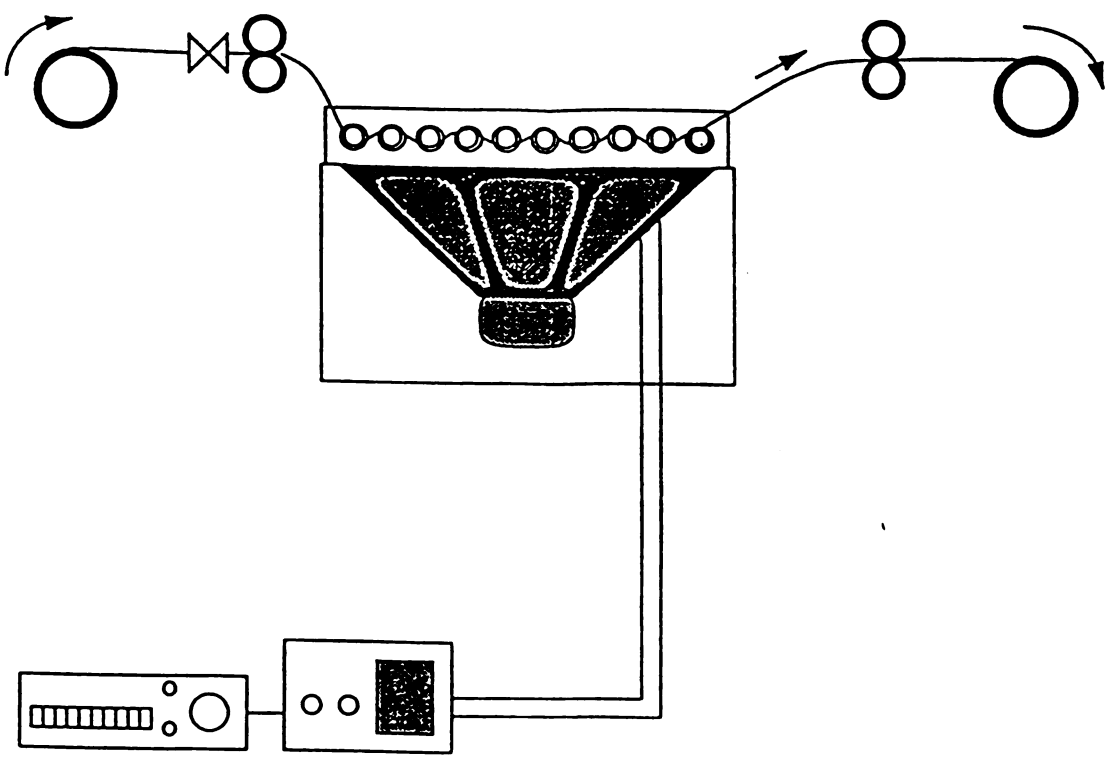

Figure 7.5: Fiber spreading operation using speaker [55].

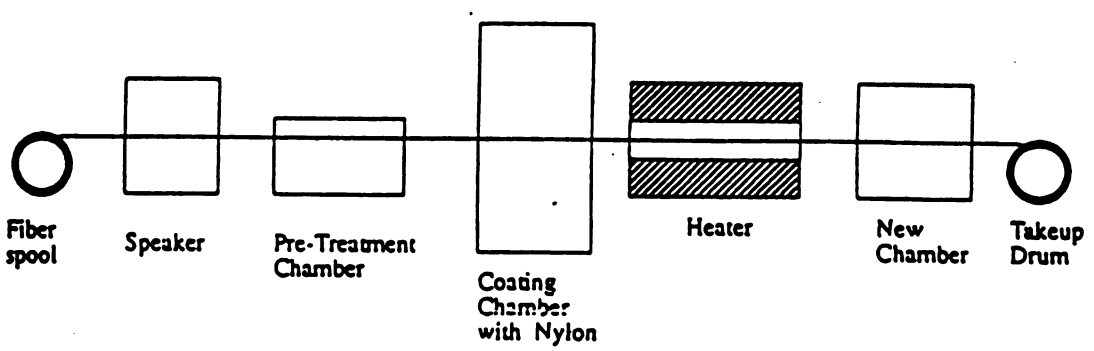

Figure 7.6: Modified experimental set up to coat the fibers with metal powder.

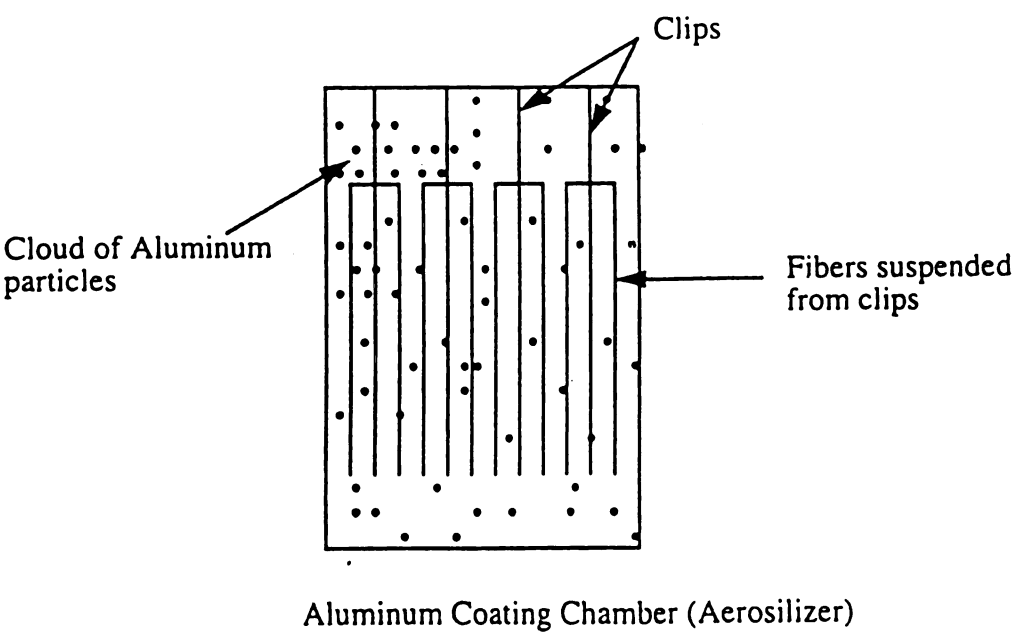

Figure 7.7: Aerosolizer to coat the fibers with metal powder.

Advantages of the Proposed Process

1. Minimizes undesired interface reaction products since the precursors are produced at lower temperatures (in case of precursors produced using a binder).

2. Homogeneous fiber distribution can be achieved by spreading operation that in turn reduces the fiber damage usually caused by fiber-to-fiber contact.

3. With the help of the aerosolizer and fine (5.5μm dia.) metal powders with smaller size than the diameter of the fibers (8μm), a uniform distribution of matrix around each fiber can be achieved.

4. The spreader and fine metal powders help to obtain high fiber volume fractions.

5. A homogeneous fiber distribution, minimum interface reaction, and high fiber volume fractions yield high quality composites.

6. New processing technique is less expensive than the existing techniques because of its simplicity and automation.

7. The process becomes less complex if binder is not used since no vacuum burnout of the polymer (binder) is needed.

CHAPTER 8

Experimental Procedure

8.1 Experimental Chamber System

The chamber to coat the fibers with metal powders is made of plexiglass because of the necessity of visual adjustments to determine the appropriate frequency of the speaker for fluidization of powder particles. All the experiments were done in an independent chamber and once consistently good results were obtained, the chamber would be added to the original system.

The chamber consists of a speaker, wooden box enclosing the speaker, a glass tube, and an aluminum flange that connects the speaker, lower membrane, and the glass tube (Figure 8.1). The outside tube contains two lids made of aluminum at the top and bottom (Figure 8.2). Both lids have an O-ring inside to prevent the leakage of vacuum. The two lids are held onto the chamber by three stretch cords. Calculations have shown that the plexiglass tube and the aluminum lids are capable of withstanding atmospheric pressure [56].

The coating process takes place in the inner glass tube (Figure 8.3). The O-ring at the top is held in place by a small indentation made at half an inch from the top. Six tungsten pins are provided at three inches from top to serve as electrical feedthroughs for the heating system (if binder is used). Two gas ports are provided to pump Argon into the

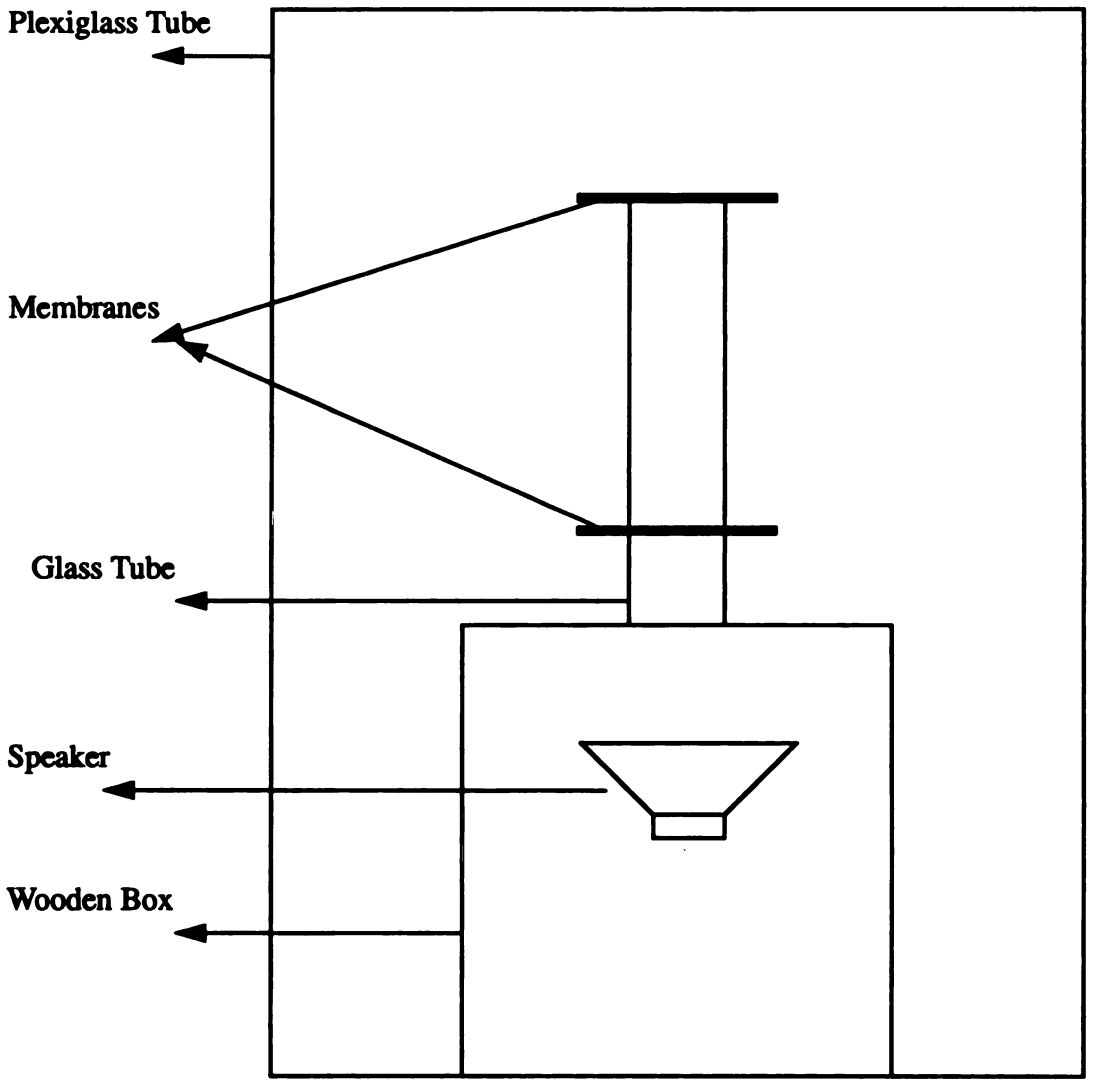

Figure 8.1: Chamber to coat fibers with metal powders [56].

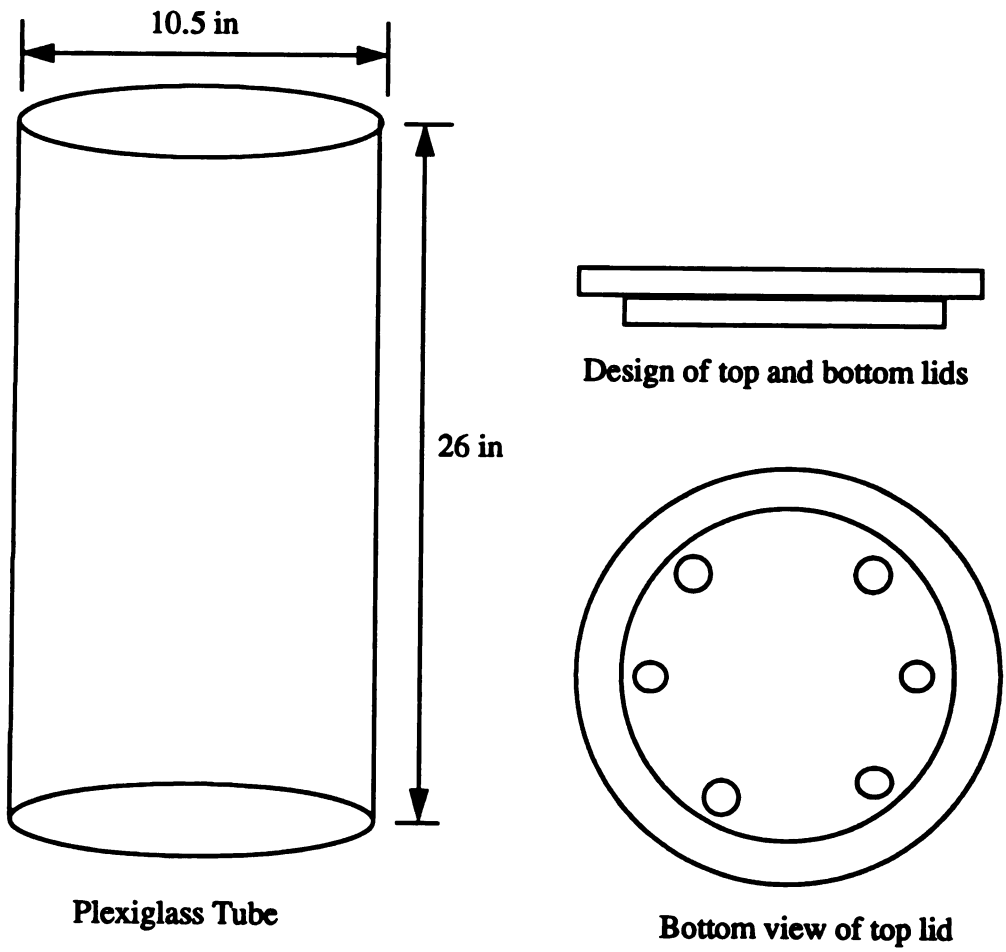

Figure 8.2: Outer tube [56].

chamber through air filters. The inside tube is placed on the aluminum flange which is held by a wooden box that surrounds the speaker. A membrane between the glass tube and the aluminum flange serves as the fluidization bed.

The heating system is a flexible heating element wound around a metal tube hung on two tungsten pins in the inner glass tube. The prepreg tapes with binder are suspended in the heating chamber (metal tube) by spring clips (Figure 8.4). Electrical feedthroughs made of O-ring sealed bulkhead unions filled with vacuum epoxy that fit through the holes of the top lid are provided to transmit a signal from outside to the inner chamber without interfering with vacuum level.

The speaker is mounted inside a wooden box with a circular opening on top to permit upward propagation of sound waves. The speaker box is connected to the inner tube by an aluminum flange whose circular base covers the opening of wooden box. The aluminum flange has a circular indentation for an O-ring to hold the bottom rubber membrane where the inner tube is fitted. A frequency generator and an amplifier are provided to control the speaker.

The vacuum system is shown in Figure 8.5. Thick wall flexible vacuum hoses connect the vacuum pump to the chamber. The gas flow in and out of the chamber is controlled by ball valves. Vacuum feedthroughs consist of bulkhead unions sealed by O-rings.

8.2 Materials

PAN based high strength Hercules AS-4 fibers with 8μm diameter and Valimet Inc.'s 99.7% pure aluminum powder from Valimet Inc. have been used to make the preforms. The properties of the materials used are shown in Table 8.1.

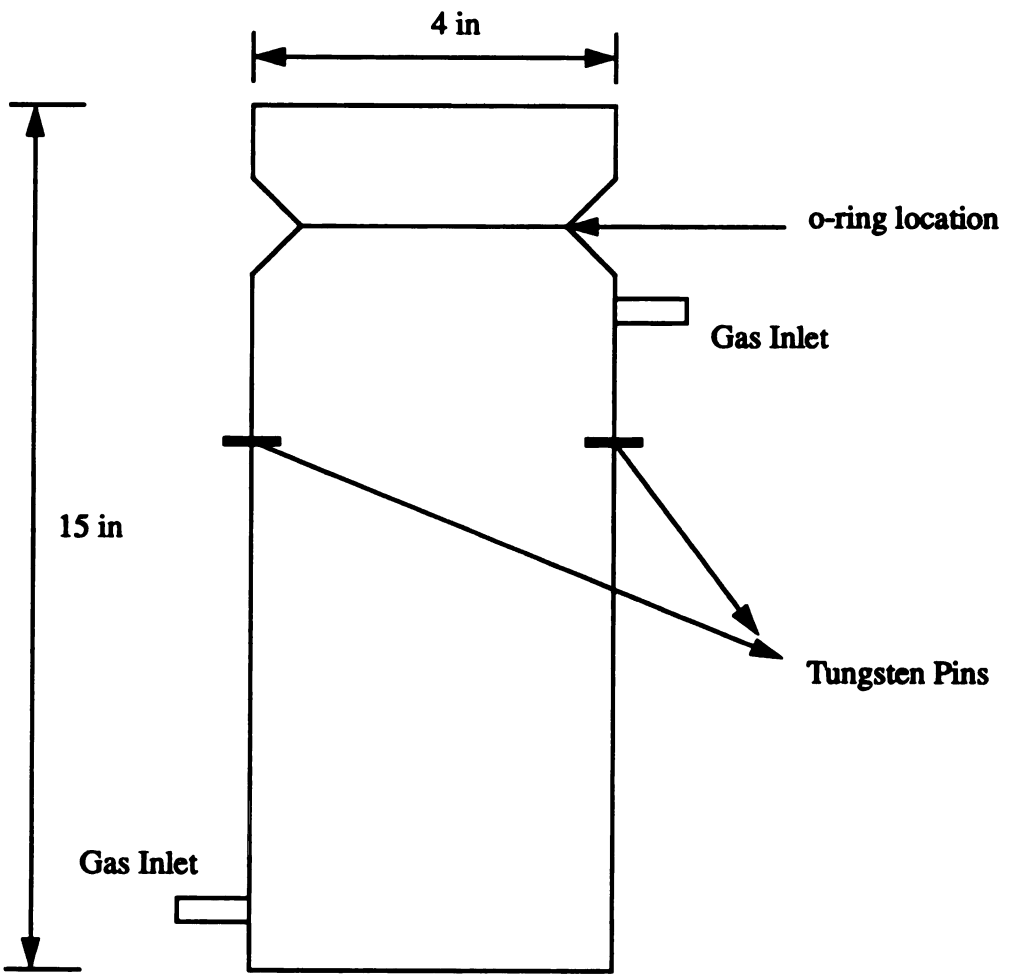

Figure 8.3: Inner tube [56].

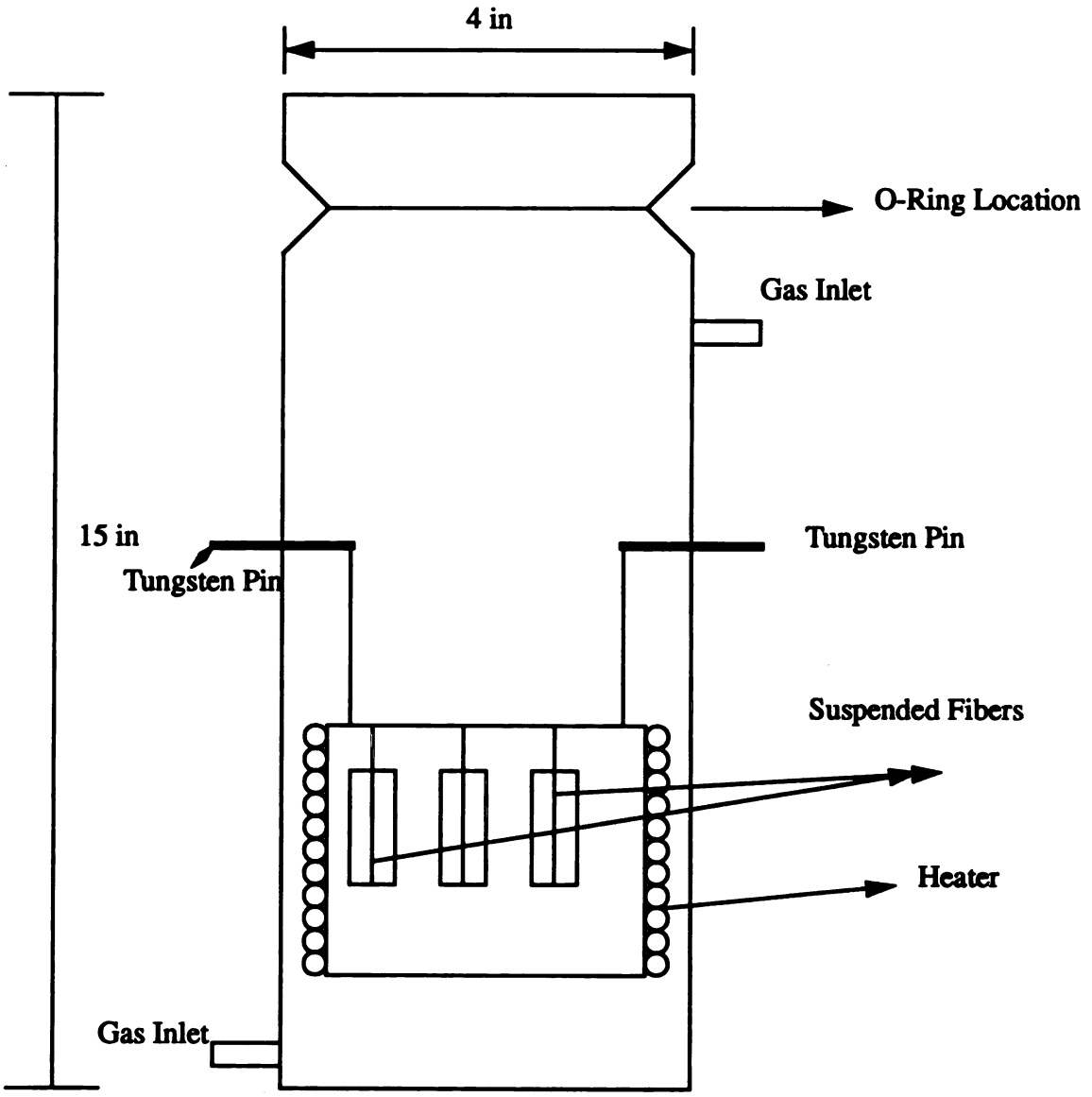

Figure 8.4: Heater in inner tube [57].

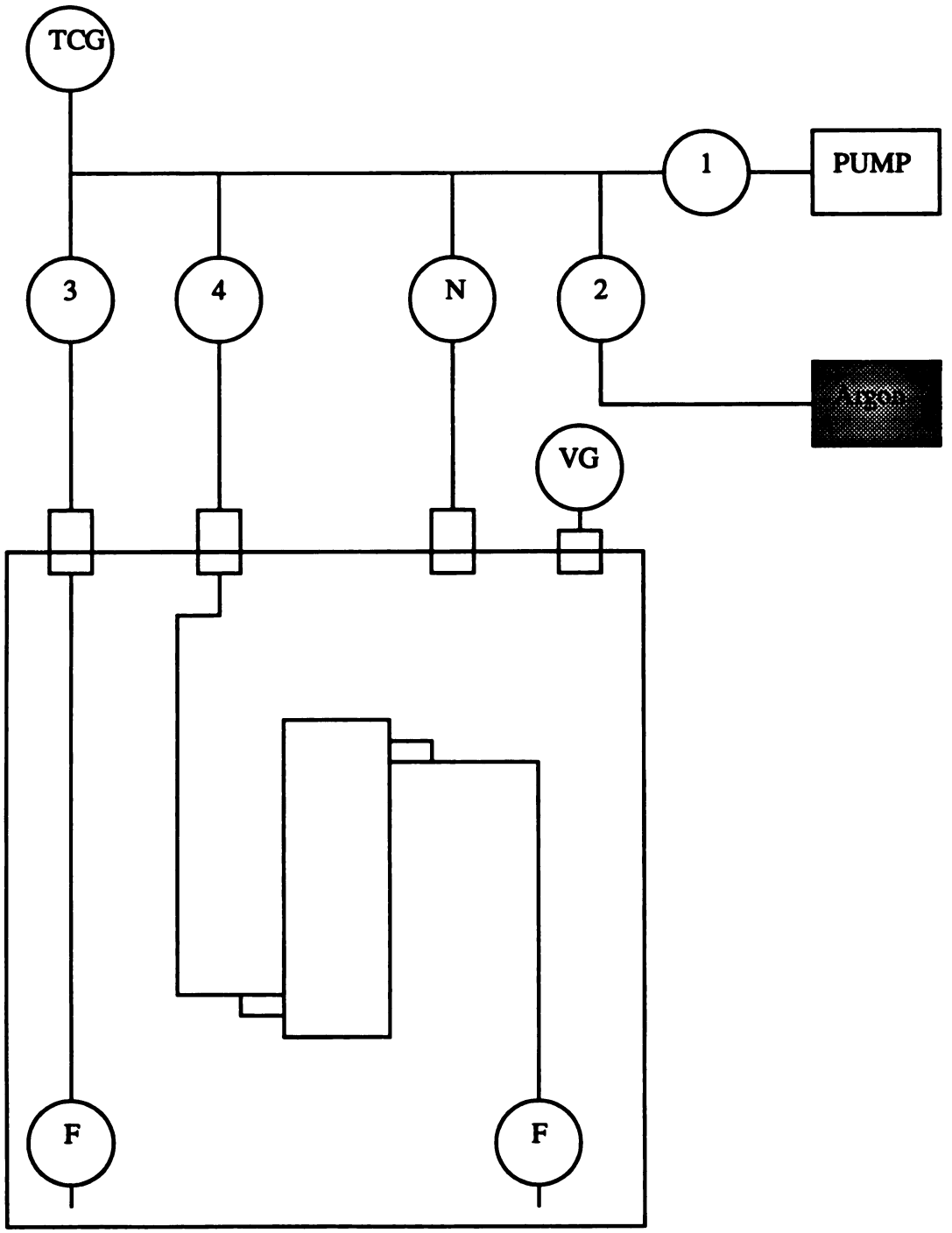

Figure 8.5: Vacuum System [56].

Table 8.1: Properties of the materials used.

Properties	Al	Fibers
Average particle (μ m)	5.5	8
Density (gm/cm^3)	2.69	1.8
Melting Point (^0C)	660	
Tensile Strength (MPa)	82.8	3100
Tensile Modulus (GPa)	69.0	220
Chemical Composition		
Aluminum	99.7%	
Iron	0.18%	
Silicon	0.2%	
Source	Valimet Inc.	Hercules Inc.

8.3 Production of Precursors Without Binder

The procedure involved in the production of aluminum powder coated prepreg precursors was

1. The prepreg tapes (bare carbon tows) were cut into 5 cm long pieces.
2. The prepreg tapes were suspended inside the metal tube with spring clips as shown in Figure 8.4.
3. The metal tube was hung on the pins inside the glass tube.
4. 5-8 gms of aluminum powder was deposited on the bottom membrane.
5. The inside tube was fitted on the top of flange.
6. The top membrane was placed in position with the help of the O-ring.
7. All the electric wires and vacuum hoses were connected properly.
8. The aluminum lid was placed on the outer tube.
9. The vacuum pump was operated until the pressure inside the tube was reduced to below 3 inches Hg.
10. Argon was slowly introduced to one atmosphere (14.7 psi).
11. The frequency generator or speaker and the power amplifier were turned on to fluidize the aluminum powder for approximately 5 minutes.

8.3.1 Consolidation by Vacuum Hot Pressing

The aluminum coated carbon fiber precursors were vacuum hot pressed (VHP) by using an MTS-810 Material Test System. The steps involved were:

1. Align dozens of prepreg layers in mats.
2. Chopp off the aligned prepregs in 2 cm long and 1 cm wide pieces.
3. Wrap the prepreg with aluminum foil.
4. Apply boron nitride paste evenly on the inner surface of the fixture.
5. Place the sample in the fixture.
6. Keep the fixture on the bottom platen inside the pressing furnace.
7. Press the top platen on the sample with pressure of a little more than zero.
8. Close the furnace and pump vacuum to less than 2×10^{-5} torr.
9. Increase the temperature to 570 ^{0}C in 30 minutes.
10. Press the sample under 30 MPa at 570 ^{0}C for 45 minutes. For each sample the load was computed with respect to cross sectional area of the sample.
11. Release the pressure and decrease the temperature to 400 ^{0}C in 5 minutes.
12. Extract the specimen after the furnace reaches room temperature.

The consolidated sample was approximately 30mm $\times$ 12mm $\times$ 3mm plate.

8.3.2 Physical & Mechanical Property Measurements

The fiber volume fraction, density, and CTE α of the composite were measured. α was measured using a dilatometer (Figure 8.6) and Archimedes principle was used to measure the density. For thermal expansion measurements, the original sample was cut into 25.4mm $\times$ 12.7mm $\times$ 3mm block. 3-point bending tests were done on composites by using United Testing System SFM-20. The results are given in the Table 9.1. For bending tests, the consolidated sample (30mm $\times$ 12mm $\times$ 3mm) was cut into 30mm $\times$ 2mm $\times$

0.5mm specimens by using a diamond-saw after the composite was trimmed to eliminate unconsolidated material at the edges. The fiber volume fraction (v_f) was also measured by counting the fibers on a composite cross section. The flexural modulus and flexural strength of the composite were evaluated using following equations:

$$S_{FC} = 3PL/2bd^2$$

$$E_{FC} = PL^3/4\delta bd^3$$

where:

S_{FC} = the flexural strength of the composite

P = the loading

L = the span

b = the width of the specimen

d = thickness of the specimen

E_{FC} = the flexural modulus of the composite

δ = deflection increment at midspan

The flexural strength of the composite from the 3-point bending test can be compared with the theoretical value calculated from equations which is derived from the rule of mixtures and the contribution of the matrix is neglected.

$$S_{FC} = 3V_f S_{Tf}/(1 + S_{Tf}/S_{Cf})$$

where:

S_{Tf} = the tensile strength of the fiber

S_{Cf} = the compression strength of the fiber

V_f = the fiber volume fraction

If S_{Cf} is not known, S_{Cf} = 0.9 S_{Tf} is a good approximation for graphite fiber/matrix composites.

For bending tests of composites, the span-to-depth ratio is recommended to be at least 16:1. This ratio shall be chosen such that failures occur in the outer fibers of the specimens, due only to the bending moment. For highly anisotropic composites, shear deflections can seriously reduce the modulus measurements. In this study, a ratio of 32:1 is a standard that should be adequate to obtain valid measurements [58].

8.3.3 Metallography & Fractography

Transverse and longitudinal sections of the consolidated samples were cut, mounted, polished, and examined using an Olympus PME 3 Microscope. The fractured surfaces of the 3-point bend specimens were also examined using Hitachi S-2500C Scanning Electron Microscope (SEM).

8.3.4 X-ray Photoelectron Spectroscopy (XPS or ESCA)

X-ray photoelectron spectroscopy (XPS) or Electron spectroscopy for chemical analysis (ESCA) of 3-point bend test specimens was used to identify the interface reaction products. Data was collected using a Perkin-Elmer Physical Electronics Model 5400 ESCA spectrometer. The spectrometer was equipped with a standard source using a Mg $K\alpha_{1,2}$ x-rays (1253.6 eV) operated at 300 watts, 15 kV and 20mA. The instrument used a 180^0 hemispherical energy analyzer operated in the fixed analyzer transmission mode at a pass energy of 35.75 eV and a position sensitive detector. Spectra were collected using an analysis area defined by a 1mm diameter spot. Samples were mounted onto a sample holder.

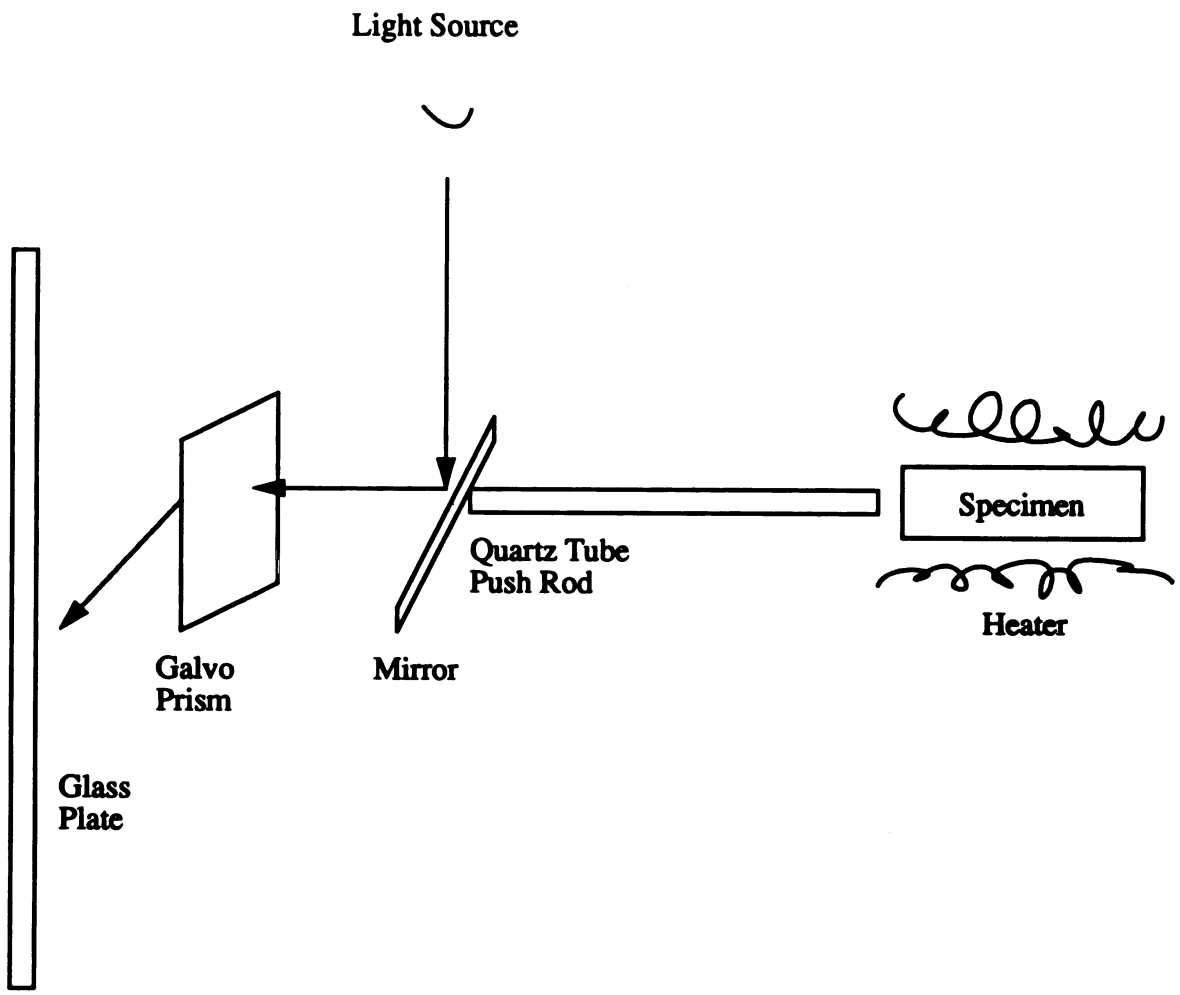

Figure 8.6: Dilatometer [1].

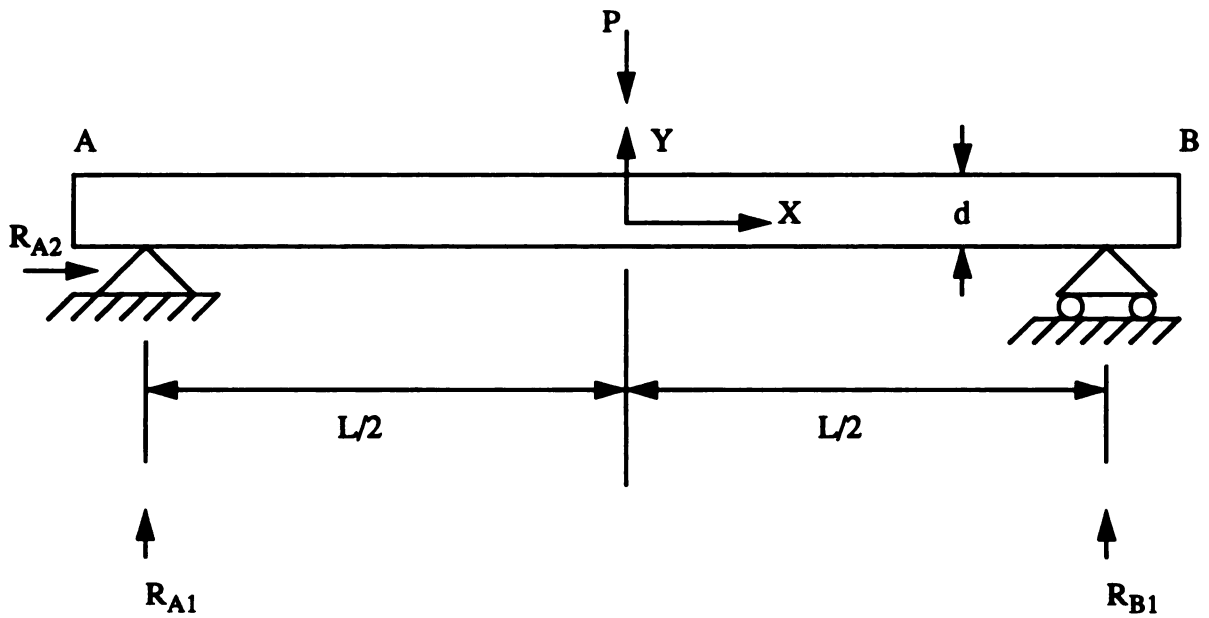

Figure 8.7: Simple beam subjected to 3-point bending.

Spectra were collected using a 45^0 take-off angle between the sample and the analyzer lens.

XPS or ESCA is a surface analytical tool to study the surface composition. In XPS, either photons of low energy or electrons can be used as exciting radiation, x-rays are normally used by the researchers. The XPS system basically consists of 5 components:1) the source, 2) sample holder container, 3) an electron energy analyzer, 4) a detector, and 5) a readout system. The source should be capable of producing intense mono-energetic stable beam of either photons, electrons, or x-rays of sufficient energy to excite the electrons in the surface of the sample being examined. The beam impinges on the surface to be studied and ejects the electrons. The electron energy analyzer sorts out the ejected electrons according to their kinetic energies and focuses them onto a detector. The detector produces an electrical signal proportional to the intensity of the electron beam, and the read system translates it into graphic form.

The XPS system measures the binding energy of the ejected electrons. Siegbahn et al. found that the binding energy (E_b) for a given electron in an atom was not constant for a series of compounds containing that atom. Siegbahn et al. also found that chemical environment had a significant affect on E_b and was roughly a function of atomic charge. The binding energy results due to combination of various forces acting on the core electrons. Depending on the magnitude of the nuclear charge or atomic number of the particular atomic species being examined , electrons in the atom experience a strong attractive force. The core shell electrons exert a repulsive force that screens the outer or valance electrons from the nuclear charge, thus diminishing the nuclear attractive force. The resultant force which binds the electron to the atom is the binding energy E_b.

If an electron is ejected from the outer shell, core electrons will have more attraction towards nucleus, since the screening of inner electrons is reduced by one electron charge. The gaining of an outer electron will have the opposite effect, i.e., increase in shielding and decrease in binding energy. The above theory indicates that binding energies depend on the chemical environment and represent a new key to the analysis of chemical struc-

ture of materials in solid surfaces. XPS can be used to study a variety of solid surfaces. However, the sample has to be in a chamber maintained at pressure of $\approx 10^{-6}$ torr or less. Gaseous samples on solid surfaces can be studied by using differential pumping techniques. The limitation of this technique is that impinging electrons should not adversely affect the surface being examined.

XPS is a surface sensitive technique requiring very small amounts of sample, typically of the order of 10^{-6}gm. XPS is extremely well suited to study solid surface films, particularly tribological films because the electrons can not be ejected from a depth more than 100 $\mathring{A}$.

The phases at the interface and the reaction products on the fiber surface was also done using EDAX.

CHAPTER 9

Results

9.1 Composite Precursors Without Binder

9.1.1 Optical Microscopy

Figure 9.1 to Figure 9.6 show optical micrographs of the transverse and longitudinal sections of the composite at different magnifications. Bare carbon fibers were used to make the composites. Figure 9.3 shows the even distribution of fibers with a very few fibers contacting each other. From Figure 9.4, Figure 9.5, and Figure 9.6 it is clear that there is no matrix material in one part of the specimen. This may account for the porosity determined from the density measurements.

These figures indicate that fiber-matrix interface is smooth with no apparent discontinuity in the interface, even at higher magnifications. This implies that the fiber-matrix bonding is good with minimal interface reaction and no fiber damage.

Figure 9.7 compares the longitudinal sections of composites made using fibers with and without a binder. Figure 9.8 compares the fiber distribution of composite made using bare carbon fibers with composite made using precoated (prepreg fiber/nylon) fibers. This Figure clearly shows that the fiber distribution is better in the former case. Figure 9.9 compares the fiber distribution in the composite made using bare carbon fibers with the

fiber distribution in the composite made using powder slurry technique [19, 29].

The main features of this new fabrication technique are:

1. It was capable of picking up a significant volume fraction of metal matrix.
2. The distribution of the matrix around the fibers was uniform.
3. Micrographs showed that the fiber - matrix bonding was good.
4. The processing is less complex since the polymer binder is not required and no vacuum burnout of the polymer using vacuum hot pressing furnace is needed.

9.1.2 Physical and Mechanical Properties of the Composite

The α value determined from the dilatometer experiments is 1.8 $\times 10^{-6}/^{0}$C for the temperature range of 25 to 270^{0}C (Figure 9.10), where the slope ($\Delta\epsilon/\Delta$T) was determined from a linear regression. The density of the material is 2.28 gm/cm^{3}. The fiber volume fraction was measured by counting the fibers on a composite cross section and it varies between 40 - 50% and based on this volume fraction, the porosity of the material is found to be 0.5-2.0%, respectively.

The results of the 3-point bend test of aluminum matrix composites made with precoated fibers and bare carbon fibers are shown in Table 9.1 Table 9.2. The flexural strengths of the two composite samples made with bare carbon fibers with 40% v_f are 629 and 439 MPa respectively as compared to the tensile strength of 82.8 MPa for unreinforced pure aluminum. Better flexural strength values are obtained for the composites made with bare carbon fibers when compared with those made with precoated fibers (343 and 328 MPa respectively (Table 9.1) having fiber volume fractions of 50%). The flexural modulus values in both cases are almost similar. The % ROM strengths in the case of composites made using bare carbon fibers are 49 and 34 respectively and % ROM modulus values are 78.6 and 67.6 respectively.

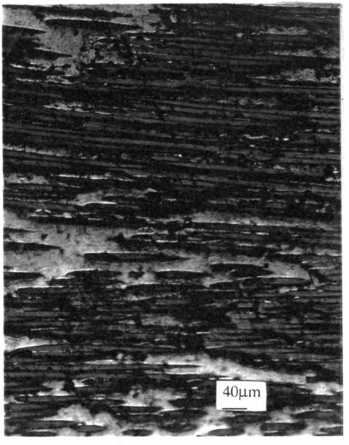

Figure 9.1: Optical micrograph of the longitudinal section of the composite (B2-1, Table 9.1).

Figure 9.2: Optical micrograph of the longitudinal section of the composite (B2-2, Table 9.1).

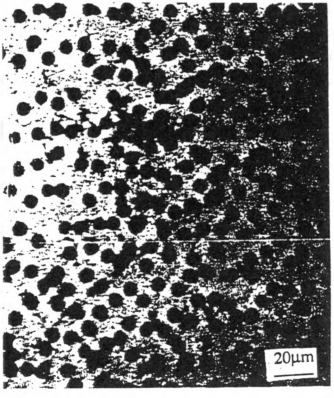

Figure 9.3: Optical micrograph of the transverse section of the composite showing homogeneous distribution of the fibers (B2-1, Table 9.1).

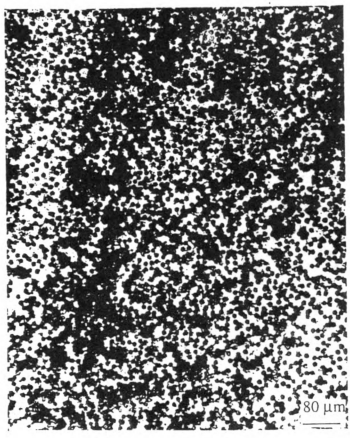

Figure 9.4: Optical micrograph of the transverse section of the composite with no matrix material in one part (B2-1, Table 9.1).

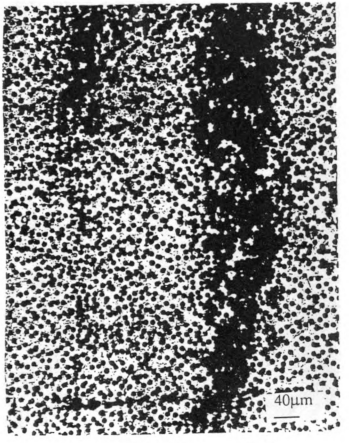

Figure 9.5: Optical micrograph of the transverse section of the composite with no matrix material in one part (B2-1, Table 9.1).

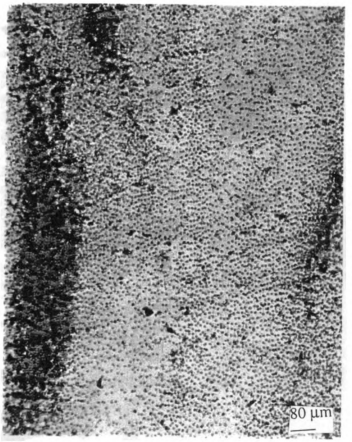

Figure 9.6: Optical micrograph of the transverse section of the composite with no matrix material in one part (B2-1, Table 9.1).

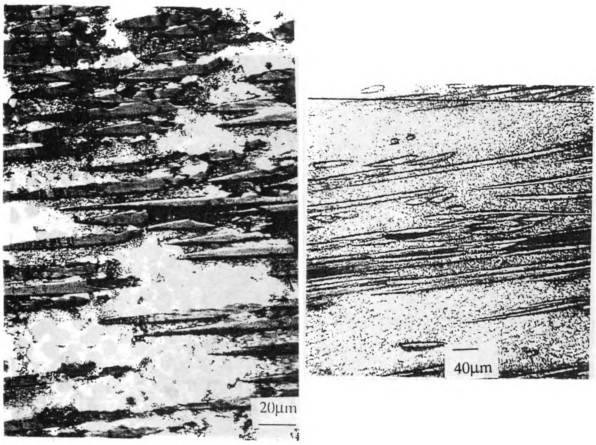

(a) (b)

Figure 9.7: a) Optical micrograph showing the longitudinal section of the composite made using bare carbon fibers (B2-1, Table 9.1), b) Optical micrograph showing the longitudinal section of the composite made using precoated fibers (C1, Table 9.1).

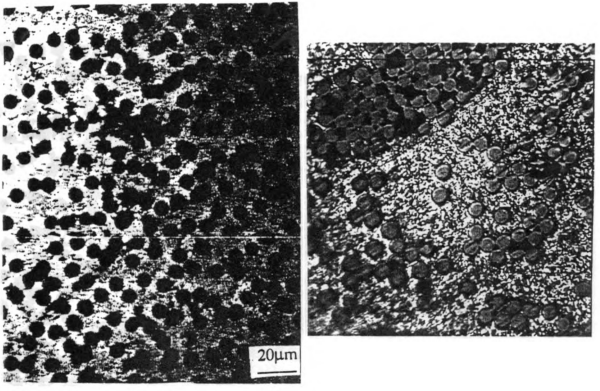

(a) (b)

Figure 9.8: a) Distribution of fibers in the composite made using bare carbon fibers (B2-1, Table 9.1), b) Distribution of fibers in the composite made using precoated fibers (C1, Table 9.1).

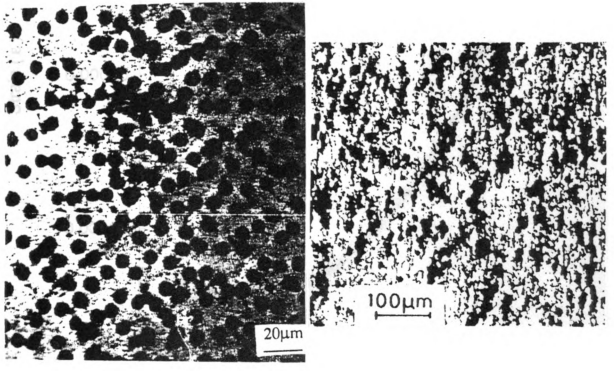

(a) (b)

Figure 9.9: a) Distribution of fibers in the composite made using bare carbon fibers (B2-1, Table 9.1), b) Distribution of fibers in the composite made using powder slurry technique [19, 29].

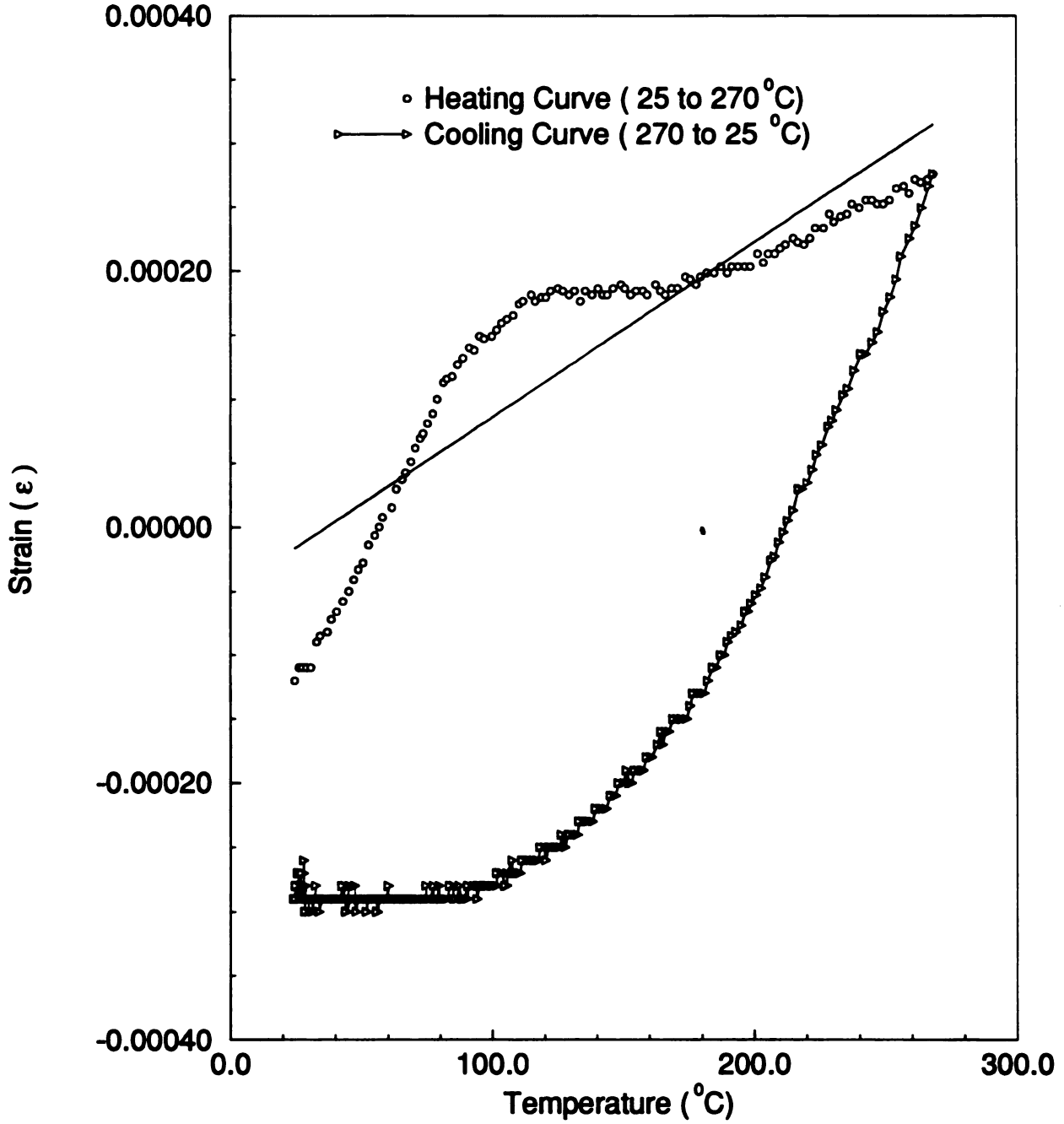

Figure 9.10: Measurement of coefficient of linear thermal expansion (CTE) (25-270 °C) (B3-3, Table 9.2).

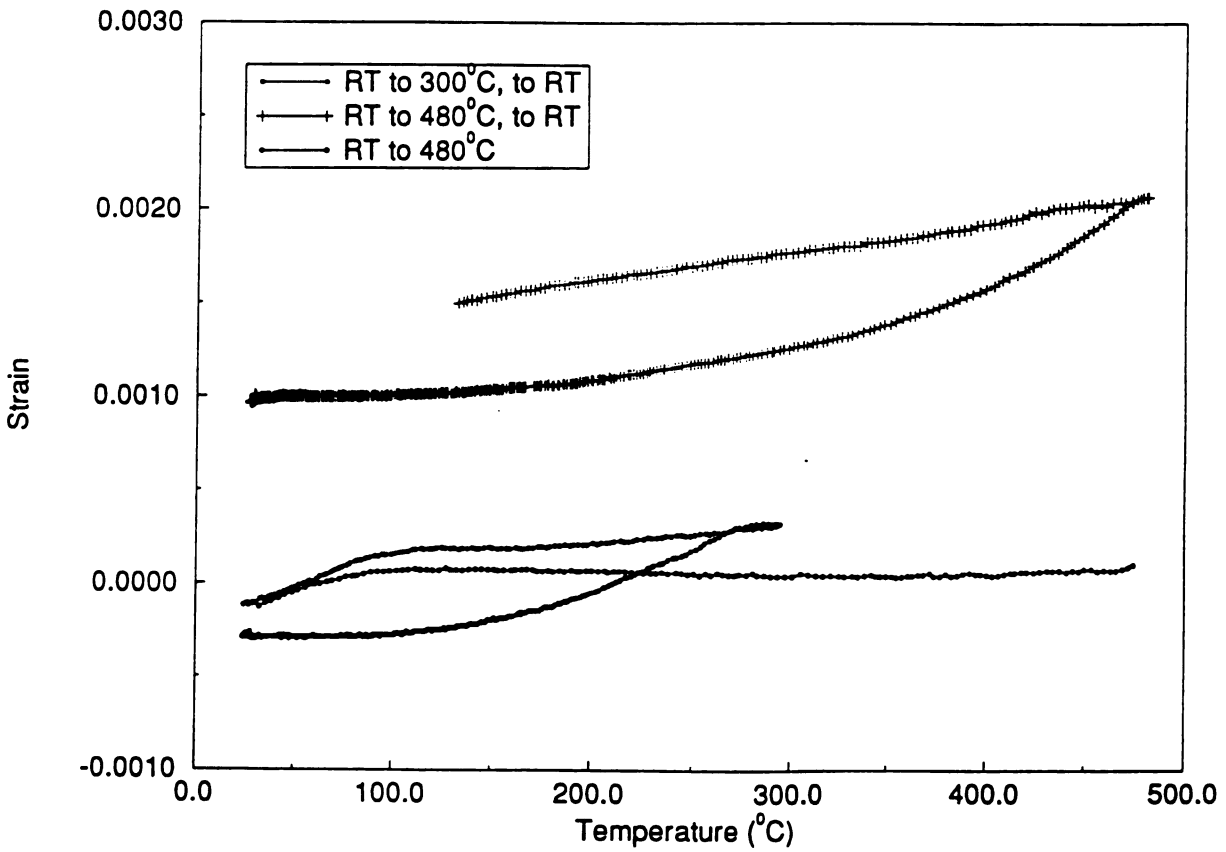

Figure 9.11: Composite subjected to thermal cycles for CTE measurement.

Table 9.1: Results of the 3-point bend test of the composite specimens made using pre-coated and bare carbon fibers.

Fibers	precoated	precoated	Bare	Bare	Bare	Bare	Bare
Specimen	C1[a]	C2[b]	B1-1[c]	B1-2[d]	B1-3[e]	B2-1[f]	B2-2[g]
Number of Fiber Layers Stacked	35-40	35-40	40-45	40-45	40-45	40-45	40-45
Span (in)	0.7	0.7	0.7	0.7	0.7	0.7	0.7
Thickness (in)	0.04	0.04	0.13	0.13	0.13	0.02	0.02
Span to Thickness ratio	16.0	16.0	5.0	5.0	5.0	32.0	28.0
Yield Load (lb)	0.02	0.12	-	46.21	-	-	-
Peak Load (lb)	5.4	5.8	41.30	46.21	53.50	4.7	4.6
Yield Stress (Psi)	170.1	101.1	-	-	-	-	-
Flexural (Psi) Strength (MPa)	49775 343	47622 328	34085 235	40750 281	50430 347	91324 629.0	63697 439.0
Fiber Frac. (%)	50	50	40	40	40	40	40
%ROM Strength	13.0	13.0	16.0	19.0	23.0	49.0	34.0
Flexural Modulus (Ksi) (GPa)	17625.0 122.0	13554.0 94.0	2197.0 15.0	3733.0 25.74	4473.0 30.84	14742.0 101.7	12691.0 87.5
%ROM Modulus	80.0	62.0	11.0	19.0	23.0	78.6	67.6
Strain Fail. (%)	0.65	0.55	2.0	-	-	0.66	-

[a] Batch1,Specimen1
[b] Batch1,Specimen2
[c] Batch1,Specimen1
[d] Batch1,Specimen2
[e] Batch1,Specimen3
[f] Batch2, Specimen1
[g] Batch2,Specimen2

Table 9.2. Table summarizing the results of the various experiments done on the composite made using bare carbon fibers.

Fibers	Bare	Bare	Bare	Bare	Bare	Ramakrishnan Slurry technique[19]
Specimen	B2-2[1]	B3-1[2]	B3-2[3]	B3-3[4]	B4-1[5]	
Number of Fiber Layers Stacked	40-45	55-60	55-60	55-60	40-45	
Density (gm/cm^3) Theoretical Density		2.28 2.33				
Porosity (%) Based on V_f		~ 0.5-2.0%				
CTE ($\times 10^{-6}/^0C$)				1.8		
	XPS					
	EDAX					
Notch Tensile Test Peak Load (lb)	12.0					
Peak Stress (Psi)	3020					
Modulus (Ksi)	9.0					
Strain (%)	120.0					
Fiber Frac. (%)	40					
%ROM Strength	~ 0.1					
%ROM Modulus	~ 0.1					
Tensile Strength (MPa) 90 MPa, 600 ^{0}C, 900 sec. 16%V_f [19]						178
%ROM Tensile Strength [19]						27.7

Figure 9.12 and Figure 9.13 show the plots between load and extension for 3-point bend test composites made using bare carbon fibers.

9.1.3 Fractography

Figure 9.14 to Figure 9.18 show the SEM micrographs of the 3-point bend test specimens made of bare carbon fibers at various magnifications. These fractographs show the even distribution of fibers with a very few fibers in contact with each other. From these fractographs, it is obvious that the fiber-matrix interface is smooth with no apparent discontinuity in the interface, even at higher magnifications. This implies that the fiber-matrix is good with minimal interface reaction products and no fiber damage. The fractographs also show cup and cone mode of failure in the matrix and brittle failure in the fibers. These micrographs show less than 2% of the fibers in contact with each other in any particular cross section investigated. In addition, some fiber pull out on the order of fiber diameter is observed in the fracture surface of the 3-point bend test specimens.

9.1.4 X-ray Photoelectron Spectroscopy (XPS or ESCA) Analysis

The results of x-ray photoelectron spectroscopy (XPS) or electron spectroscopy for chemical analysis (ESCA) of the fractured composite made of bare carbon fibers are shown in Figures 9.19 to Figure 9.22. These plots show that there is no formation of Al_4C_3 at the interface. Table 9.3 gives the atomic concentration in the fractured carbon fiber reinforced aluminum composite sample. Si is found in the fractured sample.

Si is not found in the fractured sample using EDAX. Only aluminum is identified.

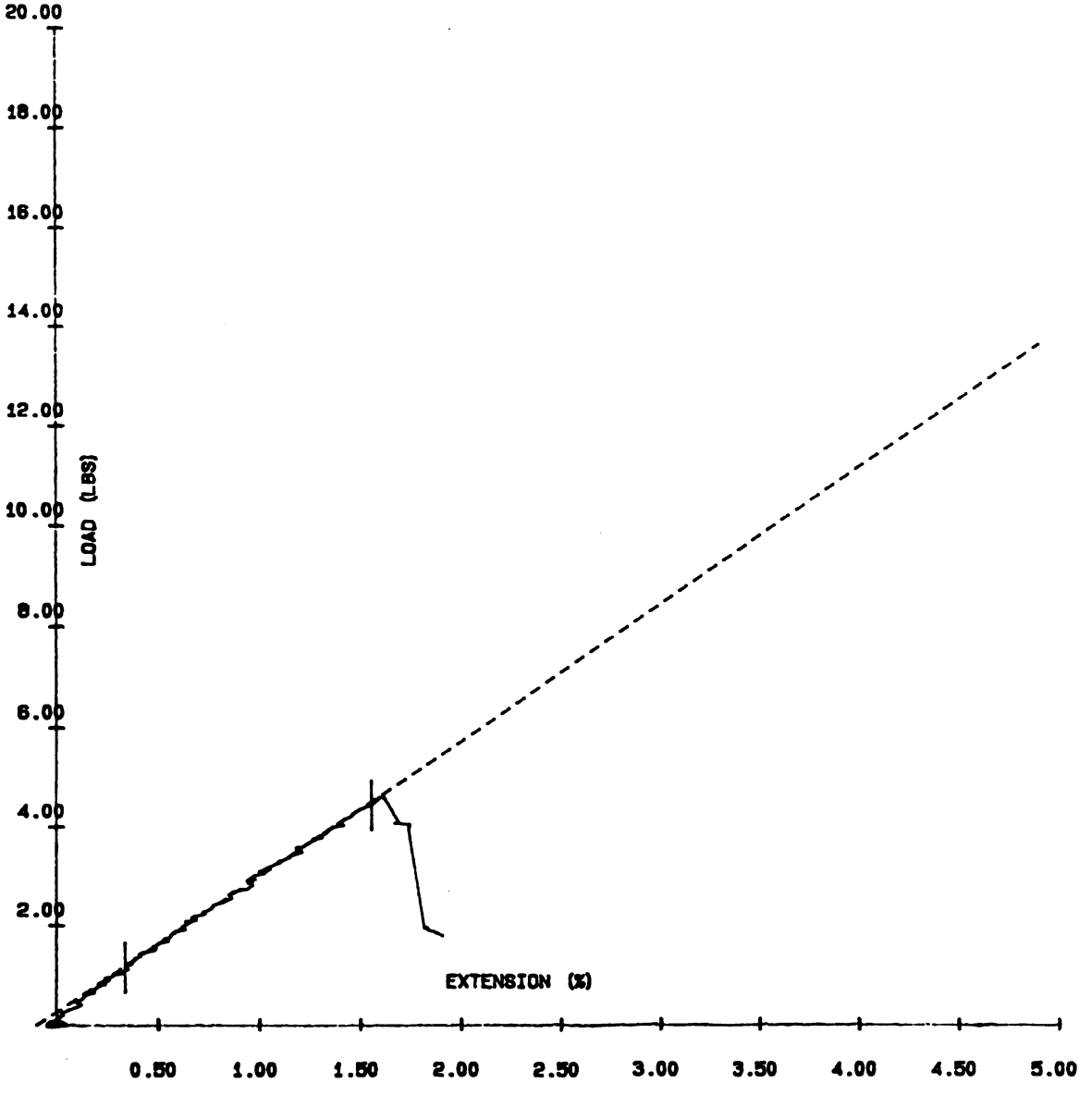

Figure 9.12: Load-Extension curve for 3-point test specimen made using bare carbon fibers (B2-1, Table 9.1).

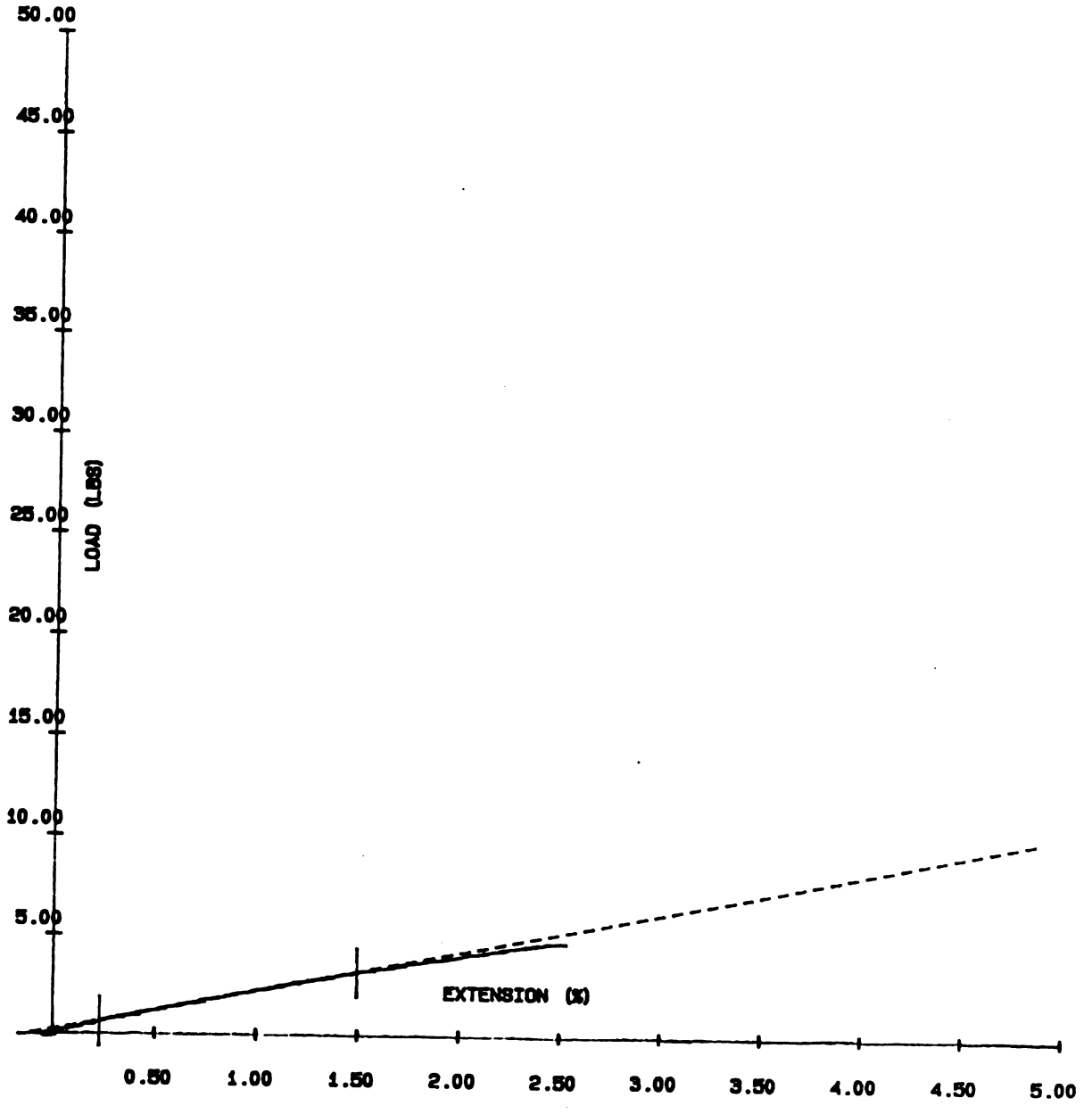

Figure 9.13: Load-Extension curve for 3-point bend test specimen made using bare carbon fibers (B2-2, Table 9.1).

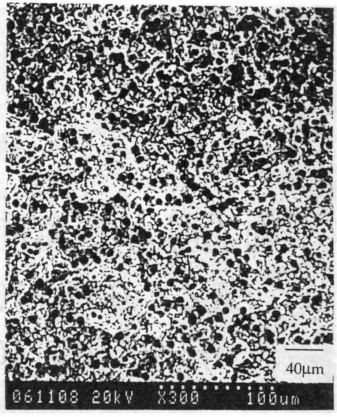

Figure 9.14: Fractograph of the 3-point bend test specimen (bare carbon fibers used) at 300X showing uniform distribution of fibers in aluminum matrix (B2-1, Table 9.1).

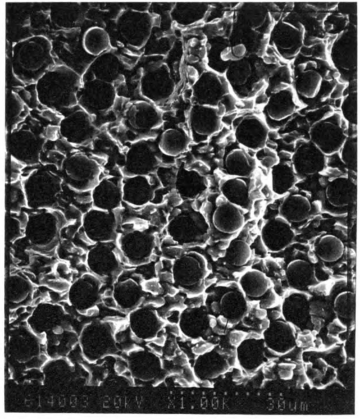

Figure 9.15: Fractograph of the 3-point bend test specimen (bare carbon fibers used) at 1000X showing uniform distribution of fibers in aluminum matrix (B2-1, Table 9.1).

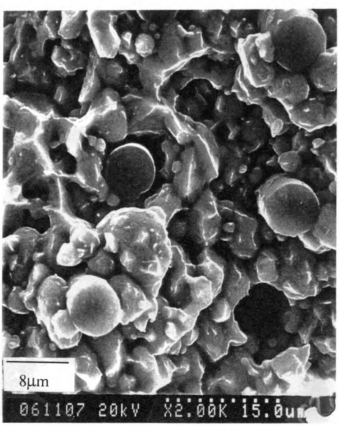

Figure 9.16: Fractograph of the 3-point bend test specimen made using bare carbon fibers) at 2000X showing ductile failure in aluminum matrix and brittle failure in carbon fibers (B2-1, Table 9.1).

Figure 9.17: Fractograph of the 3-point bend test specimen made using bare carbon fibers at 5000X showing ductile failure in aluminum matrix and brittle failure in carbon fibers (B2-1, Table 9.1).

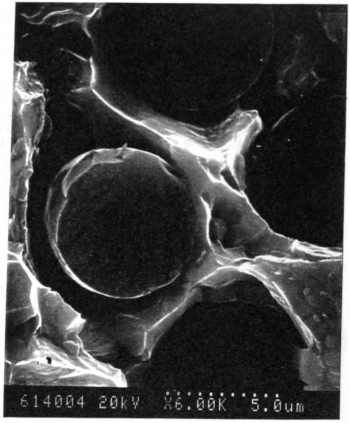

Figure 9.18: Fractograph of the 3-point bend test specimen made using bare carbon fibers at 6000X showing brittle failure in carbon fibers and ductile failure in aluminum matrix (B2-1, Table 9.1).

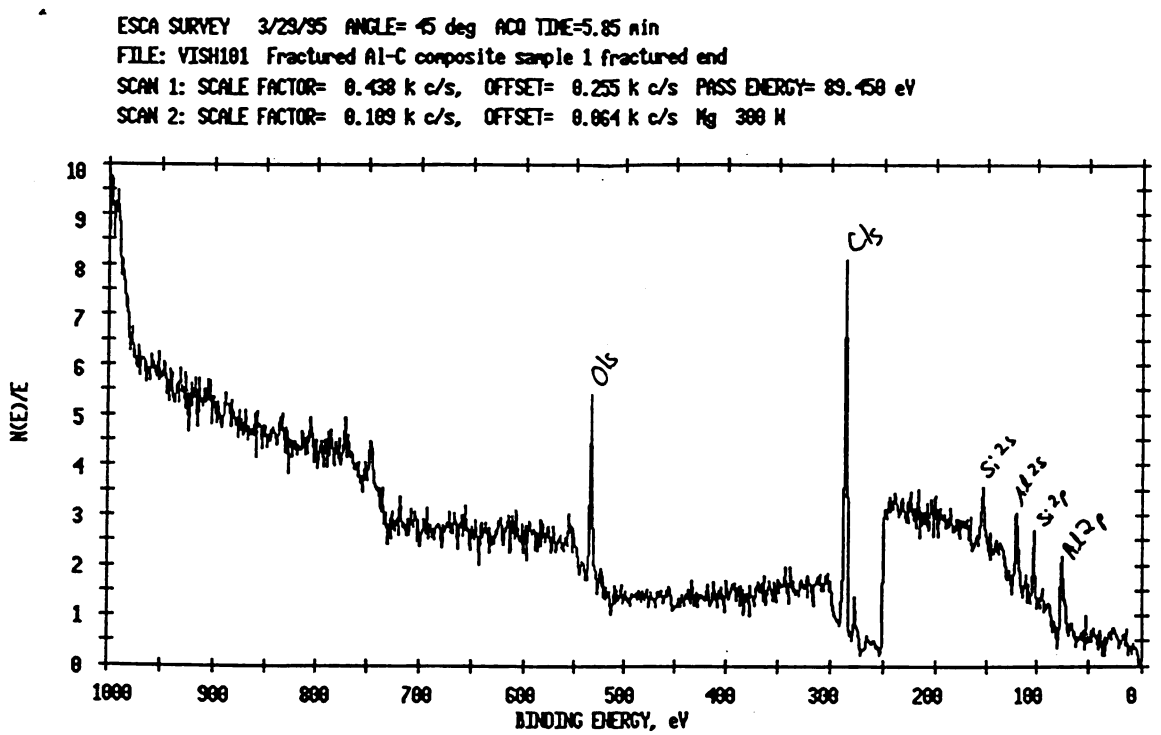

Figure 9.19: XPS analysis for the carbon fiber reinforced aluminum matrix composite showing the presence of different elements present in the fractured surface (B2-2, Table 9.1).

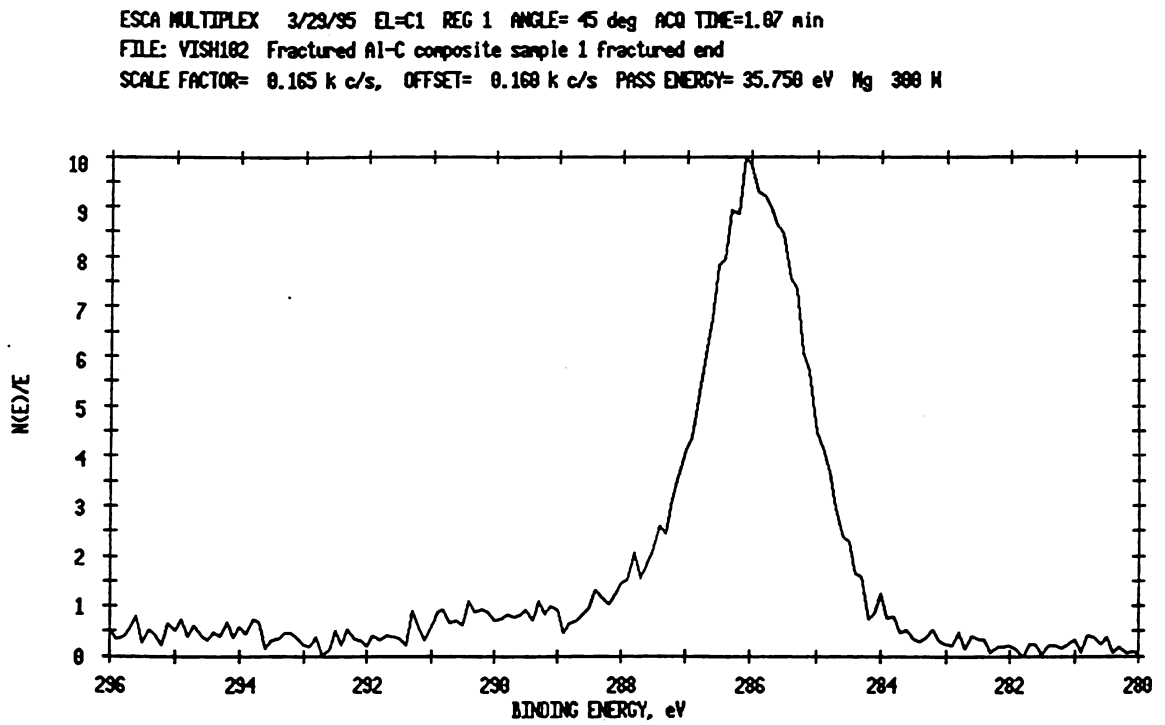

Figure 9.20: XPS analysis for carbon in the composite (B2-2, Table 9.1).

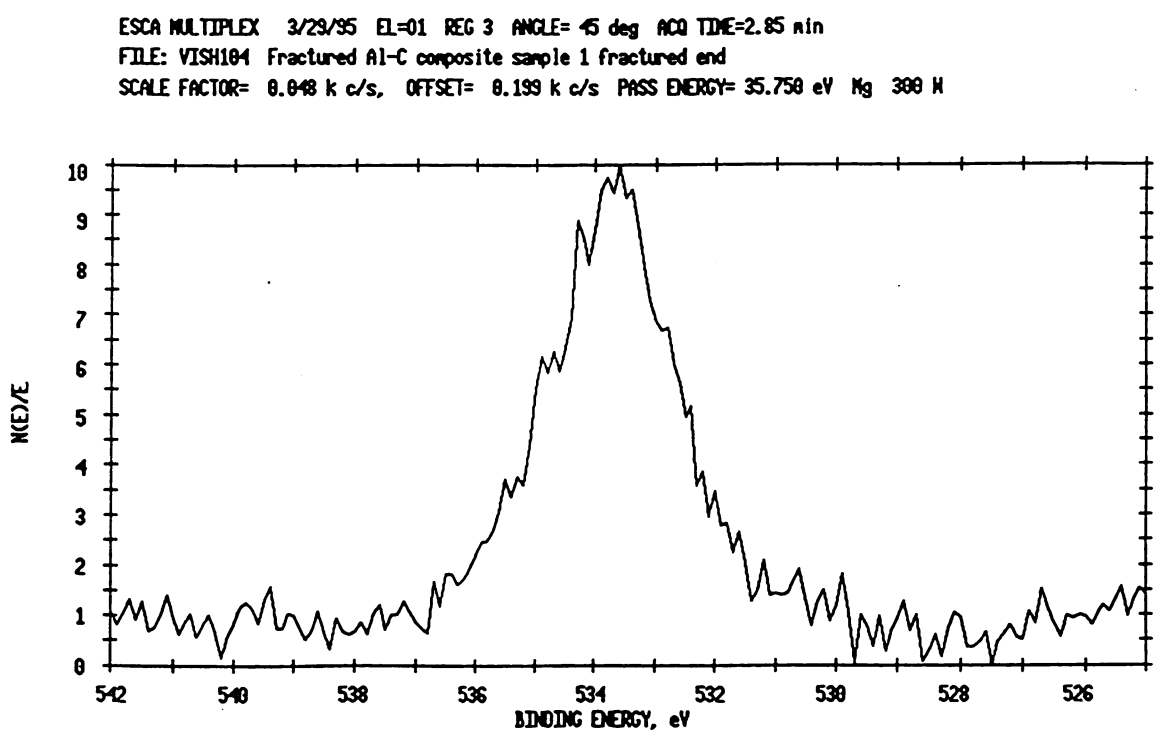

Figure 9.21: XPS analysis for oxygen in the composite (B2-2, Table 9.1).

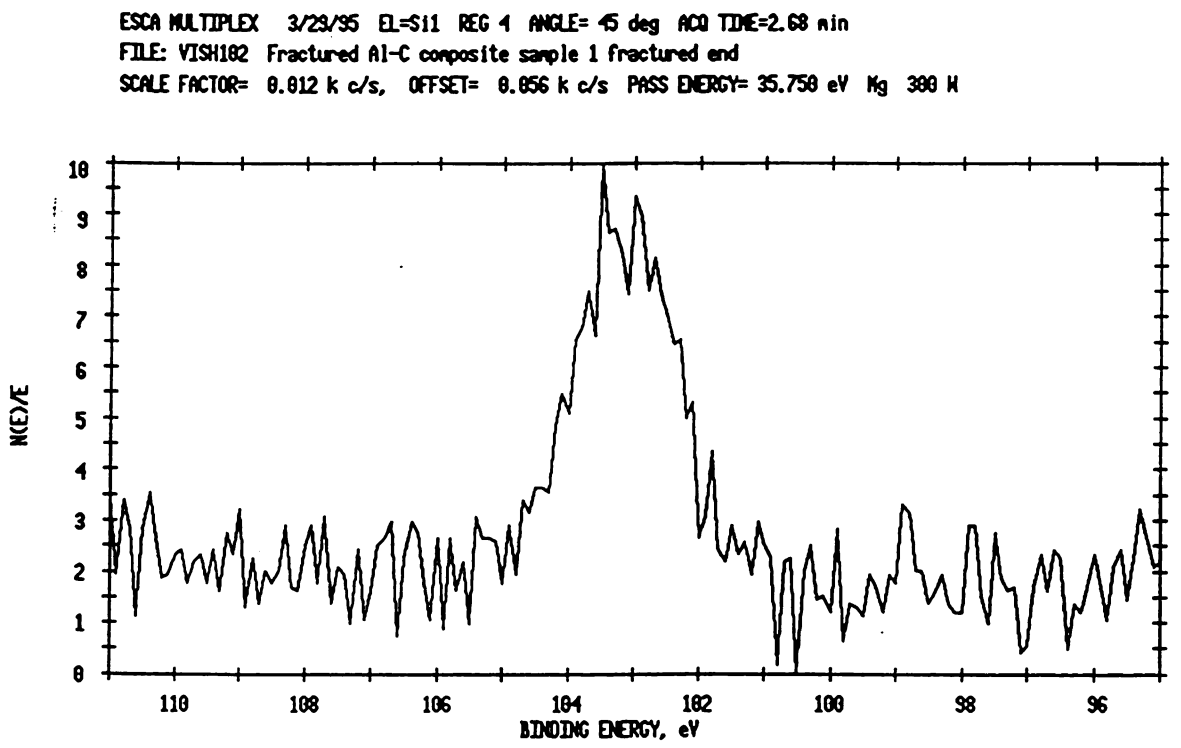

Figure 9.22: XPS analysis for silicon in the composite (B2-2, Table 9.1).

Table 9.3: Atomic concentration in fractured carbon-aluminum composite sample (fractured end is exposed).

Element	Area (cts-eV/s)	Sensitivity Factor	Concentration (%)
C 1s	3670	0.296	74.21
Al 2p	265	0.234	6.78
O 1s	1841	0.711	15.50
Si 2p	199	0.339	3.51

CHAPTER 10

Discussions

The new fabrication method of making continuous fiber reinforced metal matrix composites with out using any binder is capable of producing composites with uniform fiber distribution. It has the potential to attain higher fiber fractions (40-50%) leading to low density and low CTE. In the experiments conducted thus far, several issues that relate to the quality of the composite are discussed with a view toward future processes where automation is possible. Several micrographs showed that the matrix was missing in some parts of the composite or unsintered aluminum particles indicating poor consolidation indicating the potential problems existed with this technique. The 3-point bending tests indicated that the %ROM strength and modulus values ranging from 50-80% could be obtained. Tensile test results also indicated the poor consolidation and fiber clusters as the probable source of failure in the composite. XPS analysis showed the presence of Si in the interface suggesting another possible source of failure. All these issues are discussed in detail in this section with special emphasis on the fracture analysis in the composite. The hysteresis loop observed from the measurement of coefficient of thermal expansion, density of the composite, phases at the fiber-matrix interface, on the fiber and matrix are also some of the issues addressed in this section.

10.1 Adding Powder to the Fibers, Handling Fibers, and Continuous Processing

Some fibers lost aluminum powder when the fibers were taken out of the aersolizer, and during the layup procedure, because the powder particles were loosely attached to the fiber surface. The layers that had lesser amount of powder had additional powder sprinkled on top of the layer. This was done manually using a spatula to make sure that each layer had enough powder for consolidation. The carbons fibers are not easy to handle with no binder and much care was needed during the layup procedure. These fibers move relative to each other and powder is knocked off leading to fiber clustering and in nonuniform distribution of fibers. This indicates that the adhesion of powder to the fiber is not strong enough for the human handling needed for these exploratory experiments.

Continuous processing of the composite with and without using a binder is possible. Each element in the experimental set-up was tested (Figure 7.6). The new fabrication process of making composites without using any binder is capable of picking up any desired volume fraction of the matrix. This can be achieved by either suspending fewer fibers in the aerosolizer (at a given time of powder fluidization) which provides lower fiber fraction, or, suspend more fibers in the aerosolizer (at a given time of powder fluidization) which provides a higher fiber fraction in the composite. The volume fraction of fiber can also be controlled by altering the time of powder fluidization.

10.2 Density Measurements

The density of the composite is 2.28 gm/cm^3 with 40% V_f. As the fiber volume fraction increases the density of the composite decreases. The porosity of the composite varies approximately from 0.5-2.0% for 40-50% V_f. It is noticed that matrix material is missing in some parts of the optical micrograph of the transverse section composite (Figure 9.4 and

Figure 9.5). From these micrographs, it is evident that the porosity should be more than 1% and the density of the composite should be less than the measured 2.28 gm/cm^3. The uncertainty in the fiber fraction may be one of the reasons resulting in the ambiguity of the density measurements of the composite. The fiber volume fraction was measured by counting the number of fibers in a certain cross section of the composite. Therefore, the fiber volume fraction was estimated approximately and the uncertainty in V_f and porosity is bounded by the observations of the cross section of the composite. The porosity observed on the fracture surface is consistent with the calculated range of porosity. The thickness ($\sim$10nm) of Al_2O_3 layer presents on the aluminum particles (5μm dia.) was also taken into consideration for calculating the variations in the density measurements. The density of this layer is very negligible and the effect of this density on the variation in density measurements is practically nil.

10.3 Coefficient of Thermal Expansion-Hysteresis Loop

If a material is subjected to thermal cycling in its service environment, the response of the material during these cycles must be understood. A dilatometer was used for expansion measurements during continuous thermal cycling. The specimen was first heated from room temperature to 250 ^{0}C and then cooled to room temperature (Figure 9.10). The expansion is characterized by large hysteresis loop and a large positive residual strain after the cycle, which is typical of Gr/Al [59]. This behavior can be explained qualitatively. During the initial heat-up from room temperature, the matrix (Al) expands while the graphite fibers contract due to negative CTE. At higher temperatures, the matrix yields under compression and the CTE of the composite decreases due to the strong influence of the fiber on the expansion of the composite. The yielding of the matrix continues to maximum temperature in the cycle. During cooling down from the maximum temperature the fiber expands while the matrix contracts leading to the reversal of thermal strains until the matrix yields

under tension. As the matrix yields the composite follows the fiber response. If the fiber is again heated to high temperatures, the fiber contracts and matrix expands. If the composite is subjected to many thermal cycles, the difference in the expansion behavior between the first and the subsequent cycles is attributed to the reduction in the residual stresses by plastic deformation during the first thermal cycle.

10.4 %ROM Values

The flexural strength and modulus values obtained for the specimen B2-1 and B2-2 are 629 MPa and 101.7 GPa, and 439 MPa and 87.5 GPa respectively. These values corresponds to 49%ROM strength and 78%ROM modulus, and 34%ROM and 67%ROM modulus respectively. These values are from the second batch of the specimens made using bare carbon fibers, and they are comparable to the good results reported in the literature [30]. These higher values may have resulted from the following factors:

- In these specimens, the fiber distribution is homogeneous (Figure 9.3 and Figure 9.15), minimum fiber-to-fiber to contact (Figure 9.3), and the span to thickness ratios (Table 9.1) satisfy the ASTM standards. The fractographs did not show any significant fiber pull-out which suggests that the fiber-matrix bonding was good. Therefore, the homogeneous fiber distribution, good fiber-matrix bonding, and high span to thickness ratios resulted in good %ROM values for the composite specimens B2-1 and B2-2.

  The span to thickness ratios for specimens B2-1 and B2-2 satisfy the standards recommended ASTM handbook for bending tests of composites [58]. For bending tests of composites, the span-to-depth ratio is recommended to be at least 16:1. This ratio shall be chosen such that failures occur in the outer fibers of the specimens, due only to the bending moment. For highly anisotropic composites, shear deflections can se-

riously reduce the modulus measurements. In this study, a ratio of 32:1 is a standard that should be adequate to obtain valid measurements [58].

In the case of specimens from the batch2 (B2-1 and B2-2), the span to thickness ratios are 32 (B2-1) and 28 (B2-2) respectively which satisfy the recommended ASTM standards. For the specimens B1-1 to B1-3, the span to thickness ratios are only 5 which is much below than the recommended ASTM standards. The flexural strength and modulus values have obtained from these specimens are 235 MPa and 15 GPa, 281 MPa and 25.74 GPa, and 347 MPa and 30.84 GPa respectively. These results are from the first batch of the specimens made using bare carbon fibers. These values corresponds to 16%ROM strength and 11%ROM modulus, 19%ROM strength and 19%ROM modulus, and 23%ROM strength and 23%ROM modulus respectively. These results clearly show lower span to thickness ratios for the specimens B2-1 to B2-3 resulted in lower %ROM values and also indicates that the 3-point bending results are strongly influenced by span to thickness ratios.

For specimens C1 and C2, the %ROM strength and modulus values have obtained are 13.0 and 80.0, and 13.0 and 62.0 respectively. In these specimens, the fiber distribution was not uniform and this affected the maximum fracture load. The micrographs showed some areas that had higher fiber density of fibers and other areas that had lower fiber density. There were some fiber clusters (fiber-to-fiber contact) in the composite. The fractographs did show fiber pull-out which suggests that fibers had not worked as good reinforcements. The fractographs at higher magnifications showed some fiber in contact with each other and the fracture initiated at the fiber-to-fiber contacts. This explains why the fracture strength (~300 MPa) and load (~5lb) are low for these specimens.

- The optical micrographs of the transverse sections of the composite showed that matrix material was missing from some parts of the composite. The composite also had

some porosity and the uncoated regions resulted in some voids in the fiber-matrix interface, where the powder particles were not consolidated completely due to the fact that the pressure could not reach these regions during consolidation. Therefore the bonding in these regions is very poor since unsintered aluminum particles could be found (Figure 9.15). The stiffness of the composite was reduced since some portions of the fibers could not transfer elastic loading to the matrix.

- The matrix material and the characteristics of the reinforcing fibers have a significant influence on the strength of the composite.In general, aluminum composites were produced using aluminum alloys. So the use of the pure aluminum matrix material could be a factor because pure aluminum has lower strength and is more highly reactive than aluminum alloys. In the case of the reinforcing component, high modulus carbon fibers have a high content of crystallized carbon and good chemical compatibility but they are expensive because they are carburized at 2000-3000 ^{0}C. In contrast, the high strength carbon fibers are much cheaper because they are processed at much lower temperatures (1000-1500 ^{0}C). But they are more reactive with aluminum than high modulus fibers. Although some successful results have been reported on composite made using high modulus fibers, very few results have been reported on composites with high strength carbon fibers as reinforcements [14]. In view of lower costs, the use of high strength carbon fibers should be significant in the production of C/Al composites although it's strength is lower.

- The strength of the composite increases as the fiber volume fraction increases. The strength is directly proportional to the fiber volume fraction. Hence, reducing the time of aluminum powder fluidization can increase the fiber volume fraction and the strength of the composite (%ROM values).

10.5 Phases at the Interface of Fiber and Matrix

The XPS analysis of the fractured surface of the 3-point bend specimen(B2-1) indicated no formation of Al_4C_3 at the interface (Figure 9.3). This is one of the reasons for achieving good %ROM strength and modulus values in the case of batch2 (B2-1 and B2-2) specimens. The XPS analysis showed the presence of Si on the fracture surface. This amount of Si is much higher than 0.2% present in the aluminum powder used as matrix material. The fractographs showed some phases on the fiber surface and matrix (Figure 10.1). These phases were analyzed using EDAX and the results did not show the presence of Si in those phases (Figure10.2 and Figure 10.3). The results only indicated the presence of aluminum in those phases. Therefore, the Si peak in the XPS analysis is anomalously high, and it suggests that the fracture path follows any Si particles that are present, but they are not easily identified with EDAX (Figure 10.2 and Figure 10.3).

10.6 River Patterns on the Fractured Surface of the Fiber

River patterns are observed on the fractured surface of the fiber at higher magnifications (Figure 9.17 and Figure 9.18). In general, a cleavage fracture represents brittle failure occuring along crystallographic planes. The characteristic feature of this type of failure is flat facets exhibit river marking. The river markings are caused by the crack moving through the crystal along a number of parallel planes which form a series of plateau and connecting ledges. These are indications of the absorption of energy by local deformation. The direction of river pattern represents the direction of crack propagation [60].

The river pattern observed in the micrographs originated at different points and followed no particular direction in the specimen. This makes it difficult to find the origin of the crack in the composite, but it indicates that each fiber fracture occurs at local flaw rather than from a macroscopic stress concentration.

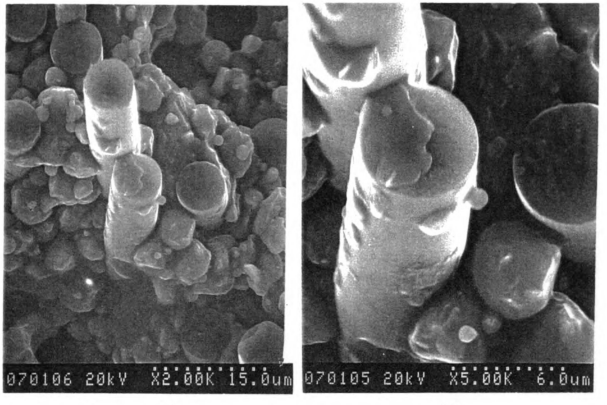

(a) (b)

Figure 10.1. a) Fractograph of the tensile specimen showing the area analyzed using EDAX, b) Fractograph of the tensile specimen showing the fiber surface analyzed using EDAX

X-RAY: 0 - 20 keV
Live: 100 S Preset: 100 S Remaining: 0 s
Real: 136 s 26% Dead

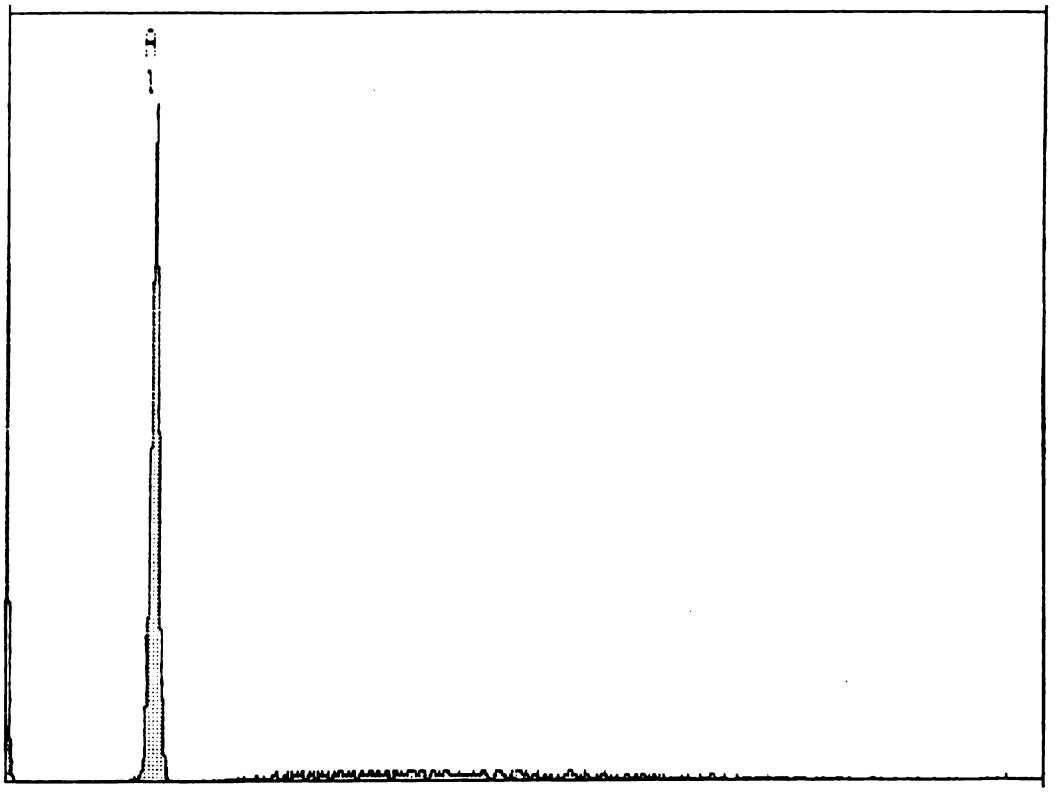

< .0 5.140 keV 10.3 >
FS = 2K ch 268= 29 cts
MEM1 :

Figure 10.2: Results obtained by analyzing the area in the micrograph (Figure 10.1) using EDAX.

X-RAY: 0 - 20 keV
Live: 100 S Preset: 100 S Remaining: 0 s
Real: 136 s 26% Dead

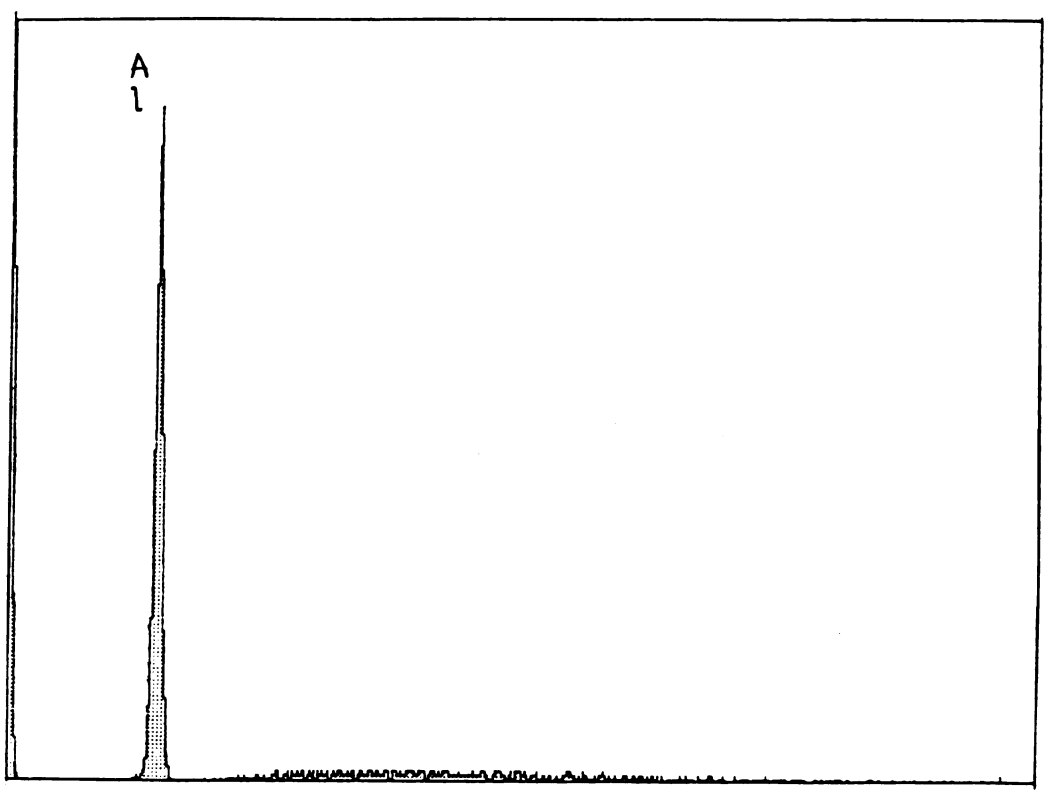

< . 0 5.140 keV 10.3 >
FS = 2K ch 267= 32 cts
MEM1 :

Figure 10.3: Results obtained by analyzing the fiber surface using EDAX.

10.7 Tensile Testing-Poor Consolidation

The fractographs of the tensile specimens showed unsintered aluminum particles indicating poor consolidation resulting in very poor mechanical properties. Fiber clusters were observed in fractographs that indicated fiber fracture at the fiber-fiber interfaces. This indicates that the poor mechanical properties resulted due to fiber-to-fiber contact. The powder particles observed in the matrix suggests that the pressure could not reach these regions to consolidate the powder particles completely and this may account for the low strength of the composite. The bonding in these regions was poor since unsintered aluminum particles were found. Therefore, combination of fiber contact and unsintered matrix resulted in poor load transfer which in turn resulted in poor mechanical properties. The tensile fracture surface represents the weaker part of the fracture, where poorest consolidation occured. 3-point bend does not sample the weakest part, only an arbitrary part of the microstructure, and thus representative of the potential properties if flaws are controlled/minimized, which will be substantially improved when the process is automated.

10.8 Summary

The processing of the composite using the new fabrication technique was not done continuously. Continuous processing would reduce the flaws introduced by the human handling involved in the new technique and also improves the tensile properties of the composite. Therefore, continuous processing of continuous fiber metal matrix composites using new technique should be the next step in the future work.

The effect of consolidation on the coefficient of thermal expansion measurements should be investigated. CTE has to be evaluated by subjecting the composite to number of thermal cycles and the influence of voids in the composite on coefficient of thermal expansion should be investigated.

CHAPTER 11

Conclusions

The new fabrication technique for making continuous fiber reinforced metal matrix composites was investigated and the following conclusions were made:

- The new fabrication technique of making continuous fiber reinforced metal matrix composites without using any binder was capable of picking up any desired volume fraction of metal matrix.
- The processing is less complex since the polymer is not required and no vacuum burnout of polymer is required.
- Following hand layup and consolidation at 570 ^{0}C, 30 MPa, and 45 minutes (consolidation parameters), the distribution of the fibers was uniform.
- Fractographs of the composite showed that the fiber-matrix bonding was good, and that fibers fractured due to brittleness of the fibers rather than due to the global stress state.
- The highest mechanical properties obtained in bend tests were 629 MPa flexural strength and 101.7 GPa flexural modulus which were 49 and 78% of ROM values.
- The CTE of the composite measured using the dilatometer is 1.8 $\times 10^{-6}/^0$C.

- XPS analysis of the fractured surface of the 3 point bend test specimen indicated no apparent formation of Al_4C_3.
- Continuous processing should improve the properties by reducing the flaws introduced by human handling.

BIBLIOGRAPHY

BIBLIOGRAPHY

[1] M. Taya and R. J. Arsenault, *Metal Matrix Composites-Thermomechanical Behavior.* Pergamon Press, 1989.

[2] K. G. Kreider, "Introduction to Metal-Matrix Composites," in *Composite Materials-Metallic Matrix Composites* (K. G. Kreider, Ed.), vol. 4, pp. 1–35, Academic Press, 1974.

[3] M. Robert, "New Pathways to Processing Composites," in *High Temperature/High Performance Composites* (F. D. Lemkey, Ed.), Material Research Society Symposium., Proc. Symposium held April 1988, Reno, Nevada, 1988.

[4] A. A. Kelly and S. Mileiko, *Fabrication of Composites*, vol. 4. Elsevier Science Pub. Co., 1983.

[5] K. K. Chawla, *Composite Materials: Science and Engineering.* Springer-Verlag, 1987.

[6] T. W. Chou, A. Kelly, and A. Okura, "Fiber-Reinforced Metal-Matrix Composites," *Composites*, vol. 46(3), pp. 188–206, 1985.

[7] A. Mortensen, M. Gungor, J. Cornie, and M. Flemings, "Alloy Microstructures in Cast Metal Matrix Composites," *Journal of Metals*, p. 30, 1986.

[8] E. J. Lavernia and N. J. Grant, "Spray Deposition of Metals: A Review," *Materials Science and Engineering*, vol. 98, p. 381, 1988.

[9] J. H. Zaat, *Ann. Rev. Mat. Sci.*, vol. 13, p. 9, 1983.

[10] M. F. Amateau, "Progress in the Development of Graphite-Aluminum Composites using Liquid Infiltration Technology," *Journal of Composite Materials*, vol. 10, p. 279, 1976.

[11] A. A. Baker *et al.*, *Fibre Sci. Tech.*, vol. 5, p. 213, 1972.

[12] P. W. Jackson, *Fibre Sci. Tech.*, vol. 5, p. 219, 1972.

[13] A. Miyase and K. Piekarski, "Compatibility of Chromium Carbide Coated Graphite Fibres with Metallic Matrices," *Journal of Materials Science*, vol. 16, p. 251, 1981.

[14] T. Ohsaki and M. Yochida, *Thin Solid Films*, vol. 45, p. 563, 1977.

[15] J. M. Harper and J. J. Cuomo, *Ann. Dev. Mater. Sci*, vol. 13, p. 413, 1983.

[16] P. D. Funkenbusch, T. H. Courtney, and D. G. Kubisch, "Fabricability of and Microstructural Development in Cold Worked Metal Matrix Composites," *Scripta Metallurgica*, vol. 187, pp. 1099–1104, 1984.

[17] P. D. Funkenbusch and T. H. Courtney, "On the Strength of Heavily Cold Worked In-Situ Composites," *Acta Metallurgica*, vol. 33(5), pp. 913–922, 1985.

[18] D. L. Erich, "Metal-Matrix Composites: Problems, Applications, and Potential in the P/M Industry," *The International Journal of Powder Metallurgy*, vol. 23, pp. 45–54, 1987.

[19] P. Ramakrishnan, "Continuous Carbon Fiber Reinforced Aluminum Matrix Composites through Powder Metallurgy," in *Advanced Powder Metallurgy Particulate Materials; Particulate Materials and Processes* (J. M. Campus, Ed.), Proceedings of the 1992 Powder Metallurgy World Congress, June 1992, San Fransisco, 1992.

[20] T. Koppenaal and N. Parikh, "Fiber-Reinforced Metals and Alloys," tech. rep., Armour Res. Foundation, Chicago, 1961.

[21] R. Sara, H. Volk, H. Nara, and D. Hanely, "Integrated Research on Carbon Composite Materials," tech. rep., AFML (Part I to Part V), 1966-1969.

[22] A. Bushow and C. Esola, "Electroforming of Aluminum Composite Structures by Codeposition of High-Strength High-Modulus Fibers or Wiskers," Tech. Rep. CR-66749, 1969.

[23] F. P. LaIaconna, "Graphite Aluminum Composites." NASA/MSPC, 1971.

[24] B. Howlett, D. Minty, and C. Old, 1971. Plast. Inst. (London).

[25] E. DeLamotte, K. Phillips, and H. Killias, "Continiuosly Cast Aluminum-Carbon Fiber Composites and Their Tensile Properties," *Journal of Materials Science*, vol. 7, pp. 346–349, 1971.

[26] L. W. Davis and S. Bradstreet, "Metal and Ceramic Matrix Composites," tech. rep., 1970.

[27] A. Baker and R. Bache, "Experiments on Fracture Behavior of Single Fibre-Brittle Zone Model Composites," *Composites*, vol. 2(3), 1971.

[28] G. Blankenburgs, "The Effect of Carbide Formation on the Mechanical Behavior of Carbon-Aluminum Composites," *The Journal of the Australian Institute of Metals*, vol. 14, pp. 236–241, 1969.

[29] P. R. Soni, "Studies on the Room Temperature and Elevated Temperature Tensile Strength of Carbon Fiber Reinforced Aluminum Matrix Composites," in *Advanced Powder Metallurgy Particulate Materials and Processes* (P. Ramakrishan, Ed.), Proceedings of the International Conference on Advances in Composite Materials, Jan 1990, Bombay, India, 1990.

[30] M. U. Islam and W. Wallace, *Adv. Mat. Manufact. Process.*, vol. 3(1), 1988.

[31] S. N. Patankar, V. Gopinathan, and P. Ramakrishnan, "Processing of Carbon Fiber Reinforced Aluminum Composite Using K_2ZrF_6 Treated Carbon Fibers: A Degradation Study," *Journal of Materials Science Letters*, vol. 9, pp. 912–13, 1990.

[32] H. Asanuma and A. Okura, "Report of the Research Group for Fiber Reinforced Aluminum Matrix Composites," tech. rep., The Light Metal Education Foundation Inc., Osaka, Japan, 1986.

[33] N. Eustathopoulos, J. C. Joud, P. Desre, and J. M. Hicter, "The Wetting of Carbon by Aluminum and Aluminum Alloys," *Journal of Materials Science*, vol. 9, p. 1233, 1974.

[34] S. Kohra and N. Muto in *Proceedings of the 5th International Conference on Composite Materials, San Diego, California* (W. C. Harrigan Jr., J. Strife, and A. K. Dhingra, Eds.), TMS, Pensylvania, 1986.

[35] J. W. Upp, R. T. Pepper, E. G. Kondall, and R. C. Rossi Tech. Rep. TR-0059(6250-10)-9, Aereospace Corporation, E. Segundo, California, Oct. 30, 1970.

[36] I. H. Khan, "The Effect of Thermal Exposure on the Mechanical Properties of Aluminum-Graphite composites," *Met. Trans.*, vol. 7A,(1281), 1976.

[37] W. C. Harrigan *Met. Trans.*, vol. 9A,(503), 1978.

[38] S. Baker and W. Bonfield, "Fracture of Aluminum-Coated Carbon Fibers," *Journal of Materials Science*, vol. 13, pp. 1329–1334, 1978.

[39] I. G. Greenfield, "Measurements of Physical Properties of Hot Graphite/Copper and Graphite/Aluminum Composites - Specimen Preparation," in *Metal & Ceramic Matrix Composites: Processing, Modeling & Mechanical Behavior* (Bhagat, Ed.), Proceedings of an International Conference held at the TMS Annual Meeting in Anaheim, California, 1990(Feb.).

[40] D. K. Hale, "The Physical Properties of Composite Materials," *Journal of Materials Science*, vol. 11, pp. 2105–2140, 1976.

[41] Y. Takao and M. Taya, "Thermal Expansion Coefficients and Thermal Stresses in an Aligned Short Fiber Composite with Application to a Short carbon fiber/aluminum," *Journal of Mechanics*, vol. 52, pp. 806–810, 1985.

[42] P. J. Withers, "The Determination of the Elastic Field of an Ellipsoidal Inclusion in a Transversely Isotropic Medium, and its Relevance to Composite Materials," *Phi.Mag*, vol. 59(4), pp. 759–781, 1989.

[43] J. D. Eshelby, "The Determination of the Elastic of an Ellipsoidal Inclusion, and Related Problems," vol. 241 of *A*, pp. 376–396, Proc.Roy.Soc of London, 1957.

[44] D. Aylor, R. Ferrara, and R. Kain, *Materials Performance*, vol. 23(7), pp. 20–22, 1984.

[45] R. Paciej and V. Agarwala, *Corrosion*, vol. 42(12), pp. 718–729, 1986..

[46] E. Kendall, "Development of Metal-Matrix Composites Reinforced with High-Modulus Graphite Fibers," in *Composite Materials-Metallic Matrix Composites* (K. G. Kreider, Ed.), vol. 4, pp. 319–395, Academic Press, 1974.

[47] H. S. Yoon, A. Okura, and H. Ichinose, "Study of the Interface of Carbon Fiber Reinforced Aluminum Composite Materials," in *Interfacial Phenomena in Composite Materials* (F. R. Jones, Ed.), Proceedings of the International Conference on Interfacial Phenomena in Composite Materials, Sep. 1989, UK, 1989.

[48] Q. Li, G. D. Zhang, J. T. Blucher, and J. A. Cornie, "Microstructure of the Interface and Interfiber Regions in P-55 Reinforced Aluminum Alloys Manufactured by Pressure Infiltration," in *Controlled Interfaces in Composite Materials* (H. Ishida, Ed.), Proceedings of the 3rd International Conference on Composite Interfaces (ICCI-3); Cleveland, Ohio, 1990.

[49] G. D. Zhang, S. R. Feng, Q. Li, and J. A. Cornie, "Control of Interface Reactions between P-55 Fibers and Aluminum Alloy Matrices during Pressure Infiltration Processing," in *Controlled Interfaces in Composite. Mater.* (H. Ishida, Ed.), pp. 343–57, Proceedings of the 3rd international conference on composite interfaces (ICCI-3); Cleveland, Ohio, 1990.

[50] V. Gupta, A. S. Argon, and J. A. Cornie, "Interfaces with Controlled Toughness as Mechanical Fuses to Isolate Fibers from Damage," *Journal of Materials Science*, vol. 24, pp. 2031–2040, 1989.

[51] J. A. Cornie, W. R. Lovic, and A. T. Male, "Failure Modes in Composites IV," pp. 236–264, TMS-AIME, 1977.

[52] S. Ochiai, S. Urakawa, K. Ameyama, and Y. Murakami *Metallurgical Transactions*, vol. 11A, p. 525, 1980.

[53] M. Shorshorov, L. Ustinov, A. Sirlin, V. Olefirenko, and L. Vinogradov, "Brittle Interface Layers and the Tensile Strength of Metal-Fibre Composites," *Journal of Materials Science*, vol. 14, pp. 1850–1861, 1979.

[54] C. He, G. Zhang, W. Cai, and R. Wu, in *Proceedings of the Materials Research Society, Boston*, 1989.

[55] S. Iyer, *Continuous Processing of Unidirectional Prepregs.* PhD thesis, Michigan State university, 1990.

[56] A. Saoudi, "A New Fabrication Method of Continuous Fiber Reinforced Metal Matrix Composites," Master's thesis, Michigan State university, 1992.

[57] H. Wang, "A New Fabrication Method of Continuous Fiber Reinforced Metal Matrix Composites," Master's thesis, Michigan State university, 1994.

[58] ASTM, Annual Book of ASTM Standards, *Standard Test Methods for Flexural Properties of Unreinforced and Reinforced Plastics and Electrical Insulating Properties (D790-92)*, 1994.

[59] S. Tomkins and A. Dries, "Thermal Expansion Measurement of Metal Matrix Composites," in *Testing Technology of Metal Matrix Composites* (Digiovanni and Adsit, Eds.), ASTM Committee D-30 on High Modulus Fibers and their Composites, 1985.

[60] D. George, *Mechanical Metallurgy.* McGraw-Hill Company, 1986.